U.PORTO

FEUP FACULDADE DE ENGENHARIA
UNIVERSIDADE DO PORTO

INTEGRATED MASTER IN ENVIRONMENTAL ENGINEERING 2019/2020

MICROBIAL FUEL CELLS FOR ENERGY PRODUCTION AND WASTEWATER TREATMENT

RICARDO CORREIA

Dissertation submitted for the degree of

MASTER ON ENVIRONMENTAL ENGINEERING

President of the jury: Cidália Maria de Sousa Botelho
Auxiliary Professor at Department of Chemical Engineering of the Faculty of Engineering of the University of Porto

---

Supervisor at the University: Alexandra Maria Pinheiro da Silva Ferreira Rodrigues Pinto - PhD
Associate Professor at Department of Chemical Engineering of the Faculty of Engineering of the University of Porto

---

Academic coSupervisor: Vânia Sofia Brochado de Oliveira - PhD
Auxiliar Researcher at Department of Chemical Engineering of the Faculty of Engineering of the University of Porto

coSupervisor: Joana Isabel Gonçalves Vilas Boas - PhD
Student at Department of Chemical Engineering of the Faculty of Engineering of the University of Porto

---

Junho, 2020

Dedicatória

Esta dissertação é dedicada às minhas avós.

Agradecimentos

O meu primeiro agradecimento é dirigido à Professora Doutora Alexandra Pinto e à Doutora Vânia Oliveira, pela oportunidade que me deram de fazer parte de uma fração de estudos do grupo de energia CEFT.

Um agradecimento especial à coorientadora Joana Vilas Boas, pela disponibilidade, pela simpatia, pela amabilidade, e, pela preciosa orientação neste trabalho num contexto assaz difícil de emergência de saúde pública de âmbito internacional, devido à situação pandémica Covid-19.

À minha mãe agradeço toda a calma e sabedoria emocional que me transmitiu, ao meu pai agradeço o acompanhamento e todas as sugestões dadas ao longo deste projeto, ao meu irmão agradeço o entusiasmo que demonstrou na minha evolução, e aos meus avôs agradeço toda a preocupação e carinho.

À Mafalda, por ser quem é e por estar sempre ao meu lado.

Aos meus queridos amigos que me acompanham nas etapas cruciais da minha vida, dedico aquela música de sempre: “A tout le monde a tout mês amis”.

Um obrigado a todos quantos têm estado comigo ao longo deste percurso.

“We each need to find our own inspiration. Sometimes is not easy”

Hayao Miyazaki

Abstract

Climate emergency awareness compromised an energy transition all around the world. Search for new and clean technologies is now a reality and a microbial fuel cell (MFC) relays on this field as an exciting and unique technology capable of energy production and simultaneously treatment of wastewaters. Wastewater is generated globally and can be harmful for living beings and lead to environmental problems due to the need of treatment before being rejected in the receptor medium, conventional treatments are expensive and generate significant amounts of sludge. Wastewater chemical and biological composition contains useful energy and microorganisms to be used in the MFC since organic matter is degraded by microorganisms in the anodic chamber converting the chemical energy of wastewater in electrical energy. This work includes a brief history of electrochemistry from the birth to the appearance of microbial electrochemical technologies with focus on MFC. Electron transfer mechanisms and energy conservation are exposed, plus detailed content of parameters and configurations that directly affect the performance of the MFC are discussed as well as diagnostic and techniques for electrochemical and biofilm characterization. Finally, the integration with other technologies and the future challenges and perspectives of MFC are approached.

At the experimental level, two experiments, A_0 and A_1, were studied in a bottle MFC configuration for the treatment of a synthetic winery wastewater. The two experiments differed in the superficial area of the electrode anode (carbon brush with a diameter of 2.5 cm and 5 cm). Results evaluated biofilm and organic content, Chemical Oxygen Demand (COD) removal and power output presented better performance for experience A_1 (34% and 0.89 mW/m^2 for COD removal and power density respectively) due to the larger anode active area and short electrodes spacing. Microorganism inoculated in the synthetic winery wastewater was the yeast *Zygosaccharomyces bailii* (*Z. bailii*) which is an aggressive food spoilage microorganism and is often isolated as a contaminant during wine fermentation. Assessing yeast grow (CFU/mL) in the bulk of the anodic chamber and measuring the pH and conductivity of solution it was possible to infer as expected the adaptability of the microorganism, nevertheless MFC performance was weak.

Keywords: Renewable Energy, Microbial Fuel Cell, Electrochemistry, Wastewater Treatment, *Zygosaccharomyces bailii.*

Resumo

A emergência climática levou à consciencialização da necessidade da transição energética por todo o mundo, a procura de energias limpas é agora uma realidade, neste âmbito as células de combustível microbianas (MFC) são uma tecnologia renovável única capaz de produzir energia e tratar águas residuais em simultâneo. As águas residuais são produzidas a um nível global e podem ser nocivas aos seres vivos e meio ambiente pelo que têm de ser tratadas antes de serem rejeitados no meio recetor. Os tratamentos convencionais usados são dispendiosos e produzem substanciais quantidades de lamas. As águas residuais apresentam concentrações de microrganismos e contêm energia na sua composição química, aspetos úteis no princípio de trabalho das MFC, uma vez que a matéria orgânica é degradada na câmara anódica por microrganismos que convertem a energia química proveniente do substrato (águas residuais) em energia elétrica, produzem ainda uma pequena quantidade de lamas.

Neste trabalho é apresentado uma história sumária sobre as origens da eletroquímica e o seu desenvolvimento até ao surgimento de tecnologias microbianas eletroquímicas, com foco na MFC. É discutida a transferência de eletrões e conservação de energia com informação detalhada sobre parâmetros e configurações que afetam diretamente o desempenho das MFC. São também abordadas técnicas de caracterização eletroquímica e de quantificação do biofilme. Por último refere-se a importância da integração desta tecnologia com outras já conhecidas e os desafios e perspetivas futuras da mesma.

A nível experimental foram realizadas duas experiências, A_0 e A_1, numa configuração de MFC em garrafa, “Bottle MFC”, para o tratamento de água residual sintética vinícola. As experiências continham uma área superficial do elétrodo do ânodo diferente (2,5 cm diâmetro e 5 cm diâmetro). Os resultados avaliados relativos aos biofilme e conteúdo orgânico do mesmo, remoção da Carência Quimica de Oxigénio (CQO) e potência específica foram melhores na experiência A_1 (34% e 0.89 mW/m^2 para remoção de CQO e potência específica respetivamente) devido à maior área ativa do ânodo e distância entre os elétrodos. O microrganismo inoculado na água residual sintética foi a levedura *Zygosaccharomyces bailii* (*Z. bailii*), uma vez que é um microrganismo muito resistente e usualmente isolado na fermentação de vinho devido a poder ser um contaminante. Avaliando o crescimento de leveduras (UFC/mL) em suspensão na câmara anódica e medindo o pH e a condutividade da solução, foi possível inferir adaptabilidade do microrganismo, verificando-se, no entanto, um fraco desempenho das MFC.

Palavras chave: Energia Renovável, Células de Combustível Microbianas, Eletroquímica, Tratamento de Águas Residuais, *Zygosaccharomyces bailii.*

Declaração

Declaro sob compromisso de honra, que este trabalho é original e que todas as contribuições não originais foram devidamente referenciadas com identificação da fonte.

Ricardo Correia

_____

29/06/2020

Index

Nomenclature

Symbol

Symbol	Meaning	Units
A	Area	m^2
A_e	Working electrode area	cm^2
BOD	Biological oxygen demand	mg/L
CE	Coulombic efficiency	%
COD	Chemical oxygen demand	mgO_2/L
D	Diffusion coefficient	cm^2/s
ε_E	Energy efficiency	%
G°	Gibbs free energy	J, J/mol
F	Faraday constant	C/mol
I	Current density	mA/m^2
M	Molar concentration	mol/L
P_{out}	Power Output	W
P_w	Electric Power	W
P	Power density	mW/m^2
R	Resistance	Ω
	Specific power	kW/kg
T	Temperature	ºC or K
	Volumetric power	kW/m
U or E	Voltage	V or mV
V	Volume	L or m^3
V_{an}		
v	Scan rate	V/s
ΔH	Heat of combustion	J/mol

Abbreviation

Abbreviation	Meaning
II	Reaction quotient
$\Delta G‡$	ΔG
ΔE_p	Anodic to cathodic peak separation
A_{An}	Anode area
AEM	Anion exchange membrane
AS	Activated sludge

BPM	Bipolar membranes
B_t	Total volatile solids of the biofilm attached to the anode electrode
CA	Chronoamperometry
C_0	Concentration of redox species
CC	Coefficient correlation
CEM	Cation exchange membrane
C_{CFU}	Concentration of CFUs presented at the anode electrode
CLSM	Confocal laser scanning microscopy
CNF	Carbon nanofiber
CNTs	Carbon nanotubes
COD_{SWWW}	COD concentration of the SWWW feed to the reactor at the beginning of the experiment
COD_{CycleX}	COD concentration at the end of the batch cycle
CO_2	Carbon dioxide
CV	Cyclic voltammetry
CW-MFC	Constructed wetland-microbial fuel cells
DC-MFC	Dual chamber microbial fuel cell
DEET	Direct extracellular electron transfer
DIET	Direct interspecies electron transfer
DO	Dissolved Oxygen
EAB	Electroactive bacteria
EAM	Electrochemical active molecules
EET	Extracellular electron transfer
EMF	Electromotive force
E_{pa}	Potential anionic peak
E_{pc}	Potential cationic peak
EPS	Extracellular polymeric substances
FAD	Flavin adenine dinucleotide
FRA	Frequency response analyser
FC	Fuel Cell
H_2O	Water
H^+	Proton
IEM	Ion exchange membrane
I_p	Analytic current
I_{pa}	Current anionic peak

I_{pc}	Current cationic peak
MBR	Membrane bioreactor
MDC	Microbial desalination cell
MET	Microbial electrochemical technology
MEET	Mediated extracellular electron transfer
MFC	Microbial fuel cell
MFCs	Microbial fuel cells
n	Number of electrons
NAD	Nicotinamide adenine dinucleotide
NHE	Normal hydrogen electrode
OCV	Open circuit voltage
OD	Optical density
OLR	Organic loading rate
OMPs	Outer membrane proteins
P_{An}	Anode power density
Pt	Platinum
PL	Polysaccharides
PEM	Proton exchange membrane
PEMFC	Proton exchange membrane fuel cell
Pp	Phosphorus
R_{act}	Charge transfer resistance (activation losses)
R_{conc}	Diffusion-limited concentration losses
R_{int}	Internal resistance
R_{Ω}	Ohmic resistance
R_p	Polarization resistance
R_p^a	Polarization resistance at the anode
R_p^c	Polarization resistance at the cathode
rxn	Change in a reaction
SWWW	Synthetic winery wastewater
SBR	Sequencing batch reactor
SC-MFC	Sing chamber microbial fuel cell
SHE	Standard hydrogen electrode
SCE	Saturated calomel electrode
SLR	Sludge loading rate
TOC	Total organic carbon

TOC_{SWWW}	TOC concentration of the SWWW feed to the reactor at the beginning of the experiment
TOC_{cycleX}	TOC concentration at the end of the batch cycle
TSS	Total suspended solids
TVS	Total volatile solids
SEM	Scanning electron microscopy
UASB	Up-flow anaerobic sludge blanket
WW	Wastewater
WWT	Wastewater treatment
WWW	Winery wastewater
WWWT	Winery wastewater treatment
YPD	Yeast extract peptone dextrose
YNB	Yeast nitrogen base

List of Figures

List of Tables

1

Introduction

1.1 - Technology Pertinence

The current energy production system is unsustainable and is increasingly contributing to global environmental problems such as climate change. Harmful liquid and solid wastes and air emissions must be treated or mitigated. Based on that new energy policies and developing strategies are being implemented to meet global goals [1]. Renewable energies are secure and clean energy supply technologies and are a fraction of sustainable development strategies, the current energy transition is unique and unprecedent characterized by a fast shift never seen before [2], [3]. Inherent pollutants on liquid waste - wastewater (WW) result in risks for public health and environment [4]. Any water that has been once used by humans could be termed as WW since its properties would no longer be the same as that of natural water [5]. It is necessary to combat the negative impacts of WW with efficient and sustainable treatment methods. To accomplish that new technologies and the upgrade of old technologies have been developed, as cutting edge anaerobic biotechnologies, enhance anaerobic membrane bioreactors and microbial electrochemical systems, among others [6].

WW is characterized in terms of physical, biological, and chemical composition and is removed from residences, institutions, commercial, agricultural, and industrial establishments [5]. Wastewater treatments (WWT) are composed by different treatment levels and grouped in two types of units (Table 1), unit operations for physical treatment and unit processes when biological and chemical reactions are conducted. The combination of these units provides better results [7], [4]. Although traditional WWT meets legislation requirements and achieves satisfactory removal efficiencies, biological treatment presents several drawbacks due to energy demand, sludge generation and incapability of recovering the potential resources available in WW [8]. Traditional WWT requires about 0.5-2 kWh/m^3 depending on the process and WW composition and holds about 3-10 times the energy required to treat it [9]. An activate sludge process due to aeration may count up to 75% of WW treatment plant energy costs, and treatment and disposal of sludge may count up to 60% of the total operation costs [9]. A positive aspect in traditional WWT plants

is the biogas (methane) produced from anaerobic digestion providing energy savings to the plant [10]. Regarding these problems and the need of meeting global goals and energy transition new technologies are being studied. On this field microbial fuel cells (MFCs) are a promising lead.

Table 1: Levels of WWT and type of unit [7].

Treatment Level	Description	Type of Unit
Preliminary	Removal of large solids such as rags, sticks, floatables, grit and grease;	Physical
Primary	Removal of suspended solids and organic matter;	Physical and Chemical
Secondary	Removal of biodegradable organic matter, suspended solids, inorganic and non-biodegradable compounds;	Biological and Chemical
Tertiary/Advanced	Removal of residual suspended/dissolved solids and disinfection.	Physical, Chemical and Biological

1.1.1 - Microbial Fuel Cell as a Sustainable Technology

A microbial fuel cell (MFC) provides dual benefits as they treat a WW while simultaneously generate power [11]. These devices have indeed the ability of directly convert the substrate energy into electricity. Potential energy stored in a WW due to the organic compounds (substrate energy) ranges from 4.92 to 7.97 kWh $kgCOD^{-1}$ [12]. All the biochemical energy can potentially be converted into electricity since rarely the energy is released in the form of heat during fermentation [13]. In addition, zero net carbon emission can be assumed since the carbon dioxide (CO_2) produced is removed from the atmosphere by the photosynthesis process [14]. It is a system that produces less sludge providing economic gains in comparison with traditional treatments, it is insensitive to the operation environment, does not require gas treatment due to recycling and conversion mechanisms and can play a crucial role in locations with an insufficient electrical structure [14]. WWT might become a net energy producer rather than a consumer, although some barriers need to be overpassed such as low electricity production, current instability, high internal resistance and costly materials [15], [16].

1.1.2 - Wine Industry

Wine production takes place in many regions of the globe by the fermentation of grape juice and grape pines, are cultivated across the North and Southern Hemisphere under diverse climate conditions [17]. In 2019, 260 million hectolitres of wine were produced worldwide. Portugal comes in the first 15th largest wine producers which gives a significant contribution to the economy [18] (Figure 1). With heavy commercial production large volumes of winery wastewater

(WWW) are generated, predominantly as result of cleaning operations (washing equipment and bottles) and purge from cooling [19] .

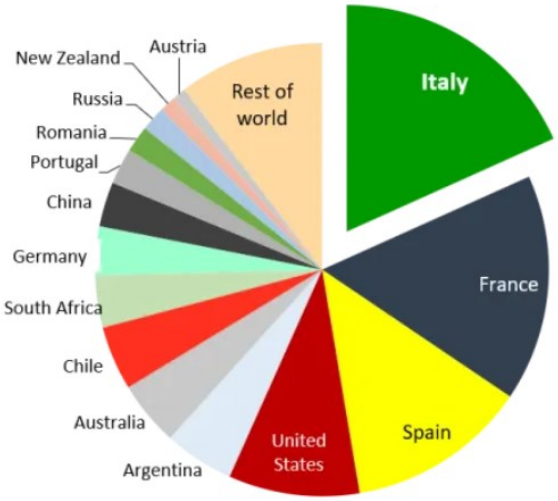

Figure 1: World Winery Production (2019) [20].

WWW quality and quantity vary from winery to winery and over the year, due to vat size, type of wine press, working period (vintage, racking, bottling) and significantly by climate and wine type produced (red or white) [21]. The WWW composition is unique for each winery however studies indicate that is composed by a high organic content, predominantly sugars (fructose, glucose), followed by organic acids (acetic, tartaric, propionic), esters and polyphenolic compounds, still suspended solids, grape juice and cleaning agents [19]. Ethanol and sugars represent more than 90% of the winery effluent, therefore it is worthwhile to recover the organic load of WWW than transforming it into sludge and CO_2 [22]. Winery water footprint range can vary greatly, from 9.6-12.7 L of water per wine bottle (75 cl) and 0.5-14 L per litter of wine produced [21], [23], [24]. Likewise, the chemical oxygen demand (COD) ranges from 320 to 49105 mgO_2/L and in Portugal from 5000-10000 mgO_2/L [21], [25]. It's a reality that these volumes of WWW and highly pollutant loads have a notable environmental impact if discharged without treatment [26]. A summary of a winery wastewater characterization is shown in Table 2.

Table 2: Typical chemistry of untreated vintage and non-vintage winery wastewater (Griffith, Riverina wine - Australia), samples collected weekly from a large winery (annual crush +/- 80 000 tonnes); DO – Dissolved Oxygen, TSS – Total Suspend Solids; COD – Chemical Oxygen Demand; Adapted from [27], [28].

Data collected (2007)	Raw flow in (kL)	DO (mg/L)	pH	Conductivity (µS/cm)	TSS (mg/L)	COD (mgO_2/L) unfiltered
February	137-184	2.5-4.0	4.07-4.14	1491-1571	513-577	8630-10590
March	132-240	4.5-4.8	4.52-4.58	918-1493	487-610	3440-7820
April	72-168	0.8-1.4	4.53-6.0	1530-1793	437-560	378-6860
May	68-168	0.8-8.6	4.72-6.0	674-1149	163-320	1750-4390
June	57-92	1.0-3.3	4.9-6.3	626-1447	450-6170	620-3350
July	39-352	2.4-7.7	2.4-7.7	657-1241	450-507	1090-3930

Regarding wastewater treatment and the search for new and clean technologies the present work goal is to study the novel technology MFC for the treatment of an wastewater effluent of winery industry (synthetic formulation) and energy production by action of the yeast *Zygosaccharomyces bailii* (Z. *bailii*).

1.1.3 - Yeast *Zygosaccharomyces bailii*

Winery effluents are charged with microorganisms and yeasts that are frequently found different quantities over the year [29]. *Z. bailii* is well known as being one of the most aggressive food spoilage microorganisms and is often isolated as a contaminant during wine fermentation [30]. Moreover, Thomas and Davenport [31] recognized Z. *bailii* as a dominant organism in an 18-month period of selected food spoilage yeasts.

Yeast *Z. bailii* has relevant physiological characteristics like being osmotolerant, highly fermentative, and is the most preservative-resistant organism known, resisting at high concentrations of acetic acid, sorbic acid and ethanol [30], [32]. In Kalathenos et. al, [33] *Z. bailii* presented the greatest potential resistance at higher ethanol concentrations and great tolerance to the most common preservatives, namely sulphite and dimethyl decarbonate. Z. *bailii* can grow in fortified wines of 18% (v/v) alcohol and shows remarkable tolerance to pH being able to grow at a pH as low as 2.2 into 7.0 [31]. The ability to endure low pH and high weak organic acid concentrations make Z. *bailii* promising for application in industrial bioprocesses [30]. All these characteristics combined bear potential for growth and secure the survival of these species against other competitors [34]. Furthermore, Z. *bailii* has the ability to ferment glucose and fructose (major sugar content of WWW) converting it into ethanol (fermentative pathway) whereby is tolerant, and capable of grow under oxygen-restrictive conditions (MFC works in this conditions) [30], [35].

1.2 - Thesis Structure

The first chapter of this work frame the specular and unique characteristics of MFCs as a possible actor in the energy transition and shift of conventional wastewater treatments through a sustainable way. The composition of untreated wineries wastewaters and the yeast *Zygosaccharomyces bailii* properties are also featured.

The second chapter is divided in 6 sub chapters. The first one frame the historical origin of electrochemistry evolving electrochemistry technologies such as fuel cells where the basics of the operating principle and performance are explained into the microbial electrochemistry technologies, this chapter pretended also to reveal slight discoveries of scientists in the development of electrochemistry. The second one highlights the principles of a MFC as well as the motor of the energy production deserved by the microorganisms and the electron transfer mechanisms and energy conservation. The third one frames the calculations and procedures for data reporting concerning MFCs and additional understandings of factors and conditions affecting the performance of these systems. The fourth one provides detailed information regarding configuration parameters, such as substrates, microorganism, reactor design, anode and cathode electrodes, membrane. The fifth one indicates the applications of MFCs in wastewater treatment rendering information about the composition of wastewaters and where is presented an extended table accommodating the performance of MFCs in diverse wastewater treatments with different configuration parameters. The sixth one details characterization techniques, first on electrochemical where it is provided the experimental conditions to realize these techniques, the fundamentals of the techniques and the importance of its application in the MFCs studies, second on the biofilm quantification/characterization, where it is presented and introduction concerning the biofilm formation steps, than the different techniques and the advantageous and disadvantages of each one as well as the importance of its use on the MFCs studies, third on the wastewater treatment evaluation where is presented the common parameters used for its analysis. The seven one relays on a bigger picture for MFCs, as it intends to inform about the possibility of this technology implementation in the future through the integration of them with other systems. The eight focus on the challenges and perspectives for MFCs.

The third chapter presents the experimental work, focus on methodologies, characterization techniques used, and procedures for the system operation. Therefore, it is a chapter containing graphics and tables with subsequent discussion of the content provided. Experimental conclusions at the end.

The fourth chapter presents the considerations of this technology from the author perspective.

2

Microbial Fuel Cell Technology

2.1 - Birth of Electrochemistry

In the 21th century scientist exposed the mysteries of the physical world contributing to significant advances and knowledge of the universe. To date, electricity, magnetism, gravity, fluids, optics, acoustics, kinetics, among others, were understood, X ray, atoms, molecules, electrons, radioactivity, boson of highs, were discovered and the Ohm, the Watt, the Kelvin, the Joule, the Amp, the Volt were invented. Theoretical and practical frameworks composed the Electromagnetic Field Theory of Light, Richter's Law of Reciprocal Proportions, Charles`s Law of Gases, the Valence Concept, the Law of Mass Actions, the Laws of Thermodynamics, the Planks Law, Theory of Electrolyte Dissociation, and the list goes on [36]. A contributor for these understandings was Alessandro Volta that in the beginning of the 19th century developed an electrochemical cell, named Volta Pile, made by two different metals (copper and zinc) emerged in an aqueous salt solution, experiments with this electrochemical cell introduced the terms "electric current" and "electromotive force" [37]. Further, Sir Humphry Davy at the Royal Institution in London related chemical and electrical effects on the Volta Pile and that was the genesis of electrochemistry. Michael Faraday in 1834 empowered the nomenclature that is still used today [37], Faraday also defined electrode (anode or cathode) as a solid substance providing electrochemical reactions and electrolyte as a chemical compound that provides electrical conduction among the electrodes, as show in Figure 2 [38].

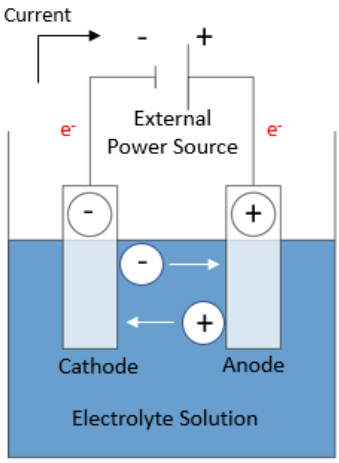

Figure 2: Electrolytic Cell; Adapted from [37].

2.1.1 - Fuel Cell Electrochemical Technology

Fuel Cells (FCs) are electrochemical devices that convert chemical energy of fuels into electrical energy directly operating in the reverse manner to an electrolysis cell. The anode of the electrolysis cell plays as the cathode (positive electrode) and the cathode as the anode (negative electrode) (Figure 3) [39].

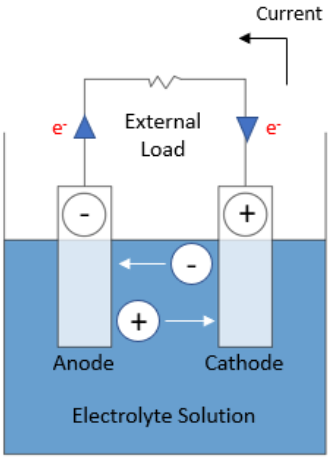

Figure 3: Fuel Cell; Adapted from [37].

FCs can process a wide variety of fuels and oxidants being the oxygen the most common oxidant due to is availability in the air and sustainability [40]. Table 3 presents six principal types of FCs [37]. These FCs share the same problems that lead to lower their performances: (1) the slow reaction rates, particularly at the cathode, reducing current and power output and (2) limited availability of hydrogen [37].

Table 3: Description of the main FC types [37].

Fuel Cell Type	Mobile Ion	Operating Temperature (ºC)	Fuel
Alkaline (AFC)	OH^-	50-200	H_2
Proton-exchange membrane (PEMFC)	H^+	30-100+	H_2
Direct methanol (DMFC)	H^+	20-90	Methanol
Phosphoric acid (PAFC)	H^+	~220	H_2 (low S, low CO, tolerant to CO_2)
Molten carbonate (MCFC)	CO_3^{2-}	~650	H_2, various hydrocarbons fuels (no S)
Solid Oxide (SOFC)	O^{2-}	500-1000	Impure H_2, variety of hydrocarbons fuels

In a FC, the fuel is oxidized at the anode and the oxidant is reduced at the cathode [41]. The reactions incite an electric current flow that performs work on the load [42]. The principle of operation of a hydrogen FC (PEMFC) is shown on Figure 4.

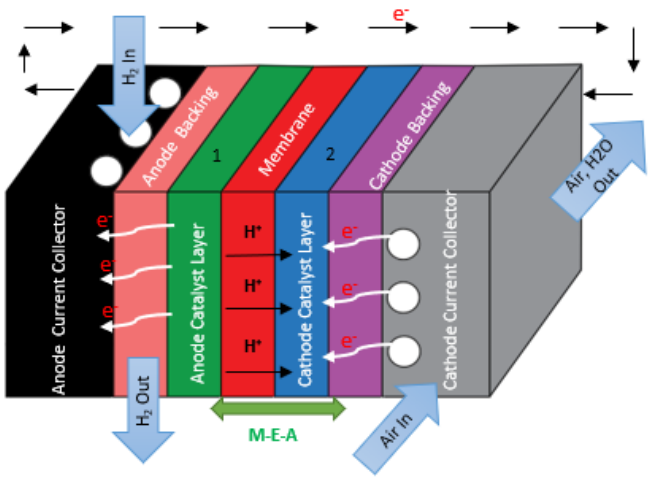

Figure 4: Principle of operation of a FC; M-E-A refers to membrane electrode assembly; Adapted from [43].

The nature of the electrolyte is a crucial factor on the FC performance. The electrolyte must allow proton transfer exclusivity, letting the electrons flow to the external circuit preventing the occurrence of short circuit [44]. The equations 1-3 demonstrate the reactions of a FC with an acid electrolyte, the system used by Grove known as "The Father of the Fuel Cell" [45]. At the anode, hydrogen is oxidized, generating electrons and H^+ ions (protons) are generated and energy in the form of heat that is released:

$$2H_2 \rightarrow 4H^+ + 4e^- \quad (1)$$

At the cathode, oxygen reacts with the electrons and protons, to form water:

$$O_2 + 4e^- + 4H^+ \rightarrow 2H_2O \quad (2)$$

Thus, the overall reaction is,

$$2H_2 + O_2 \rightarrow 2H_2O + heat \quad (3)$$

The stoichiometry of the reaction reveals that two hydrogen molecules are needed for one oxygen molecule.

The chemical reaction of the oxidation of hydrogen at the negative electrode requires first the use of some energy to excite the atoms or molecules, when the "activation energy" is supplied the reaction can proceed (Figure 5). The energy is found in the form of heat, electromagnetic radiation or electrical energy. The change in the enthalpy will be negative, as the total energy of the products is less than the total energy of the reactants. As mentioned above one of the problems of a FC is its slow reaction rates, when an atom or molecule hold low energy the reaction proceed slowly, to act on this hassle three main paths are adopted (1) use catalysts, (2) raise the temperature and (3) increase the electrode area [37].

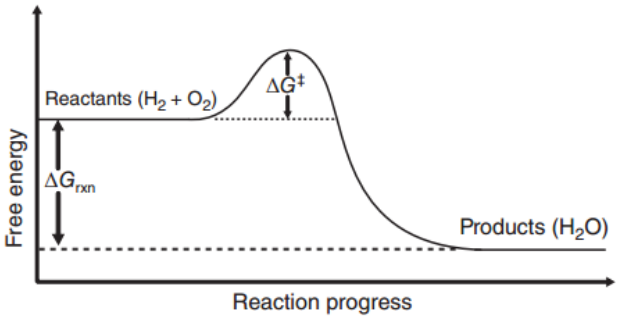

Figure 5: Energy level diagram for a simple exothermic chemical reaction; ΔG‡ - Activation energy barrier; Adapted from [45]

The evaluation of FCs systems requires standardized performance indicators such as the current density (current per unit area) (mA/cm^2), the specific power (kW/kg^1) and volumetric power (kW/m^3) [46]. Polarization curves allow a rapid comparison among FCs behaviour by showing the voltage output for a given current [47]. Figure 6 a shows typical polarization curve of a FC.

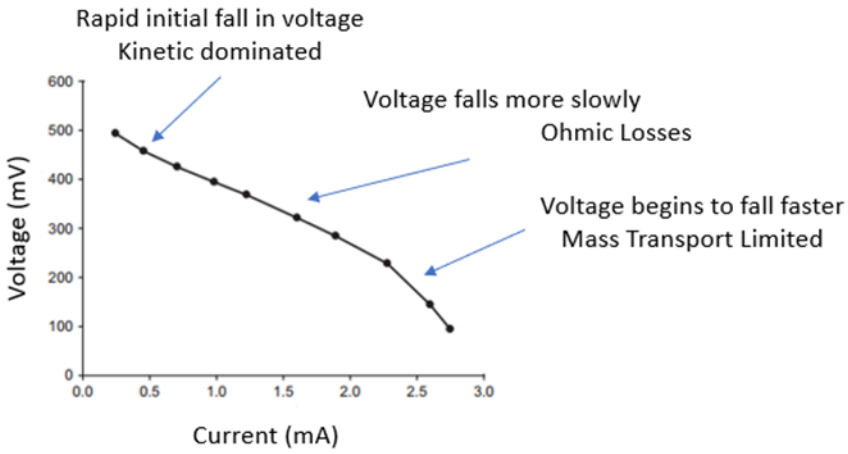

Figure 6: Typical polarization curve of a FC; Adapted from [49].

As seen in the figure a typical FC polarization curve show three distinct regions [47], [48], [49], [50].:

(1) Activation polarization: Predominant at low current densities. This represents the slowness of the oxidation and reduction reactions. The first voltage slope is related with phenomena's involving adsorption or desorption of reactant species, electrons trasnfer and the nature of the electrode surface. Factors associated to these losses are related to the electrode surface area and operating temperature.

(2) Ohmic polarization: Predominant at intermediate current densities. The FC voltage drops linearly with current by predominant ohmic losses. All the individual FC components have an associated resistance provoking the resistance to the ions and electrons flow. High electrode spacing, lower solution conductivity and fuel cell assembly contribute to these losses;

(3) Concentration polarization: Predominant at high current densities. A pronounced drop is observed as the result of an insufficient species mass transport determined by diffusion processes of the reactants to the electrode surfaces. The nature of the reactants, and its concentration, the products removal and the nature of the anode are factors associated with these losses.

The FC performance is also affected by other important losses. In fact, the real open circuit voltage is always inferior than the theoretical reference value. Electric short circuit can happen, as the electrolyte presents electrical conductivity and the crossover of the reactants thought the electrolyte can present undesirable permeability the other electrode [43].

2.1.2 - Microbial Electrochemical Technologies

The discovery of electrical effects through biological catalysed reactions was reported by Luigi Galvani in 1789 [51]. In 1910, Potter [52] observed the ability of *Escherichia coli* to produce electricity and show that bacteria are able to transport electrons and electrically interact with their environment. The discovery led to different studies using microbes to produce electric potentials and the development of the microbial electrochemical technologies (METs) [53], [54].

The MET operating principle share similarities with FCs, since convert the chemical energy into electrical energy. However, the MET utilizes microorganisms in the process which requires a multidisciplinary knowledge in the fields of engineering, microbiology and electrochemistry [55]. METs are also able of using waste in solid, liquid, or gaseous state to produce a range of products in a sustainable way, having different classification and versatile applications (Figure 7). The METs can be classified in MFC to produce electricity and treat wastewaters, microbial electrolysis cell (MEC) to produce methane and hydrogen, microbial desalination cell (MDC) to separate ions and electrofermentation (EF) to improve bio-based product synthesis (Figure 7) [53], [56].

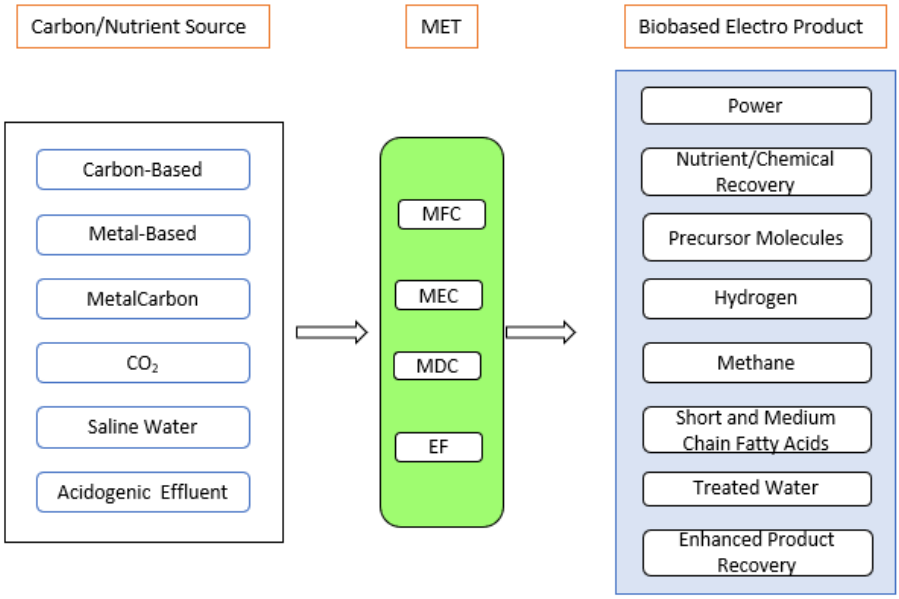

Figure 7: MET characteristics and applications; EF - Electrofermentation; MDC - Microbial Desalination Cell; MEC - Microbial Electrolysis Cell; MET - Microbial Electrochemical Technology; MFC - Microbial Fuel Cell; Adapted from [53].

2.2 - Electron transfer and conservation of energy

A MFC is a MET with many potential applications, such as electricity generation, wastewater treatment and have been analysed for application as biosensor [14], [57]. These systems facilitate the remediation of pollutants by converting the chemical energy presented in the organic matter directly into electricity as a by-product of anaerobic oxidation of biodegradable organic substrates [58]. A traditional MFC incorporates two electrodes, the anode and the cathode that may or may not be separated by a proton exchange membrane (PEM) [12], [59]. The anode is placed in an anaerobic chamber and the cathode is kept aerobic, opened to the air or emerged in a liquid solution [56]. In the anodic chamber microorganisms oxidize organic matter to CO_2 producing electrons and protons. Electrons are transferred to the anode surface and flow to the cathode through an external circuit. Simultaneously, protons diffuse through the membrane or simply diffuse to the cathode to get reduced by the arriving electrons and reacting with a final electron acceptor with high reducing potential, usually oxygen, but can be potassium ferrocyanide, potassium dichromate, among others to produce water, and complete the circuit [12], [43], [56]. Figure 8 displays a schematic illustration of a single-chamber MFC, formed by an anodic chamber, a membrane (PEM) and a cathode using oxygen as final electron acceptor

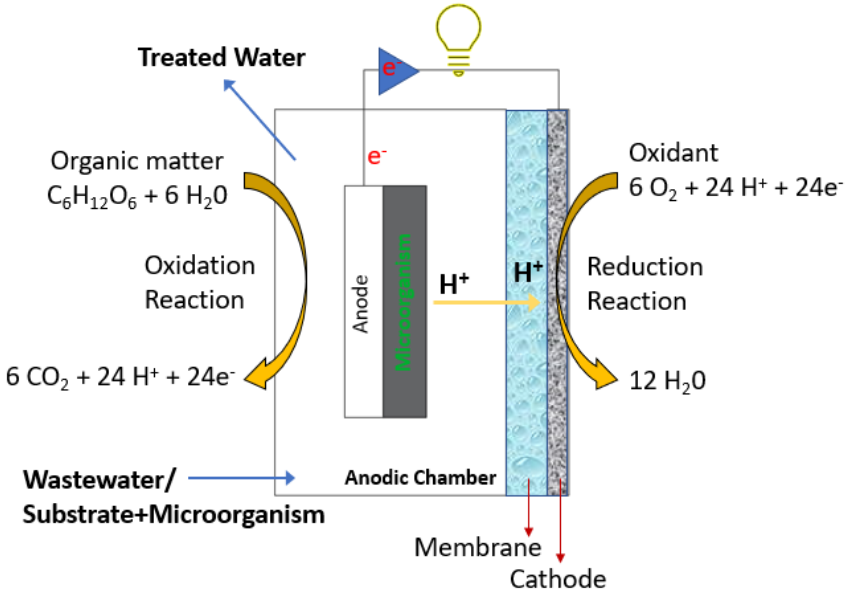

Figure 8: Schematic illustration of a Single Chamber MFC with glucose oxidation reaction at the anode (left) and oxygen reduction reaction at the cathode (right); Adapted from [60], [61].

Fermentative activity of yeast and bacteria generates current, to ensure this principle simple experiments on galvanic cells with yeast in glucose medium, or bacteria (*bacillus spp.*) in nutrient medium were conducted, both generating electromotive force (EMF) what confirmed the principle [62].

Microorganisms capture energy by transferring electrons derived from a donor substrate to the anode [62]. The electron transfer depends on the redox potential between the electron donor and the final acceptor, electrons flow from the lower reduction potential to the higher reduction potential [63] [64]. Standard reduction potential and the respiratory chain for *Paracoccus denitrificans* is displayed on Figure 9, the green arrow reveals the energy consumption for the flow of electrons of this bacteria, between NADH and cytochrome c. *P. denitirifcans* must capture this energy in order to overpass the intracellular and extracellular losses, that involve energy retained in the electrolyte as residual electron donors, biomass synthesis, microbial metabolism, activation potentials, internal resistance and diffusion limitations, the blue arrow represents the electrical energy production, this is the energy that could be recovered in the MFC [49], [65]. The compounds with positive standard reduction potential act as strong oxidizing and will have the tendency to accept more electrons while its conjugate reductant is a weak electron donor [49].

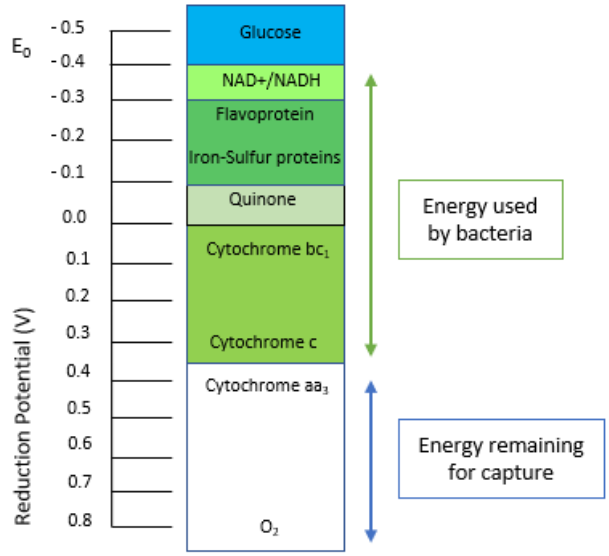

Figure 9: Standard potentials and respiratory-chain for Paracoccus denitrificans; Adapted from [49].

Electroactive bacteria (EAB) or equally referred as exoelectrogens, electrogens, electricegens, exoelectrogenic or anode respiring bacteria are microorganisms with the ability to conserve energy from electron transfer to an electrode [66]. The majority of EAB are anaerobic or facultative anaerobic and form a biofilm at the anode surface [67]. The release electrons are transferred to outer membrane proteins (OMPs) via specific diffusible intracellular electron structures such as nicotinamide adenine dinucleotide (NAD), flavin adenine dinucleotide (FAD), and from the OMPs to the anode electrode via extracellular electron transfer (EET) (Figure 10) [62]. EET occurs by two main mechanisms: direct extracellular electron transfer (DEET) and mediated extracellular electron transfer (MEET) [66], [68]. The two mechanisms relay on electrical conduction, but the potential gradient and related parameters are different like the concentration of extracellular co-factors and conductivity of nanowires or the co-factors [62]. The

ability and efficiency of the EAB to exchange electrons with an electrode and link the EET to its cellular carbon metabolism influences the current production in a MFC [54].

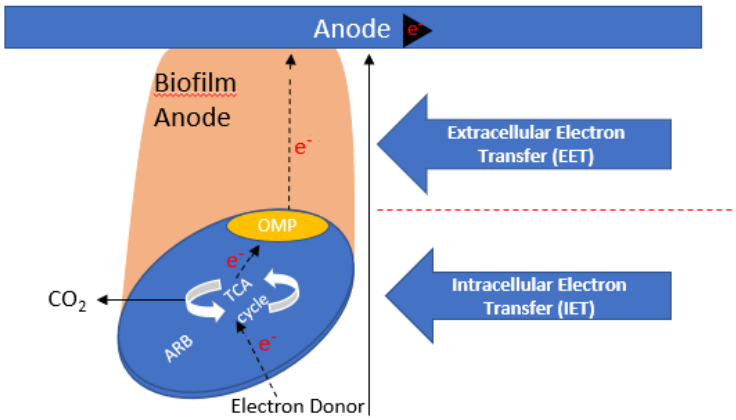

Figure 10: Schematic representation of electron transport in biofilm anode; ARB – Anode respiring bacteria; TCA – Citric Acid Cycle; Adapted from [62].

EET requires physical contact of the OMPs with electrode or via mediators, however this will lead to low current densities (<10 A/m^2) due to diffusion limitations of mediators and limited surface area for the direct contact [62]. Some microbial species present nanowires or pili useful to reach distant insoluble electron acceptors or to interconnect inner layers in the biofilm, allowing that not only the first monolayer of EAB at the anode surface is electrochemically active (Figure 11). Another DEET in some species is among microorganism cells: direct interspecies electron transfer (DIET) [62], [66], [69].

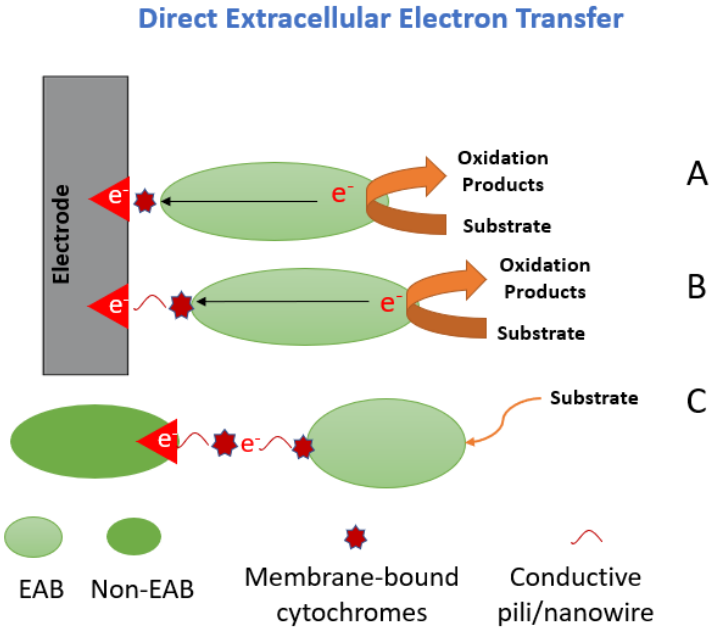

Figure 11: Simplified representation of direct extracellular electrons transfer. A) Cell membrane-bound cytochromes. B) Electrically conductive pili/nanowire. C) Direct Interspecies Electron Transfer (DIET); Adapted from [69], [66].

In alternative to DEET, electrons can be transported to the anode by successive oxidation-reduction reactions among nanowire-bound or biofilm-bound extracellular redox cofactors [62] [66], [70].

Mediated electron transfer is facilitated by either adding artificial mediator compounds (such as dyes and metalorganics) or by the inherent capability of a microorganism in secreting the compounds that act as redox carriers. In the oxidized form mediators can collect electrons either from inside the bacteria cell or form their outer membrane, becoming reduced and oxidized after transferring electrons to a final electron acceptor [71].

The transport of electrons from the cells in the biofilm to the anode can be linked to an hop between redox cofactors which turns up to a diffusion of electrons from areas of high to low concentrations [72]. MEET process can occur through the anodic reduction of primary metabolites derived from fermentation and anaerobic respiration processes or by secondary metabolites (Figure 12).

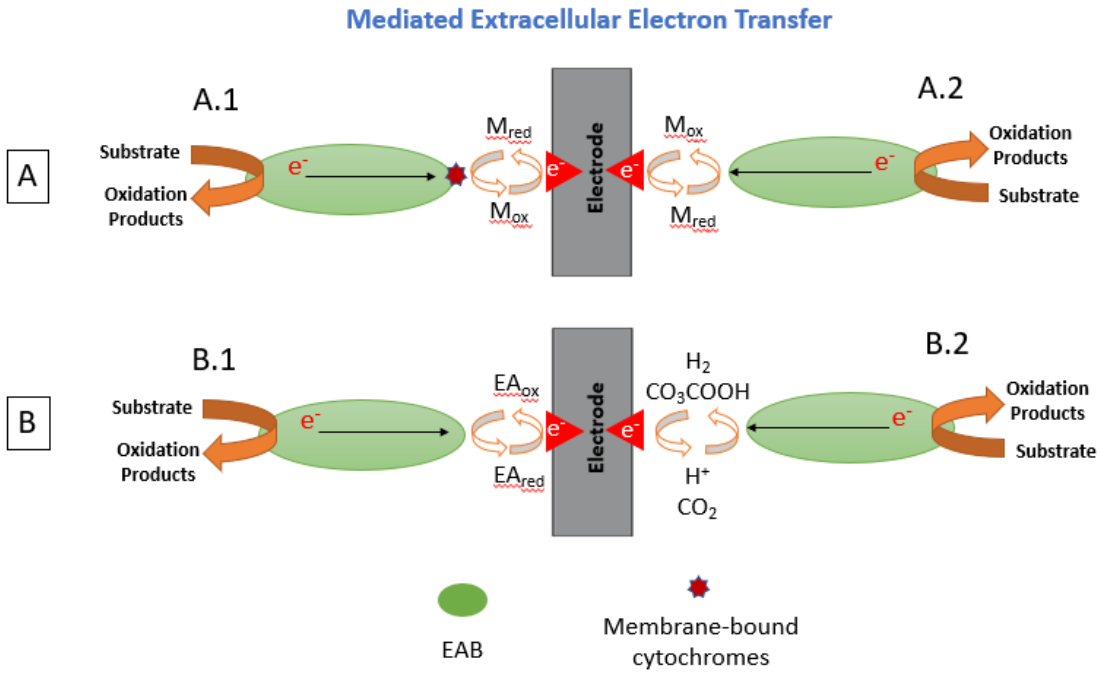

Figure 12: Simplified representation of mediated extracellular electron transfer (MEET). A - by secondary metabolites, A1) by outer cell-membrane cytochromes and e-shuttles, and A2) by self-produced or external redox mediators. B - by primary metabolites; B1) by reduced terminal electron acceptors (EA) and B2) by oxidation or reduced fermentation products; Adapted from [69], [66].

2.3 - Electrochemical Principles and Characterization

The breakdown of organic matter to produce electricity in an MFC is a dynamic and multifaceted process. MFC performance is influenced by physical, physiochemical and bioelectrochemical

processes and reactions such as the substrate degradation rate, activation losses, electron transfer rate, circuit resistance, mass transfer losses, electrode nature, external operation conditions, and inoculum type [73], [74].

MFC power density increased from 0.00-0.01 mW/m^2 in 1999 to 2000-3000 mW/m^2 in 2012 [73]. This increase was followed by and uniformization of important MFCs parameters, as power density and voltage to give a better comparation of the systems performance between different studies and researchers [73].

From a thermodynamic point of view the theoretical potential of an electrode is calculated, as the reference potentials of the components of the reaction or the Gibbs free energy of the reaction, given by (eq.4) [75]. The Gibbs free energy of a reaction measures the maximum amount of useful work that can be obtained from a reaction of a thermodynamic system [49].

$$U^0 = \frac{-\Delta G^0}{nF} \tag{4}$$

Where G° changes of Gibbs free energy (J) under standard conditions usually defined as 298.15K, 1 bar pressure and 1M concentration for all species, n is the number of electrons per mol, F the Faraday constant (96 486 C/mol),

The theoretical potential at nonstandard conditions is given with the combination of Nernst equation and reaction quotient (II), given by (eq.5),

$$U = \frac{-\Delta G^0}{nF} - \frac{-RT}{nF} \ln (II) \tag{5}$$

Where R (8.3144 J/mol.K) is the universal constant, T(K) is the absolute temperature and II (unitless) is the reaction quotient calculated as activities of the products divided by those of reactants.

For MFC calculation, it is more adequate to calculate the theorical cell voltage or electromotive force (emf) of the overall reaction, (eq.6) determines if the system is capable of electricity generation [49].

$$\Delta Ucell^0 = \Delta U^\circ_{cathode} - \Delta U^\circ_{anode} = \frac{-\Delta G^0}{nF} \tag{6}$$

In an MFC, the Gibbs free energy of the reaction is negative. Therefore, the cell voltage is positive, indicating the potential for spontaneous electricity generation from the reaction [9].

Power output is an essential key to evaluate MFC performance, that can be calculated by, (eq.7),

$$P_{out} = IU_{cell} \quad (7)$$

Power is calculated by measuring voltage and current. Voltage is frequently measured across a fixed external resistor (R_{ext}) while the current is calculated from Ohm's Law as $I=U_{cell}/R_{ext}$, the direct measured of the electric power comes, (eq.8), [76],

$$P_w = \frac{U_{cell}^2}{R_{ext}} \quad (8)$$

The power output is usually normalized to the projected anode surface, allowing the measure of the power density (mW/m^2) [77]. Power density refers to power per specific electrode or membrane areas [73].

$$P = \frac{U_{cell}^2}{A_{An}R_{ext}} \quad (9)$$

Polarization curves and power curves represent a powerful tool for MFC performance since they express the cell voltage and power density as a function of the current density [56]. Additional information is provided on chapter 2.5.1.1.

Coulombic efficiency (CE) is another parameter to evaluate the performance of MFCs, that indicates the extent to which the produced electrons end up in the desired product, this is a ratio of charge of microbial fuel cells output conducted from the substrate to the anode, (equation 10), [56], [73].

$$CE\ (\%) = \frac{M\int_0^t Idt}{FBV_{An}\Delta COD} * 100 \quad (10)$$

Where M =32 is the molecular weight of the oxygen, b = 4 is the number of electrons exchanged per mole of oxygen and V_{An} the liquid volume (L) in the anode compartment, ΔCOD is the change in COD over time (t). F is faraday constant.

The CE is negatively affected by competitive processes such as the microbial growth, the utilization of alternate electron acceptors by microorganisms and the design configurations such as membrane material and area, distance between anode and cathode, among others [73], [76], [78].

A really important factor relating the performance of the MFC and capacity to produce electricity is the energy efficiency (ε_E) that describes the energy recovery for power production and the theoretical energy release of the MFC, by the ratio of power produced by the cell over time (t) to the heat of combustion of the organic substrate (eq. 11) [76], [78].

$$\varepsilon_E = \frac{\int_0^t U_{cell} I dt}{\Delta H m_{added}} \quad (11)$$

Where ΔH is the heat of combustion (J/mol), m_{added} is the amount (mol) of substrate added.

In MFCs ε_E range from 2% to 50% or more if easily biodegradable substrates are use [76].

Many operational parameters affect power generation, (Table 4) summarizes some of them.

Table 4: Summary of the main parameters that influence MFC performance.

Parameter	Comment	Reference
Temperature	Affect system kinetics and mass transfer (activation energy, mass transfer coefficient, and conductivity), thermodynamic (free Gibbs energy and electrode potentials), nature and distribution of the microbial community (optimal temperature for different species), biofilm formation, ohmic resistance.	[50]
pH	Affect microbial activity, concentration of ions, membrane potential, proton-motive force, and biofilm formation. pH gradient between anode and cathode is one of the main causes for the sink of voltage efficiency in microbial systems, since pH interfere in chemical reactions, in the microbial physiology, in solution conductivity, among others.	[50]
Organic Loading Rate (OLR) & Sludge Loading Rate (SLR)	MFC should be operated at an optimum SLR or OLR for better organic matter removal and power production, SLR and OLR applied will have relation with the substrate conversion rate and consequently with the performance of the MFC.	[50]
Feed-rate and shear-stress	Affect behaviour of biofilm and have relation with hydrodynamic challenges (flow rate) In continuous mode an increase on the flow rate leads to an increase of the power output, although COD removal and CE decreases. High shear enrichment can be used to obtain better performing anodic microbial consortia.	[50]
Biofilm biomass concentration	Active biofilm has a direct impact on biocatalytic activity.	[73]
Growth yield	Cell growth will reduce CE due to diversion of electron into the biomass. Low biomass production in MFC is an attractive benefit related with less sludge formation.	[76]

Oxygen reduction rate (ORR)	Improving ORR enhance the power density. Electro-catalysts or electrode materials that exhibit good electrochemical properties must be used.	[79]
Ion conductivity	Represents the degree of permeability of ions through the membrane. It is a measurement of resistivity of the proton-conductive membrane against the flow of current.	[61]

MFC improvement is limited by the higher internal resistance, R_{int}, to the flow of current during the MFC operation. The R_{int} account three different resistances that are responsible for the losses that occur during the polarization curves (Figure 6). An estimation of R_{int} can be given by the sum of charge transfer resistance (activation resistance), R_{act}, ohmic resistance, R_{Ω}, and diffusion resistance (concentration/mass transfer), R_{conc}, all this resistances are estimated [80], [81]. The quantification and contribution of the different resistance must be estimated to better understand the MFC system. Further information is provided in chapter 2.5.

Microbial interaction with the electrode surface plays a key role in MFC performance. In fact, electrochemical behaviour of a MFC is linked on how well the microbial cells interact with the electrode/anode surface [82]. The inefficient electron transfer and the decline of the electrode electrochemical properties is observed over time caused by three main phenomena: excessive growth of biofilm, biofouling and membrane blockage and catalyst inactivation, Figure 13 [65].

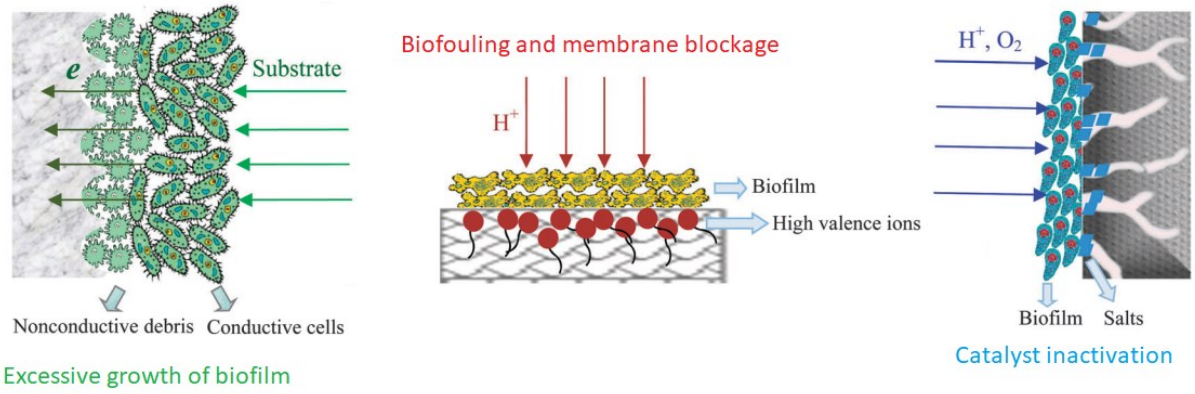

Figure 13: Schematic illustration of ways in which performance of MFC is degraded by microbial/electrode interaction [65].

Biofouling leads to a reduction of available surface area to the flow of protons and consequently reduction of current generation. Catalyst inactivation or excessive biofilm growth results in production of non-conductive residues such as dead cells, isolating the electrochemically active biofilm from the electrode surface, reducing the surface area to the flow of electrons decreasing current generation [79].

2.4 - Configuration Parameters

The MFC configuration parameters play an important role on its energy production. Several studies conclude that the MFC electrical generation and stability is affected by the activity of microorganism, nutrients availability, temperature, pH, cell configuration, electrodes, etc [12], [50], [78] .

2.4.1 - Substrates

Substrates influence the performance of the microorganisms on the anode surface. Synthetic wastewaters used in MFCs for microbial oxidation in the anode are mainly composed of acetate, glucose, sucrose and xylose [83]. Electricity can be generated from any biodegradable material, including pure compounds (mentioned above) and complex mixtures of organic matter, such as domestic wastewater, animal manure, food processing wastewater, among others [84]. Figure 14 displays the substrates (wastewater) used in MFCs dividing it in simple or defined substrate and complex or undefined substrate.

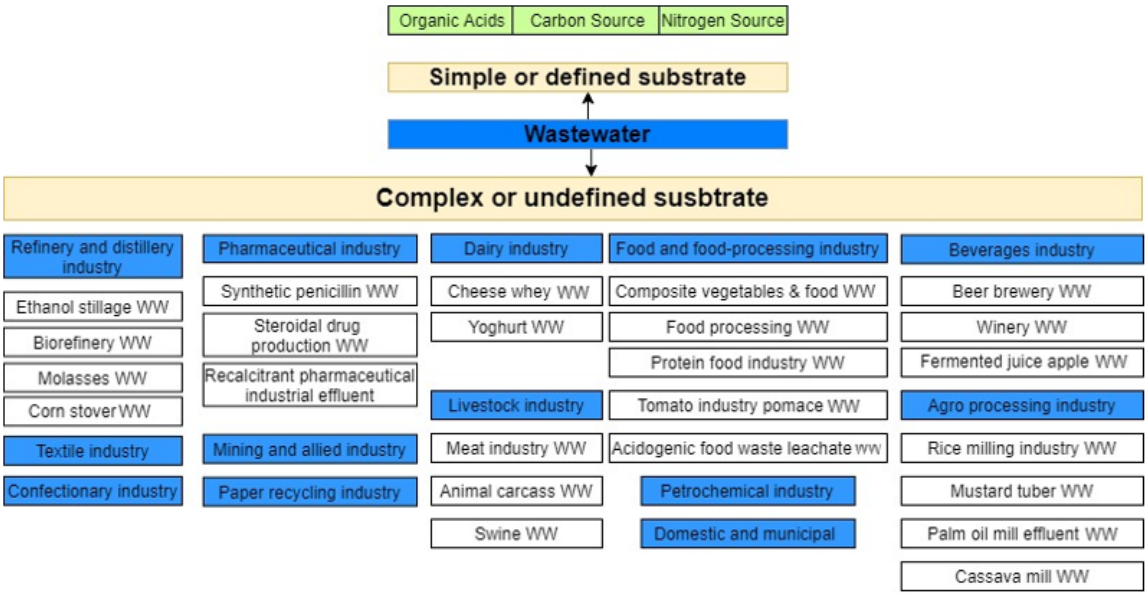

Figure 14: Type of substrates (wastewater) used in MFC; Adapted from [85], [86].

Acetate (carbon source) is the most used substrate in MFCs since induces the growth of EAB [87]. For new studies on components, reactor designs, or operational conditions, acetate-based substrate is used along with pure culture as inoculum to avoid fermentation and simplify the anodic reaction, replicability of studies turns to be easier [74]. Furthermore, MFCs with acetate

as substrate produce higher power densities compared to glucose (also commonly used as carbon source) [86].

Lignocellulosic biomass such as agricultural residues and woody biomass are promising feedstocks for energy cost-effective production because of their readily availability and abundance [86] However, this biomass cannot be directly used by microorganisms, being necessary to convert it to monosaccharides or low-molecular-weight compounds before their use in MFCs [85]. Cellulose and chitin are cheap and readily available biopolymeric materials that can be used for electricity generation as well. In MFCs direct conversion of cellulose into electricity must be conducted in the anode while the produced metabolites must be used as electron acceptors [85].

Additional information about complex substrates is given in the chapter 2.5

2.4.2 - Microorganisms

The microbial activity has the potential to generate electrons and protons enabling current production on MFCs. Thus, electron transfer mechanisms play a crucial role in maximizing the performance of microbe-electrode interaction [88]. The composition of the microbial community is not the most important factor to achieve high power densities on MFCs, although it is important to understand the dynamic between electroactive microorganisms and electrodes as they work as electrode-reducing and electrode-oxidizing microorganisms [84], [89].

Geobacter sulfurreducens and *Shewanella oneidensis* are identified as EAB models. However, analysis on communities showed a wide range of different bacteria that can persist in anodic biofilms and generate power [84]. Around 35 pure cultures including the two mentioned above, *Pseudomonas aeruginosa*, *Rhodoferax*, *Cupriavidus basilensis*, *Lactococcus lactis*, four of five classes of Proteobacteria, Firmicutes, Acidobacteria phyla, among others were capable to produce current in MFC [12], [88].

G. sulfurreducens and *S. oneidensis* belong to gram-negative bacteria, using nanowires and MtrAB (protein complex composed of cytochrome) as EET pathways respectively [89]. In gram-positive bacteria, the outer membrane is absent, the cell outer wall acts as barrier between the cell and the mineral surface. Different gram-positive were identified in electrogenic consortiums but no EET mechanism was defined until recent studies, for example Wrighton et. al, [90] with a *Thermincola potens* strain achieved a columbic efficiency of 91% when acetate was used as substrate using direct EET to transport electron to the electrode [89].

Yeasts are utilized for centuries in large biotechnological processes of the food industry, generating huge amounts of wastewaters rich on organic matter. Based on the point that yeast is used in production they could also be used as biocatalysts instead of using other microbial species [91]. This Eukaryotic organism have some characteristics suitable to MFCs: yeasts are easy to handle, easy to cultivate, can growth in different substrates and in different aerobic and anaerobic environmental conditions [89]. Yeast contains different natural electron mediators, such as azurin, ferredoxin and cytochromes, that are used by redox enzymes to transfer electrons from the cell to the anode surface, thus, a significantly amount of proteins in the yeast cell membrane is an important quality of electroactive species [92]. Yeast species like *Candida melibiosica*, *Arxula adeninivorans*, *S. cerevisiae, Pichia anomala*, were used in MFC and succeed in obtaining power production [88], [89].

At the same level of importance of the microbial species to the MFCs performance are the use of pure or complex cultures. Pure cultures have high electron transfer efficiencies, although present some limitations concerning its growth and energy transfer rates, need a specific substrate and present a continuous risk of contamination by unwanted microbes [12]. Sludge, wastewater, and marine sediments (complex cultures) provide inoculums rich in microbes which facilitate the use of different substrates or conversion of complex organics compounds to simpler compounds such as acetate, that can be used as electron donor for energy production [14], [85].

Microalgae *Tetraselmis gacilis*, *Mougeotia*, *Scenedesmus*, *Chlorella vulgaris* and mixed culture have been exploited by several researchers for electricity generation. Microalgae represent a duo interest in MFC, since in the cathode chamber can be used for supplying oxygen and in the anode as substrate for the multiplication of bacteria, as electrode donor, and to remove organic matter [9], [93].

Figure 15 displays the microorganisms used on MFCs and its EET. As shown in this Figure the EET of bacteria is by outer membrane cytochromes, nanowires, and endogenous mediators, while algae and yeast EET is by direct mediated electron transport [53].

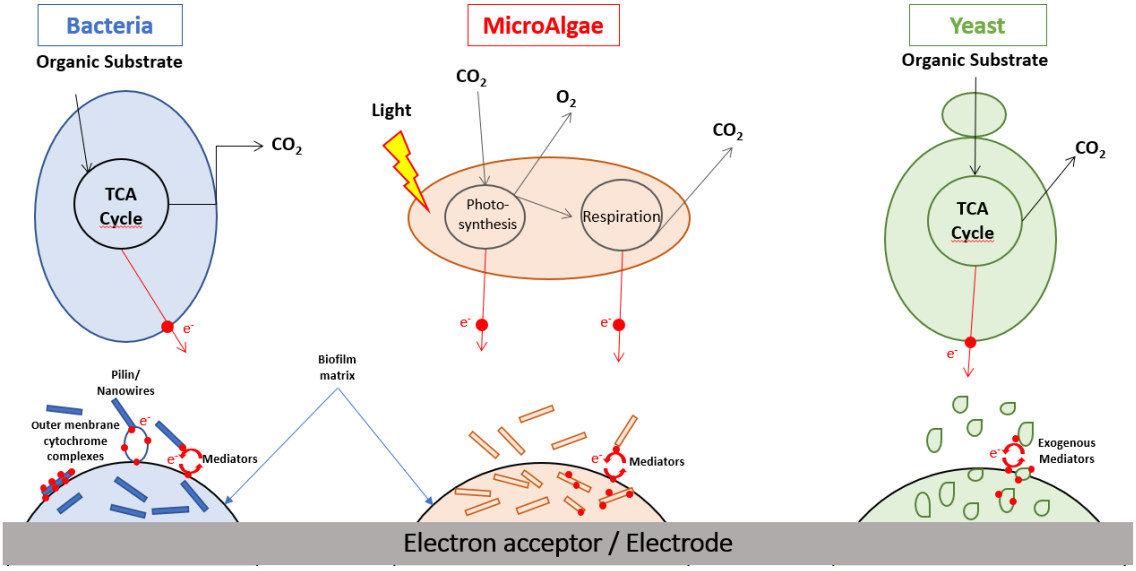

Figure 15: EET of bacteria, microalgae, and yeasts; Adapted from [46].

2.4.3 - Reactor Design

To achieve better cell performances, evaluated by its energy output and wastewater treatment ability, several studies were conducted to find the best configuration. Typically, MFC reactors are classified by the number of compartments, either single chamber MFC (SCMFC) or dual chamber MFC (DCMFC) [71]. At the beginning of the MFC research DCMFC were the most commonly used design, however they are being replaced by SCMFC due to an enhancement of the cell overall performance [74]. Different designs lead to different volumes, electrode spacing, hydraulic flow, oxygen supply and membrane area [94].

2.4.3.1 - Dual chamber microbial fuel cell

A dual chamber microbial fuel cell (DCMFC) contains an anodic chamber and a cathode chamber connected by a separator that allows the ion flow from the anode to the cathode chamber (Figure 16). Several shapes were implemented, including concentric tubular, cuboid shape, simple H shaped, double chambered, operated in batch or continuous mode [95].

DCMFC design entails some difficulties such as large volume, complex design and high internal resistance [14] The distance between the electrodes is considerable leading to an increase of the cell internal resistance, on another way the proton diffusion through the membrane increases since this configuration limit substrate and oxygen crossover [94]. With this configuration was developed a dual chambered up-flow MFC trough introducing an interior cathode to achieve continuous treatment and improve performance, this represents a combination of a up-flow anaerobic sludge blacket system (UASB) and a MFC but besides advantages in contaminants

removal, power density and current are low due to aerobic microbe metabolism in the cathode chamber [16], [71].

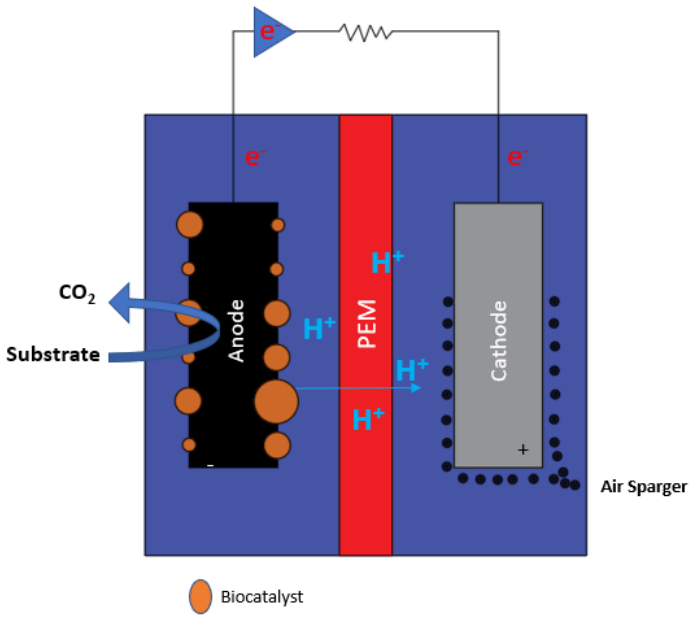

Figure 16: Schematic of DCMFC. PEM – proton exchange membrane; The biocatalyst is presented with different sizes to mimic mixed culture heterogeneity.

2.4.3.2 - Single chamber microbial fuel cell

A single chamber microbial fuel cell (SCMFC) contains only one chamber, the anodic chamber and the cathode is exposed to the air for a direct contact air-cathode (Figure 17) [95]. . A membrane can be included or not, but when is used it is designated as an electrode-membrane-assembly (MEA), composed by a membrane and a cathode catalyst and diffusion layer. This configuration has as advantages (1) no need of aeration, decreasing the energy requirements to operate and consequently the energy costs, (2) easy to handle due to a smaller volume (3) simpler operation as the recycling or chemical regeneration of the catholyte is not required, (4) short electrode distance, which decreases the internal resistances and consequently increases the power output [95], [96].

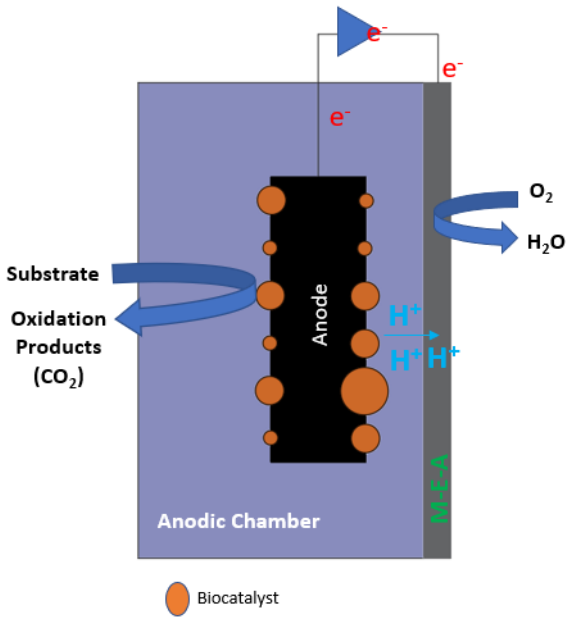

Figure 17: Schematic of SCMFC. MEA – membrane electrode assembly; The biocatalyst is presented with different sizes to mimic mixed culture heterogeneity

Several types of MFC were introduced in this configuration namely, simple Air-Cathode, single cylindrical Plexiglas chamber and tubular MFC [16].

2.4.3.3 - Stacked microbial fuel cell

Stacked MFCs can be constructed in series or parallel arrangements by electrically connecting single MFC units. The purpose is the application of this technology at large scale since generates higher power production, however are susceptible to tubing, pumping and wiring issues [16], [59], [93]. In parallel connection the current density and COD removal increases while maintain an average voltage, in series connections the voltage increase although it is a vulnerable arrangement to voltage reversal and consequently loss of bacterial activity [74], [97]. Aelterman et. al, [98] stacked six MFC units with a work volume of 60 mL (360 mL total) achieving almost a power output of 250 000 mW/m^3, it's possible to infer that this value of power output stands out.

2.4.4 - Anode

The anode material composition, morphology and surface proprieties have a clearly influence on the biofilm formation and attachment to its surface, electron transfer rate, substrate oxidation and electrochemical efficiency of a MFC [96], [99]. Therefore, they must fulfil certain requirements (1) good electrical conductivity and low resistance; (2) strong biocompatibility; (3) chemical stability and anti-corrosion; (4) large surface area; (5) appropriate mechanical strength and toughness [14], [99]. Table 5 presents materials and configurations, and comments.

Table 5: Description of the most common anode materials and configurations used in MFCs; Adapted from [99].

Anode Material	Comment	Type	Configuration	Comment
Carbon	Frequently used due to: - Chemical stability - High conductivity - High specific surface-area - Good biocompatibility - Relatively low cost	Carbon paper Carbon cloth Graphite plate Carbon mesh Activated carbon cloth	Plane	Main limitation is related to the electrocatalytic activity because the pores became clogged by the biofilm development and lose efficiency.
		Granular graphite Graphite felt Carbon felt Granular activated carbon Reticulated vitreous carbon	Packed	
		Carbon brush	Brush	Ideal electrode with high surface area, high porosities and efficient current collection.
Metals	Used due to a higher conductivity than the carbon materials. Noncorrosive requirements limit the availability. The plane surface presents poor adhesion by EAB	Stainless steel plate	Plane	Good mechanical properties expected for long-time operation; Can be suitable to scale-up applications compared with carbon electrodes.
		Pt-coated titanium	Plane	Pt is required, increasing the cost.
		Noble Metals (e.g. Gold)	Plane	Reduce the internal resistance of the cell. Have high costs and a week bacteria adhesion. Good biocompatibility and higher conductivity. Not economically viable material.
Composite Materials	Composite of metal-carbon. Developed to enhance: - Electrical performance, - Specific surface area, - Electron transfer, - Biocompatibility,	Mn^{4+} - graphite anode aluminium-allow mesh composite carbon cloth electrode. Composite graphite/PTFE electrodes. Graphite paste with an incorporated Sb(V) complex. Integration with nanoparticles	Diverse, related with novel configurations	Required studies concerning the costs, long-term stability, and knowledge of the mechanism of interaction between the bacteria and electrode
Three-dimensional microporous based	Developed for increase the performance and maximize the volumetric power density. Limitations related to the low specific surface area, poor conductivity, or reduced pore size for bacteria penetration	Potentially useful 3D structures are: Carbon foam RVC Carbon brush Granular carbon	3D structures. 3D microporous-based anode.	Contribute to substrate transfer, open 3D space facilitates microbial growth.

The two-dimensional (plane) electrodes have limited the surface area contact with the EAB. In order to improve that, besides the choice of the material used, changing the structure to three-dimensional is a promising strategy. Carbon foam, carbon brush and granular carbon are good candidates [99].

Since the anode surface characteristics amplifies the bacterial adhesion and the electrical connection between the bacteria and the electrode surface, different methods for modification the anode surface using different materials have been reported [100]. These include (1) surface treatments with physical or chemical methods, (2) addition of highly conductive or electroactive coating, and (3) use of metal-graphite composite electrodes [101].

Surface treatment was studied with ammonia, acid, thermal treatment, and electrochemical oxidation [99]. Surface coating materials have included carbon nanotubes (CNTs), conductive polymers, mediators, metals, and composites of these materials, being the most common the CNTs due to an increase of the electron transfer rate and consequently a reduction of the cell internal resistance [101].

2.4.5 - Cathode

The majority of the anode materials can work also as cathodes. However, the anode and the cathode are exposed to different environments. The anode is emerged in a nutrient rich solution anchoring the biofilm and the cathode is frequently opened to air (air-cathode) or emerged in an aqueous solution (aqueous cathode), bringing different needs [14], [96]. The air-cathode frequently includes a conductive matrix, a diffusion layer and a catalyst/binder layer (Figure 18) [101].

The catalyst layer allows water diffusion toward the matrix and extend the interface reactions, with the benefit of lowering the cathodic activation overpotential and increase of the energy production [102], [103], [104]. The diffusion layer plays an important role in the cathodic reaction, as it facilitates the oxygen transfer to the catalyst layer while maintaining the integrity at a high-water pressure [96]. Without the diffusion layer the system is vulnerable to an excess oxygen diffusion and to a risk of water leakage due to exposure of the porous matrix [103].

Carbon cloth is the most used air-cathode and the binder is often perfluorosulfonic acid (Nafion) or polytetrafluoroethylene (PTFE). Nafion grants better results justified by the development of a biofilm thickness on the cathode greater than with a PTFE, thus avoid ohmic losses but can have a price 500x times higher than PTFE [96].

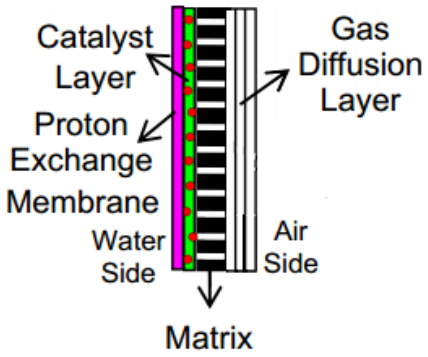

Figure 18: Schematic of an air-cathode structure; Gas diffusion layer contemplate the physical cathode; Adapted from [103].

The aqueous-cathodes are made of conductive supporting materials, such as carbon paper, carbon cloth, and Pt mesh, coated with a catalyst/binder layer, aqueous air-cathodes performance are limited by the low concentration of dissolved oxygen, require an energy source to operate increasing the operational costs, and lack in sustainability due to need of aeration [101], [105].

ORR turns out to be the most suitable cathode reaction. Oxygen is readily available in the air, has positive redox potential and generate higher power densities. The biggest limitation so far is the low solubility of oxygen in the electrolytes [106]. Generally, ORR is a slow reaction, so it is necessary to decrease the cathodic activation overpotential using of catalysts [99], [102] Pt and Pt-based materials have been applied as the most common precious metal catalysts due to the favourably low overpotential, although its higher price hinders its application [96], [102]. Pt catalyst can make up to 47% of the total capital cost of an air-cathode [106]. The first row of transition metals have been proposed as a solution to this problem, they are relatively cheap, offer good stability and do not affect the microbial activity of the cell, however these metals have lower catalytic activity toward the ORR than Pt [14], [96], [106]. Carbon nanofibers and activated carbon nanofibers have been applied as cathode catalysts since activated carbon is inexpensive and have a high surface area with good electrical conductivity [106], [107], [108].

Microorganism and/or enzymes can also substitute catalysts in the cathode by accepting electrons from the cathode to reduce the oxygen,

Summarized information on Figure 19 [107].

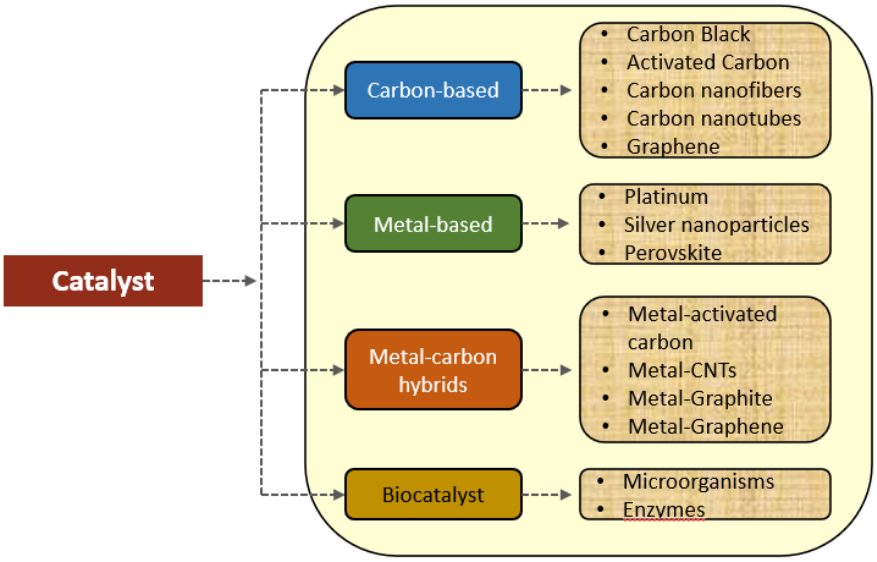

Figure 19: Schematic representation of various types of oxygen reduction reaction catalysts in MFCs; Adapted from [107].

Researchers found that the biocathodes have a low cost, good stability, high conductivity, biocompatibility and multiple functions and efficiency in WWT. Biocathodes are microbially catalysed and are an alternative to replacing expensive catalysts [94]. Biocathodes improve the overall sustainability of the technology by reducing environmental impact and cost footprint as can be a cost-effective solution for nutrient removal and waste degradation [83]. Biocathode electrodes are mainly composed of carbon-based materials, such as graphite fibber brush, graphite plate, carbon felt, granular graphite, and stainless-steel meshes, although the most suitable material for biocathodes is still unknown [101], [106]. Biocathodes have the ability to increase the spread of oxygen to the cathode and improve the oxygen reduction rate [109]. Biocathodes can be classified in two categories, (1) aerobic biocathodes where oxygen is used as electron acceptor, and (2) anaerobic biocathodes, where nitrates and sulphates are used as electron acceptor [110]. In biocathodes, both charge-transfer resistance and oxygen mass transfer are the major limiting factors for the performance of a MFC [111]. Clauwaert et. al, [112] stated a substantially viability and sustainability increase using biocathodes, since it ease the use of noble or non-noble catalyst for the oxygen reduction.

Table 6 displays a summary of the different cathode configurations. Large accessible surface areas and efficient current collection are essential to achieve high power densities [101].

Table 6: Cathode configurations, type, and comments [101], [106].

Configuration	Type	Comment
Plane Cathodes	Carbon cloth	More mechanical flexibility and is highly porous compared to carbon sheets.
	Carbon paper	Lack of durability and low specific area.
	Graphite sheets/ plates	Rough surface generates great power density compare to flat surface.
Tubular Cathodes	Tubular	Can increase surface area to volume ratio. One of the designs is the cloth cathode assembly (CCA). More studies need to be conducted.
Packed Cathodes	Carbon Cloth	Used to improve the available surface area. Low porosity, which may lead to fouling after prolonged operation. Granular bed electrodes need to be tightly packed together to maintain electrical conductivity, otherwise inactive or dead zones can appear after long term operation.
Brush Cathodes	Graphite Fibber	High surfaces areas and porosities that promote the microbial growth, a low ohmic resistance along with antifouling property improving the system efficiency. Usually attached to a noncorrosive and conductive titanium wire core.

2.4.6 - Membrane

Membrane is a very important component in FCs since physically separates the anode and the cathode and provides a selective transport of protons from the anode to the cathode. It also prevents the transport of oxygen from the aerated cathode to the anaerobic anode chamber, which is crucial in MFCs, otherwise microbial growth could be inhibited or aerobiosis occurs in detrimental to anaerobiosis [61], [113]. Therefore, a high ionic conductivity, high mechanical and chemical stability, low substrate crossover and no electronic conduction are desirable [60], [61]. Membrane fouling is also an issue (slightly addressed at sub-chapter 2.3) that can increase the capital costs and decrease system performance since limits the diffusion of protons and increase internal resistance [103], [114]. For wastewater treatment, a proper balance between the cost, durability and resistance is required towards an economically viable system. Based on that, a wide diversity of membranes and separators has been studied.

Ion exchange membranes (IEMs) are an important class of polymeric membranes and include the PEM or cation exchange membrane (CEM), the anion exchange membrane (AEM) and the bipolar membrane (BPM) [115], [116]. CEM such as Nafion, Hyflon, Zirfon and ULTREX have been used as the preferred separator for MFCs because they easily conduct protons towards the cathode [117]. Typically, problems associated these membranes include oxygen crossover,

substrate loss, cation transport, accumulation of other species than protons, such as K^+, NH_4^+, Ca^{2+}, Mg^{2+}, and biofouling [60], [61], [118]. Nafion is the most commonly used membrane due to its excellent ionic conductivity (10^{-2} S/cm), due to the negatively charged sulphonate groups (SO_3^-) presented on its structure that are responsible for a high level of proton conductivity but are very expensive and may lead to substrate crossover [61], [96], [115]. Thinner Nafion membranes, such as Nafion 112, have better performances, with higher power densities than thicker ones, Nafion 117 membranes, due to a lower ohmic resistance [117]. However, thinner membranes can lead to an increase of the oxygen permeability to the anode [117]. A higher transport rate of cations to the cathode than protons provokes a pH imbalance at the MFC that should be avoided [119]. AEM typically contain positive ionic groups and mobilize negatively charged anions [60]. RALEX a dominant AEM, improves the proton transfer due a decrease of the transfer of other cations and the pH splitting, by promoting the transport of OH^- to the anode, and provides better long-term stability. A big drawback of AEM is the substrate crossover, promoting biofouling at cathode surface and consequently reducing the MFC performance [117]. Both AEMs and CEMs have a lost on its performance after several operation cycles in a SCMFC, although AEM present a higher recovery rate after repressing (Figure 20) [117]. BPM contains both a CEM and a AEM, can efficiently conduct proton and hydroxide ion on the splitting of water interface of the membrane, the main concern is the pH gradient [61], [93].

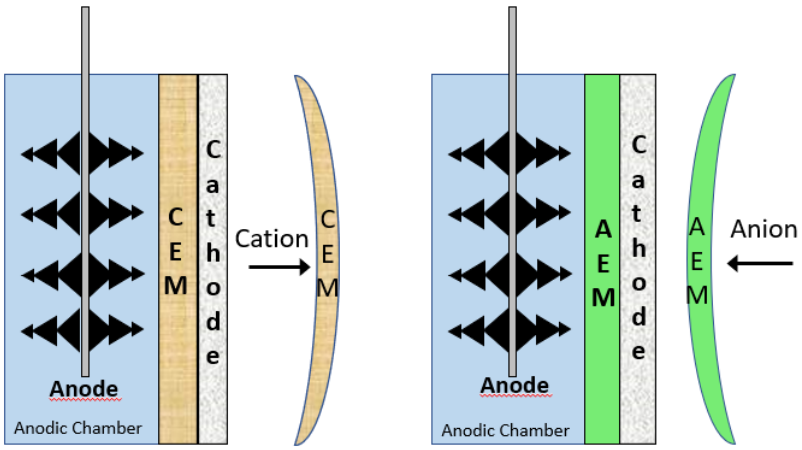

Figure 20: Deformation of CEM and EAM in SCMFC presented with a Carbon Brush anode; Adapted from [117].

Microporous separators which include nanofiltration, microfiltration and ultrafiltration membranes are able to transfer various species according to the pore size [115]. These membranes are widely used in wastewater treatment due to its good filtration performance, high durability and lower cost, increasing the interesting of its application in MFCs [60].

Some studies presented other materials as separators, like rubber, a natural material that remained intact after 500 days of work, ionic liquids (Ils), which are organic salts environmental-friendly

that are chemical and thermal stable in a wide temperatures range, and also provide high ion conductivity. Inclusion membranes (PIMs) based on ILs showed a good potential to replace Nafion membranes [96]. Glass fibre and ceramic have also been case of study [120]. Ceramic separators demonstrated similar results when compared with conventional IEM membranes, but present a considerably lower cost [79].

The use of a membrane electrode assembly (MEA) (Figure 17) in a MFC minimizes the electrodes distance and compacts the reactor design, reducing the internal resistance, which may lead to an increase on the power output [121]. The MEA also hinders the contact of the anode with the oxygen present at the cathode, which negatively affects the anode activity [122], [123].

Membraneless MFCs, which eliminate the use of a membrane, have also been studied. Some advantages are the lack of membrane biofouling, lower internal resistance and reduction of the operation costs [124]. Although, present high substrate and oxygen crossover rates, leading to lower performances and a lack of conductivity, given by the membrane [61] [124].

2.5 - Applications of MFC in Wastewater Treatment

Beyond the advantages in energy savings, MFCs also provide sludge reduction and the treatment of multiform, complex, recalcitrant and high strength wastewaters [53]. MFCs have demonstrated to be able to remove multi contaminants, such as biological wastes, organic compounds, heavy metals, polyalcohol, petroleum products, dyes and phenolic compounds of wastewater streams [16]. However, the removal efficiency of these components is very distinct maybe due to different MFC configurations and operating conditions, such as inoculum and substrate source and electrode materials. Table 7 presents a summary of MFCs performance on WWT based on different works reported in literature, using different wastewaters as organic substrate in the anode.

Table 7: Wastewater treatment using MFC, plus configuration, voltage, power density, inoculum, COD removal, and columbic efficiencies. AS – Anaerobic Sludge, CB – Carbon Brush, CC – Carbon Cloth, CCA – Cloth Cathode Assembly, CFB- Carbon Fibre Brush, DWTP – Domestic water treatment plant, DC- Dual Chamber, GAC – Granular Activated Carbon, GDAC - Gas Diffusion Air Cathode, GFA – Graphite Felt Anode SC - Single Chamber, MBRMFC – Membrane Bioreactor MFC, PBS – Phosphate Buffer Solution, Pt – platinum;

Configuration / Anode & Cathode	Wastewater/ Inoculum	Voltage (mV)	Power (density or volumetric)	COD removal (%) / CE (%)	
DCMFC	Alcohol	611	124 mW/m^2	88 / -	[86]
Ultrafiltration MFC / GFA Pt-coated Ti plate	Artificial/ Anaerobic Digested Sludge	-	53.5 W/m^2	90 / -	[12]
DCMFC packed with Activated Carbon / GAC packed bed & Graphite plate	Acrylic fiber/ Anaerobic Sludge	400	212W/m^3	-	[12]
DCMFC / Carbon felt & Carbon felt	Acidogenic food waste leachate	400	0.4W/m^3	>87 / -	[86]
DCMFC air -cathode	Agricultural	-	0.34 mW/m^2	84 / -	[16]
Up-Flow Anaerobic sludge blanker reactor MFC	Beet-Sugar	-	1402 mW/m^2	53 / -	[16]
Anaerobic baffled stacking microbial fuel cell (ABSMFC)	Beet-Sugar	-	115.5 mW/m^2	50-70 / -	[86]
SCMFC / Carbon brush & Carbon cloth	Biodiesel	470	2110 mW/m^2	90 / -	[86]
40 tubular SCMFC / Graphite & Ni-based paint, MnO_2 felt	Brewery	23000	4.1 W/m^3	87 / -	[12]
SCMFC	Brewery	-	0.03 W/m^2	90 / -	[16]
Continuous Flow DCMFC / aerated cathode	Brewery	-	0.023 W/m^2	91.7-95.7 / -	[96]
DCMFC / Carbon paper & Carbon cloth	Cheese Whey/ AS	-	46 mW/m^2	94 / 11	[86]
SCMFC/ Graphite coated Stainless steel mesh; CC with 0.5 mg/cm^2 Pt loading	Dairy/ AS from DWTP	810	20.2 W/m^3	91 / 26	[12]
SC non catalysed MFC	Dairy	-	-	95.4 / 4.24	[16]
SCMFC / Impregnated carbon based multiwalled nanotubues	Distillery	426	267 mW/m^2	-	[125]
SCMFC air cathode / Toray carbon paper & Carbon cloth Pt catalyst (0.5 mg/cm^2)	Domestic	230	494 mW/m^2	- / 12	[126]
SCMFC	Domestic	380	1.246 W/m^2	60/-	[96]
ML-MFC / Bioanode & Biocathode	DS and AS	595	0.03 W/m^2	>62.8 / max 58.1	[12]
DCMFC	Food		0.23 W/m^2	86 / -	[96]
Catalysts and mediatorless / Graphic Sheets & Graphic Sheets	Food processing/ AS	475	230 mW/m^2	86 / 21	[86]
SCMFC / Carbon-felt & Pt-deposited carbon	Fermented corn/ Anaerobic mixed consortia	-	1180 mW/m^2	- / 10	[86]
DCMFC / Graphite Granules	Hospital	670	167 W/m^3	78 / 12	[98]
SCMFC / Granular graphite & Pt 0.5 mg/cm^2	Landfill Leachate/ Enriched in Mn(IV)-reducing bacteria	-	45 mW/m^2	72 / 6.7	[127]
Air-Cathode MFC	Municipal	-	1.14 W/m^3	80 / -	[16]
Two Chamber	Municipal	-	0.025 W/m^2	30 / -	[16]
Single Chamber Air-Cathode MFC	Municipal Waste Inoculated with AS	-	4.64 W/m^2	40-50 / -	[16]

Air-Cathode MFC / PBS treated GAC & Non-PT, GDAC	Molasses mixed Sewage	765	5.06 W/m^3	70 / -	[12]
MBRMFC / CCA & 10% Pt catalyst with 4-coating diffusion layers	MBR Sludge/MBR Sludge	430	51 mW/m^2	11 / -	[12]
DCMFC / Carbon cloth & Carbon cloth Pt-coated	Oil sands tailings/ Slurry of mature fine tailings & clarified oil sand process-affected water	753	392 W/m^2	27.8 / -	[12]
SCMFC open air cathode / Carbon cloth & 20% WPTC y 10% Pt	Paper Wastewater/ ADS	-	0.125 W/m^2	78 / 26	[128]
DCMFC / Graphite felt & Graphite felt coated Pt powder	Palm Oil/ Palm oil mill effluent	800	622 mW/m^2	23 / 32	[129]
Plug Flow MFC / CFB & Pt 10% by wt on CB	Plant influent with sodium acetate	70.6	281.7 mW/m^2	70 / 3.04	[12]
SCMFC with open-air cathode / Non-catalyzed graphite	Pharmaceutical	346	177 mW/m^2	85 / -	[130]
DCMFC GC-packing type / Carbon rod & Graphite flake	Petroleum/ AS	305	330 mW/m^2	64 / -	[86]
DCMFC / Carbon cloth	Raw Sludge/50% of acclimated sludge	154	0.042 W/m^2	55 / 6.3	[12]
Anoxic/oxic MFC / Packed granular graphite & Packer granular graphite	Saline sea food/ Marine Sediments	780	16.2 W/m^2	- / 15	[86]
Air-Cathode MFC / Toray carbon paper & 5% wet proofed carbon paper, 0.5 mg Pt/cm^2	Starch Processing	490	0.239 W/m^2	98 / 15.4	[131]
SCMFC air-cathode / Carbon felt & GORE-TEX cloth	Sewage Sludge	-	73 mW/m^2	53 / 22	[132]
SCMFC air cathode / Carbon paper & Carbon paper	Starch processing/starch processing	490	239 mW/m^2	98 / 8	[86]
Tubular SCMFC / Graphite felt, Carbon fiber cloth /MnO_2	Swine	610	11.2 W/m^3	77.1 / 83.8	[12]
DCMFC aqueous cathode	Swine	-	0.045 W/m^2	-	[96]
Cube-shaped air cathode / Carbon paper & Carbon paper	Swine/Swine	400	228 mW/m^2	84 / -	[86]
DCMFC / Graphite felt & Pt mesh	Yogurt/ AS	700	53.8 mW/m^2	- / 9.6	[86]
SCMFC / Graphite brushes & Pt coated carbon cloth	White wine lees/Denitrification tank WW	420	262 mW/m^2	90 / 15	[133]
SCMFC / Graphite carbon brushes & Carbon Cloth	Winery/AS	441	31.7 W/m^3	65 / 18	[86]
DCMFC / Carbon felt & Graphite	Red wine / Mixed Culture	384	3.8 mW/m^3	89 / -	[134]
SCMFC / Carbon felt	Winery / AS		890 mW/m^2	10 / 42.2	[11]
SCMFC air cathode / Graphite brushes & Pt coated carbon cloth	Red wine lee / Denitrification tank WW	340	111 mW/m^2	27 / -	[133]

Food wastes are rich in biodegradable carbohydrates and organic acids with relatively low concentrations of organic nitrogen and represent 27% of the total municipal solid wastes. These facts persuade the researchers to study and use this substrate as organic source in MFC [86]. Depending on the BOD and volume of water used in processing food products the generated WW can allow a MFC to produce 2-260 kWh/ton of product [83].

Beverages wastewaters have a considerable COD amount, typically in the range of 3000-5000 mgO_2/L, being 10 times more concentrated than domestic waters, is nontoxic, filled with organics as sugar, starch, and protein components. The biological methods that can be used to brewery WWT are efficient but have a high energy demand due to the need of aeration, based on that MFC have been used to perform these treatments [83], [86]. Concerning WWWT Rengasamy and Berchmans [134] treat a red wine WW (7800 mgO_2/L) with a mixed culture of *Acetobacter aceti* and *Gluconobacter roseus*, achieving a COD removal rate of 89% and a power output of 3.8 mW/m^3. Penteado et. al, [11] treat a winery wastewater (COD content of 6850 mgO_2/L) in a tubular MFC with a working volume of 170 mL and achieved a maximum power output of 890 mW/m^3, a COD removal rate of 10% and a maximum CE of 42.2%, resulting in a very high power density for WWWT with MFC [135]. Penteado et. al, evaluated three different configurations for carbon materials at the electrode of a DCMFC for WWWT, concluding that the COD removal and electricity production are tightly bound to the electrode material, as the performance was affected by the biomass adhesion to the electrode surface [136]. Sciarria et. al, [133] carried a study in a SCMFC for white and red wine lees treatment, exposing that the treatment of white wine lees produce more electricity and achieve better COD removal efficiencies than the red wine lees, due to the presence of heavy polyphenols on the red wine lees. In this work they achieved a power output of 262 mW/m^2 and a COD removal rate of 90%

Dairy industry wastewater is composed of biodegradable organics, where 97% of total COD content is sugar, contains high concentration of fermentable substrates. The major waste product from dairy industry can reach up to 80 000 mgO_2/L [85], [86].

Livestock industry wastewater is characterized by being high strength, predominantly composed by biodegradable organic content (ca 100 000 mgO_2/L for animal wastes), also have resistant organic material like cellulose and may contain high levels of nitrogen-containing components, such as proteins. Livestock industry WWT is important for sustainable animal production, upon receiving a pre-treated livestock industry wastewater the MFC efficacy, resource and energy recovery can be enhanced [85], [86].

Among all types of refinery and distillery industry wastewater, it can be found cellulose and hemicellulose, lignin, xylose as acid hydrolysates, residual sugars, 5-fufural, phenolics, furan

aldehyde derivatives, allowing the conversion of compounds as substrate to feed MFCs and directly use of others to electricity [86].

Mining and allied industry wastewaters can be used in MFC for electricity production, but also to metals removal and recovery, such as iron [86], [137].

Pharmaceutical industry wastewaters are characterized by complex composition and high toxicity, having organic rates in the range of 1980-8000 mgO_2/L, being, also, investigated in MFCs [86].

Paper recycling industry wastewaters contain soluble organic. The cellulose found is this WW can be effectively treated with traditional WW technologies, opening space too MFC treatment, although the efficiency is limited by low conductivity [138] [86].

Textile industry wastewaters contain recalcitrant organic molecules, toxic, mutagenic, or carcinogenic chemicals and 60% of the total dyes manufactured are azo dyes. MFC are being tested to treat this type of WW, since physical or chemical and electrochemical methods are being used [86].

In petrochemical industry wastewaters, components such as, hydrocarbons, diesel, purified terephthalic acid (raw material for petrochemical products manufacturing with high organic materials) were used in MFC for power production, since the petroleum sludge has been reported as an electron donor, meaning that it is able to produce power [86].

Domestic and municipal wastewaters have organic matter with embedded energy content, containing almost 10 times the energy required to treat it, being for this reason suitable to use in a MFC and have been marked of big interest among the researchers [86].

2.6 - Diagnostic and characterization techniques

MFC attracts interest due to its exciting potential and applications, as explained before, however their performance must be improved. To accomplished that, a deeper knowledge on the phenomena behind the MFC behaviour is crucial to overcome its major limitations. A better understanding of how a MFC works and how its power output can be improved, can only be obtained if several electrochemical techniques along with surface and microbial analysis are conducted [139], [140].

This sub-chapter intends to describe the main diagnostic and characterization techniques used in the MFC research.

2.6.1 - Electrochemical Techniques

The study of a MFC requires detailed understanding of the bioeletrochemical processes that occur at the interface between the biological film and the electrode, covering the comprehension of different mechanism by which microorganisms enable the electron transfer between a substrate and the electrode [111]. Electrochemical techniques are employed for a qualitative and quantitative analysis of biofilms and the phenomena that influence the electrochemical behaviour of electroactive species, such as electron transfer, mass transport, coupled with the chemical reactions [141]. The most common techniques used are presented in Figure 21.

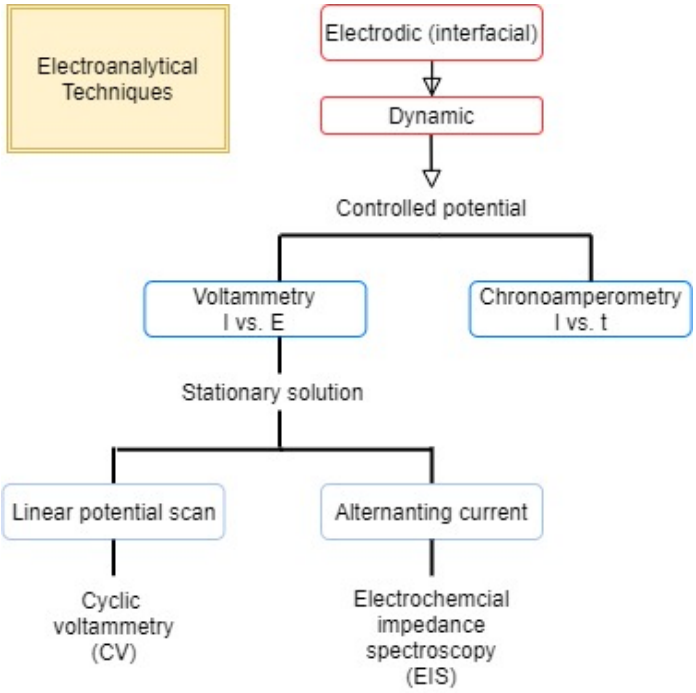

Figure 21: Electroanalytical Techniques; Adapted from [141].

2.6.1.1 - Polarization and power density curves

The polarization curves (cell voltage vs current density) can be done by the galvanostatic method, by controlling the current and measuring the cell voltage [42]. The current density is obtained from equation 12:

$$I = \frac{I}{A} \ (mA/m^2) \tag{12}$$

To perform this measurement the system must be in steady state conditions, this state is temporarily and dependents on the substrate in the anode and the biocatalyst activity at the

electrode [94] [142]. In practical measurement, the current, tension or resistance imposed must be changed in a descending order, from the highest value to the lower one, and this value depends on the system under study [94].

Analogue to FCs (explained in chapter 2.1.1) the real/actual cell potential of a MFC is always lower than its ideal value and decreases with the increase of the current due to the activation, ohmic and concentration irreversible losses [49], [50]. However, the MFCs account with an additional loss that affects the system and the other losses due to the microorganisms metabolic activity and the biofilm formed over the electrode [143]. Moreover, some of the issues that affect these losses are emphasized in MFCs, such as the electrodes distance, to prevent short circuits and the presence of oxygen at the anode, due to oxygen crossover trough the membrane from the cathode to the anode side. These losses have a visual impact on the polarisation curve shape, as shown in Figure 22 [76].

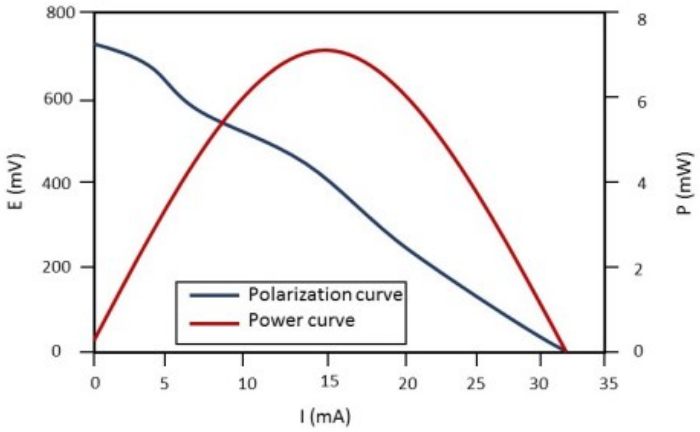

Figure 22: Example of MFC polarization curve (in blue) and the power curve (in red) [144].

Power curves describe the power or power density as a function of the current. Power density is often normalized by the anode surface area once it is in the anode that the biological reactions occur [76]. The red line presented in Figure 22 shows a typically power curve based on the polarization curve. It is noted that no power is produced when no current flows, then as the current increases the power also increases reaching a maximum point (point of interest for real applications), from which the power drops due to an increase of the performance losses.

2.6.1.2 - Chronoamperometry

Chronoamperometry (CA) is a technique where current is measured at a fixed time after applying a single or a double potential step. The independent variable time is followed by a depend variable current [141]. CA involves the application of a particular potential to the electrode at which the redox couple is active for a suitable period of time, so a specific potential measure a transient

current, demonstrating all the oxidation and reduction occurred on the surface of the electrode [78].

With the current measured over the time it is possible to calculate the electron diffusion coefficient across the biofilm by the Cottrell equation, equation 13.

$$I(t) = \frac{nFAD^{1/2}C_o}{\pi^{1/2}t^{1/2}} \quad (13)$$

Where n symbolizes the number of electrons released during the redox process, C_0 the concentration of redox species and D the Diffusion coefficient (cm^2/s).

By quantifying the electricity produced or consumed, CA expose the health of a culture in early biofilm formation either in batch or continuous mode in short-term experiments, since the current is closely related to the cell growth. In long-term experiments the CA output is affected by diffusion limitations and biofilm stratification [145]. The current can be maximized when the redox centres of the matrix are first fully reduced at a sufficiently low initial potential before being immediately re-oxidized at a sufficiently high final potential [146]. CA has been used for the identification and presence of electrogenic species in biofilms, for the formation of electroactive biofilms, and to differentiate between capacitive and faradic currents [147]. CA can be also applied to the comprehension of charge generation of a bioanode [74].

Table 8: Experimental conditions of CA applied for the characterization of electrochemical properties of specific bacterial biofilms; SHE – standard hydrogen electrode, SCE – saturated calomel electrode; Adapted from [148].

Method	Experimental Conditions	Measured property	Bacterial strain	Ref
CA	Potential: 0.242 V (vs. SHE)	The kinetics of interfacial electron transfer between bacteria and electrodes	*Geobacter sulfurreducens*	[149]
	Potential: -0.19 V, 0.21 V, 0.71 V (vs. SHE)	Bioelectrocatalytic current production	*Shewanella oneidensis*	[150]
	Potential: 0 V (vs. SCE)	Electroactivity of bioanodes	*Lactobacillus rhamnosus GG*	[151]

2.6.1.3 - Electrochemical impedance spectroscopy

Electrochemical impedance spectroscopy (EIS) is a steady-state, non-intrusive technique that studies the chemical and physical processes occurring in solutions, interfaces (solid-liquid, solid-solid) and solid phases, as it allows the separation and quantification of the different voltage losses [111]. EIS is the most precise and commonly used technique for the diagnosis of internal resistance and can be used to measure the ohmic, activation and concentration resistances that affect the FC behaviour and is considered a very important tool for studying heterogeneous systems such as MFCs [56], [77] [147].

EIS measurements can be conducted when a potentiostat is equipped with a frequency response analyser (FRA) [77]. The system is disturbed with a small magnitude alternating current (AC) and small perturbations are used to ensure that non-large overpotential is created and to prevent the damage of the biofilm attached to the electrode surface [139], [147]. Usually, the current response is analysed in the frequency range from 100 KHz to 1 mHz, and the amplitude of the AC signal is 5 or 10 mV [147]. The current response will be a sinusoid at the same frequency but shifted in phase (Figure 23) [111]. A linear response at a steady state conditions is obtained if the amplitude of the current is selected based on the polarization curve and not arbitrarily [111].

The excitation signal, expressed as a function of time, has the form [111]

$$E(t) = E_o \cos(\omega t) \tag{14}$$

Where E_t is the potential at time t, E_o is the amplitude of the signal, and ω is the radial frequency (rad/s).

In a linear system, the response signal, I_t, is shifted in phase (Φ) and has a different amplitude than I_0 [111].

$$I(t) = I_o \cos(\omega t - \Phi) \tag{15}$$

An expression analogous to Ohm's law gives the impedance of the system as [111]

$$Z(t) = \frac{E(t)}{I(t)} = \frac{E_o \cos(\omega t)}{I_o \cos(\omega t - \Phi)} = Z_o \frac{\cos(\omega t)}{\cos(\omega t - \Phi)} \tag{16}$$

The impedance is therefore expressed in terms of magnitude, Z_0, and a phase shift, Φ. The magnitude of the complex impedance is the ratio of the voltage and the current amplitude,

whereas, the phase angle of the complex impedance is the phase shift by which the current is ahead of voltage [152].

EIS measurements are commonly represent by Nyquist Plots and Bode Plots (Figure 23) [111]. In the Nyquist plot, negative values of imaginary impedance, capacitance, (-im (Z)) are plotted against the real part of the impedance, resistance, (Re (Z)). Each point of the plot represents the impedance at a specific frequency, being the low-frequency data on the right side and the high-frequency data on the left side of the Re(Z)-axis [111]. In the Nyquist plot the higher frequency limit is associated with the ohmic resistance, R_{Ω}, whereas the diameter of the semicircle projects the polarization resistance, R_p [61]. The major drawback of Nyquist plots are the fact that the frequency used is not indicated [56]. This limitation has been overcome in the Bode plot, where the logarithm of the impedance modulus |Z| and the phase angle Φ are plotted *vs* the logarithm of the frequency of the applied AC signal.

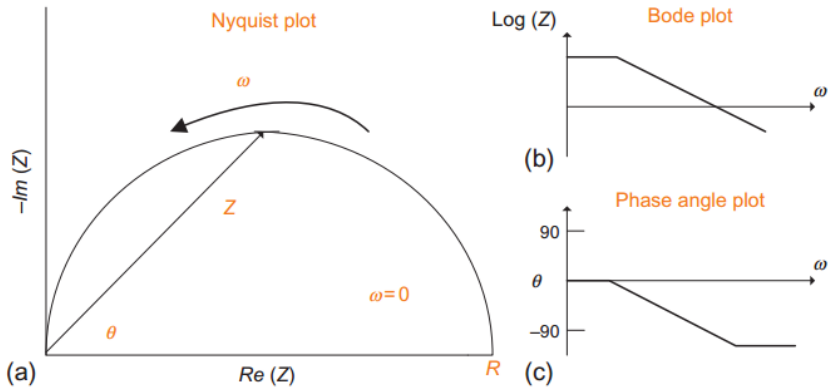

Figure 23: Representation of EIS data in (a) Nyquist plot, (b) Bode plot, (c) phase angle plot [111].

EIS incorporates relevant parameters which are, (1) electrolyte resistance: the resistance offered by the ionic solution; (2) double layer capacitances: the thickness of the double layer can be generated by the formation of biofilm on the electrode surface, getting related with the double layer capacitance of the system; (3) polarization resistance: occurs when the applied electrode potential is different from the equilibrium potential of the electrochemical reaction at the polarized electrode leading to oxidation/reduction of the species at the electrode surface; (4) charge transfer resistance: transfer of electrons from the ionic species in the solution to the solid metal; (5) diffusion: related with the path of substrates to diffuse through the biofilm. The impedance measurement of this diffusion phenomenon requires the integration of a diffusion element in the equivalent circuit model, namely Warburg impedance, a semi-infinite linear diffusion [152].

As aforementioned EIS is an important method to determine several electrochemical properties of the MFC components, such as the different resistances associated with electron transfer and ohmic losses and the identification and quantification of the different loss mechanisms [111].

When current flow due to electron transfer it can result in an electrochemical reaction where faradaic components are present, or cannot result in an electrochemical reaction, where faradaic components are not present. Faradaic components come up from the electron transfer across the interface by overcoming an adequate activation barrier resultant from polarization and ohmic resistance (R_p R_Ω). The non-faradaic current come up from charging the double layer capacitor at the interface which incorporates a double layer capacitance (C_{dl}) [152].

At very high frequencies, the impedance is majorly due to a nearly ideal ohmic resistance, R_Ω, due to the membrane ionic resistance, electrolyte solution and other electrical connections [61], [152]. The faradaic component R_p is not ideal and changes with the frequency, polarization resistance at intermediate frequency includes the charge-transfer limited activation losses (R_{act}). At low frequencies de Rp is due to diffusion-limited concentration losses (R_{conc}) [61], [152]. Both the charge transfer resistance and the diffusion resistance occur at the interface between the electrode surface and the surrounding electrolyte [152]. The internal resistance can be written as

$$R_{int} = R_\Omega + R_p^a + R_p^c \quad (17)$$

A wide range of factors affect the internal resistance of a MFC, such as the type of substrates and microorganism used in the anode chamber, types of electron acceptors, geometry and design, among others [152].

Ramasamy et. al, [153] studied the behaviour of a MFC using *Shewanella by EIS and* verified a response in the mid-frequency region that was bonded to the charge-transfer resistance of the endogenously synthetize mediators [111]. . In the study of *G. sulfurreducens* and *S. oneidensis* electron transfer mechanism, it was found that the internal impedance of *G. sulfurreducens* were much lower than that of *S. oneidensis*, revealing that the electrons transfer efficiency though conductive pili (*G. sulfurreducens*) is faster than on the flavin (*S. oneidensis*) [111]. Manohar et. al, [154] observed a decrease of the polarization resistance of the anode with the addition of *S. Oneidensis* to the anode compartment, showing that the formation of bacterial biofilm benefited the system. In fact, EIS is a strong technique to examine the resistance due to charge transfer in response to the electrode colonisation, with an expected decrease with the electroactive biofilm formation [145]. However, it is less informative in the presence of a microbial consortium, as it cannot show the contribution of individual species to the overall impedance [145].

The use of EIS for the evaluation of the effect of the pH on an SCMFC was conducted by He et. al, [155] , revealing that a neutral pH presented the lowest polarization resistance compared with the other conditions tested. This indicates that the anodic bacterial activity is optimal at neutral

pH. The EIS data demonstrated that the polarization resistance of the cathode was the dominant factor that limits the power output [155].

For accurate results, impedance data can be used to build equivalent circuits by introducing circuit elements as resistances, capacitances and inductances, this elements need to symbolize something in the real system, for exemple a resistance in an equivalent circuit can indicate an internal ohmic resistance, a second resistance can indicate the cathodic and anodic charge transfer resistance, [111]. Examples of the most common electric equivalent circuits used to describe a MFC are presented in Figure 24. Due to complexity of MFCs systems and EIS data collection, such as determination of reactions mechanisms, kinetic parameters, electrolyte and electrode conductivities, and biofilm behaviour, the build of an equivalent circuit through EIS analysis must be carefully undertaken [139], [156].

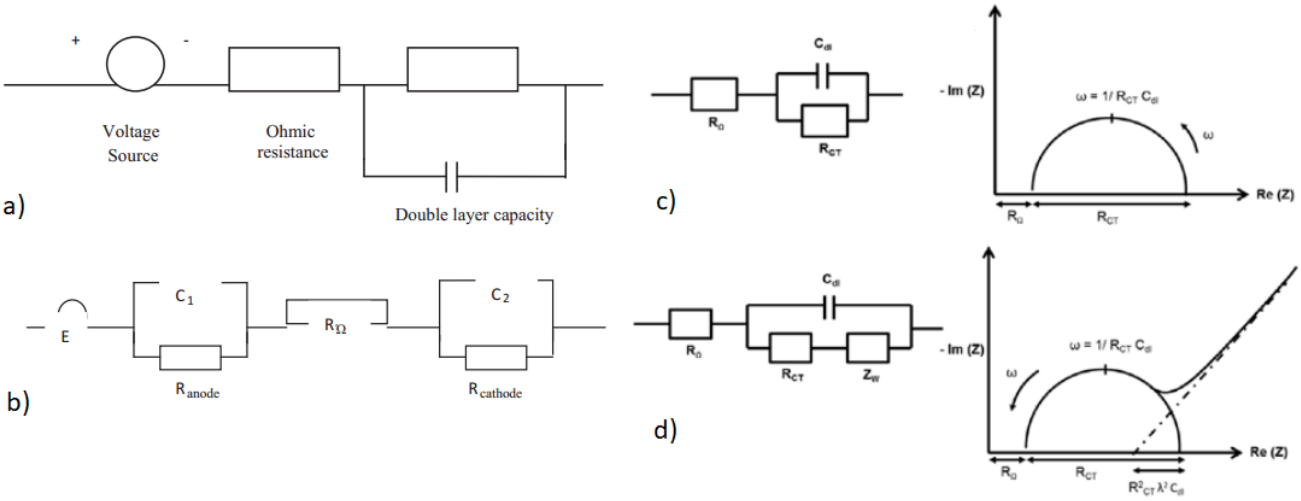

Figure 24: a) Circuit model for resistance in MFC, b) Simple equivalent circuit model for MFC [61]. c) representation of Randles circuit and its characteristic Nyquist plot, d) Randles circuit with Warburg element and its characteristic Nyquist plot; Cdl – Charge accumulated; C1, C2 – Doulbe layer capacitors; R – Polarization Resistances; Zw – Warburg impedance; [152].

2.6.1.4 - Cyclic voltammetry

Cyclic voltammetry (CV) is a dynamic electrochemical measurement, where the voltage applied to a system is swept linearly with time, back and forth between a suitable voltage window of values, measuring the respective current (Figure 25 a) [45]. The measurements are usually performed in a three-electrode-setup composed by a reference electrode, a counter electrode and a working electrode (anode or cathode) [77]. The working electrode and the reference electrode allow the current measurement in the cell [77], [78]. When changing the electrode potential between a window of values during the CV measurements, electrons generated are pushed and pulled out of the cells turning up to represent a single oxidation or reduction by each redox center

accessible to the electrode. A suitable potential scan in a potentiostat mode has to be identified and the process must not harm the cells [157]. *Geobacter* strains in voltammograms can sweep in a potential window of -0.5 to + 0.2 V. *Shewanella sp* can sweep in a potential window from -0.7 to 0.4 V [111]. Additional experimental conditions are displayed on Table 9.

A scan analysis of 25 mV/s fit for bacterial suspensions while a scan analysis of mediators in biofilms must be lower than 10 mV/s [77]. The analysis of the scan rate may reveal information about the interfacial electron transfer, or cell to cell contact properties [158]. By that CV is used for assessing the electrochemical activity of the microbial strains or consortia, determining the standard redox potentials of redox active components, and evaluate the performance of novel cathode materials [77].

Table 9: Experimental conditions used for the characterization of electrochemical properties of specific bacterial biofilms by CV; EAM – Electrochemical active molecules; SHE – Standard hydrogen electrode; SCE – Saturated calomel electrode; NHE – Normal hydrogen electrode; Adapted from [148].

Method	Experimental Conditions	Measured property	Bacterial strain	Ref
Cyclic voltammetry (CV)	Equilibrium time: 5s Scan rate: 1 mV/s Potential range: -0.558 V to 0.242 V (vs. SHE)	The kinetics of interfacial electron transfer between bacteria and electrodes	*G. sulfurreducens*	[149]
	Potential range: - 1 V to 1 V (vs. SHE) Scan rate: 100 mV/s Sampling interval: 1mV	Redox behaviour of EAM	*Staphylococcus epidermidis*	[159]
	Potential range: -0.56 V to 0.24 V (vs. SHE) Scan rate: 10 mV/s	Extracellular electron transfer	*G. sulfurreducens*	[160]
	Potential range: -0.49 V to 0.71 V (vs. SHE) Scan rate: 2 mV/s	Extracellular electron transfer	*S. oneidensis*	[150]
	Potential range: -0.7 V to 0 V (vs. SCE) Scan rate: 10 mV/s	Extracellular electron transfer	*Pseudomonas aeruginosa*	[161]
	Potential range: -0.6 V to 0.6 V (vs. SCE) Scan rate: 5 to 100 mV/s	Electroactivity of bioanodes	*Lactobacillus rhamnosus*	[151]
	Potential range: 0.1 V to 1.2 V (vs. NHE) Scan rate: 1 mV/s	Redox behaviour of biofilm	*Acidithiobacillus thiooxidans*	[162]

From cyclic voltammogram significant parameters are obtained by anionic and cationic peak, such as potentials and currents (E_{pa}, E_{pc}, I_{pa}, and I_{pc}). Representation of voltammetry is given in (Figure 25 b) The peak to peak separation (anodic to cathodic peak), ΔE_p, reflects the extent of reversibility of the electrode process, a lower ΔE_p means less irreversibility of the electrode process. In terms of the catalysts (cathode performance), it should produce the maximum current at minimum over potential [74].

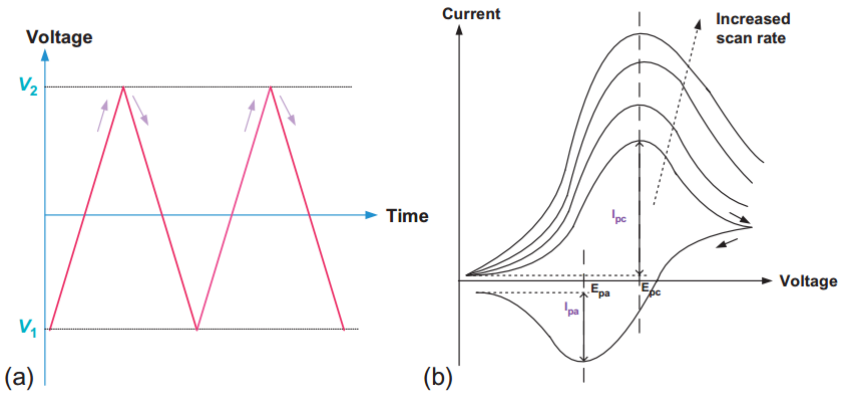

Figure 25: (a) Cyclic voltammetry waveform and (b) current versus potential for reversible and irreversible electron transfer reactions [111].

The potential of redox reaction taken place in an MFC is given by [78]:

$$E^0 = \frac{E_{pa} - E_{pc}}{2} \tag{18}$$

The analytic current is calculated by Randle-Sevcik equation [78]:

$$I_p = 0.4663\, nFAC\, (\frac{nFvD}{RT})^2 \tag{19}$$

Where C is the concentration of the analyte, A_e is the working electrode area (cm^2), D is the diffusion coefficient(cm^2/s) , v is the scan rate (V/s), and, n,F,R,T usual significance.

The cyclic voltammetry have been applied for (1) examining the direct or indirect electron transfer mechanisms between the biological membrane and the electrode, (2) determining the anodic oxidation potential and the cathodic reduction potential, (3) testing the performance of the catalyst system [78]. CV curves are affected by pre-treatment of the electrode surface, microorganism type and their thermodynamic properties, the electron transfer rate, concentration of electroactive species and their diffusion rates and sweep rate [78].

2.6.2 - Biofilm quantification/characterization

Any natural or artificial surface exposed to microorganisms have strong probability of being colonized [163]. The colonization of bacteria is commonly accompanied by biofilm formation, which are aggregates of bacterial cells encapsulated with a self-secreted polymeric matrix that works as a glue to attach to a surface or each other [147]. The matrix is a typically -mixture of polysaccharides, but can contain proteins and even nucleic acids [163]. The biofilm development is a continuous and a four step sequential process: (1) initial attachment of microorganisms to a surface or each other, (2) formation of microcolonies, (3) maturation of the biofilm (4) dispersal of the biofilm (Figure 26) [164].

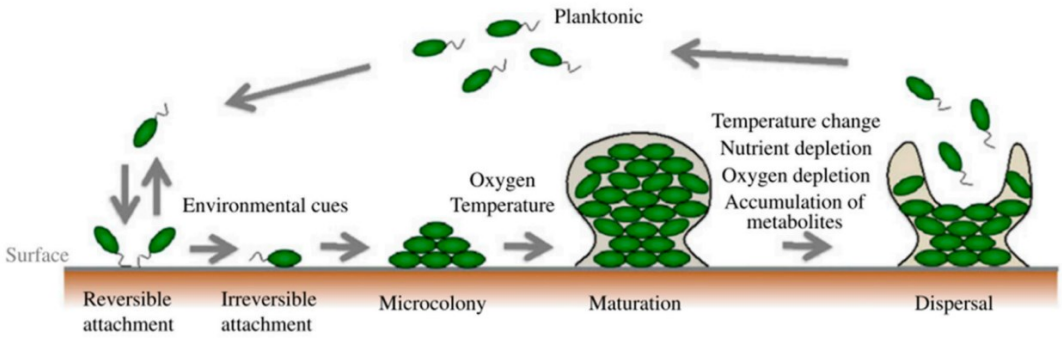

Figure 26: Biofilm development [165].

The presence of biopolymers, known as extracellular polymeric substances (EPS), in biofilms provides the biofilm attachment on surfaces and are responsible for the biofilm cohesion [166]. . Biofilm architecture is influenced by hydrodynamic conditions, concentration of nutrients, bacterial mobility, intercellular communications as well as exopolysaccharides and proteins [166].

Biofilm characterization is conducted due to the relation between biofilm thickness and MFC power output as the power generated is directly related to the electroactive metabolic action of the microbial biofilm developed [73], [147], [167]. The efficiency of electroactive biofilms is dependent on mainly three parameters as show in Table 10 [168].

Table 10: Impact of system design, operating and biological parameters on the development of electroactive biofilms and on the MFC performance [168].

Influencing factors on biofilm formation

System design parameters	Electrode Material; Electrode properties such as conductivity, hydrophilicity, porosity and chemical stability; Electrode surface area to volume ratio; Presence or absence of membrane and type of membrane used; Relative Anode and cathode surface area; Cathode type; MFCs configuration and electrodes distance;
Operating parameters and environmental conditions	Operation mode: batch vs continuous system; External Resistance; Redox potential; Shear rate; Temperature; pH; Aerobic vs anaerobic process; Ionic concentration; Substrate concentration;
Biological parameters	Microbial resource, its availability, its diversity and abundance; Type of microbial culture: Gram positive vs Gram negative and pure culture vs mixed culture; Microbial interactions including competition, complementary niche formation; Biofilm growth rate; Specific electron transfer rate; Electroactive microbial community in terms of: density, diversity, composition and abundance; Ability to synthetize redox mediators; Ability to produces nanowires and perform direct electron transfer; Relative exoelectrogens population; Bioreaction rate in terms of substrate utilization and substrate specificity;

The following sections describe techniques for biofilm characterization along with the inherent advantageous and disadvantageous.

2.6.2.1 - Scanning electron microscopy

The scanning electron microscopy (SEM) (Figure 27) is a powerful microscopic method useful to visualize the structures surface and the spatial arrangement. Therefore, can be applied to evaluate the ultrastructure of the biofilm [147]. SEM uses a beam of high-energy electrons to image surfaces of different samples, providing a high resolution and magnified image with a wide range of magnification, from 10x up to 500 000x [169], [170].

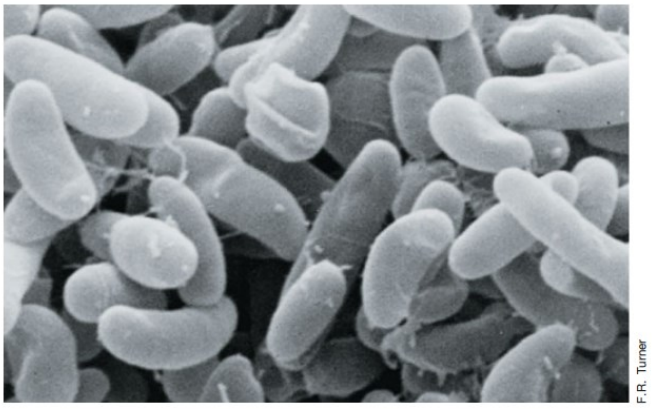

Figure 27: Scanning electron micrograph of bacterial cell [170].

The main components of the SEM include a source of electrons, electromagnetic lenses to focus electrons, electron detectors, sample chambers, computers and displays to view the images (Figure 28) [171]. The main experimental factors influencing the image quality are sample preparation, electron acceleration voltage, spot size, and the detector position [78]. The SEM operation principles are described in appendix A1.

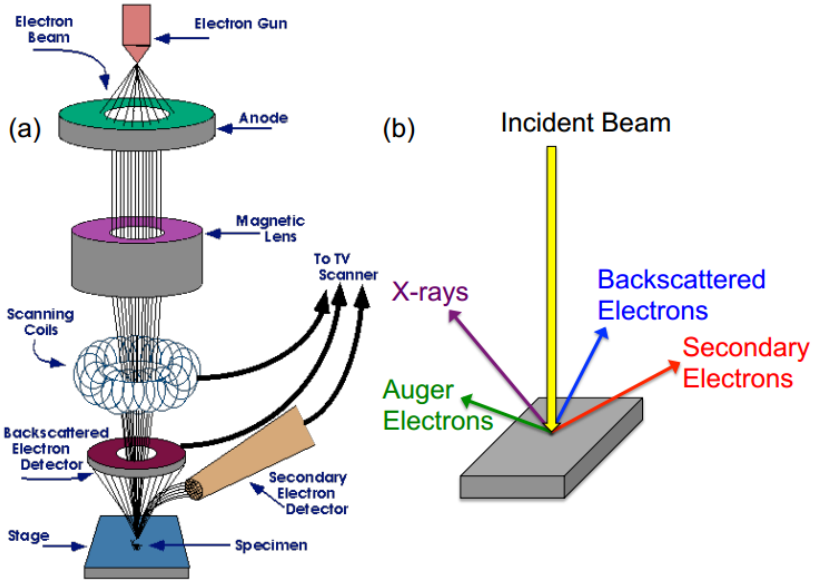

Figure 28: Schematic drawing of (a) the typical Scanning Electron Microscope (SEM) column, (b) sample beam interactions within a SEM [172].

SEM advantages include detailed three-dimensional (3D) topographical imaging and the versatile information obtained from the different detectors, (1) producing the most detailed images of an objects surface and (2) revealing the composition of a substance [171]. The microscope is easy to operate, the software is user-friendly, the source of electrons is generally a heated tungsten filament, which provides easy operation and simplicity [171], [173]. In opposition to other electron microscope techniques (transmission electrons microscope) the sample can be examined at higher pressures [173]. SEM disadvantages relay on expensive operation cost and limitations on the sample size which need to fit inside a vacuum chamber [171]. Higher voltages can provide higher power, but there is a risk of unwanted penetration that may damage the samples [173]. SEM analysis require extensive preparation, including fixation, removal of all moisture and coating the sample with a thin layer of a conductive metal (gold or platinum) that can result in the purchase of additional equipment and chemicals [169].

2.6.2.2 - Confocal laser scanning microscopy

Confocal laser scanning microscopy (CSLM) is a computerized microscope used to study biological specimens, including microorganisms. It is a non-destructively *in situ* method that

couples a laser source to a fluorescent microscope [170], [174] CSLM reduces significantly the need of a sample to be pre-treated by disruptions and fixation preparation methods, that can consequently degrade or eliminate the links for microbial relationships, complex structure and biofilm organization, crucial in the maintenance of the natural structure [175]. This microscope produces high-resolution images and provides spatial distribution of a wide range of biofilm properties (cell numbers, cell area, dimension) and simultaneous 3-D information regarding the different cellular and polymeric biofilm constituents, such as phototrophic organisms, bacteria and EPS (Figure 29) [175], [176]. Adjusting the plane of focus of the laser source it is possible to observed with 1 µm resolution cells on the surface of the biofilm and in its different layers [170].

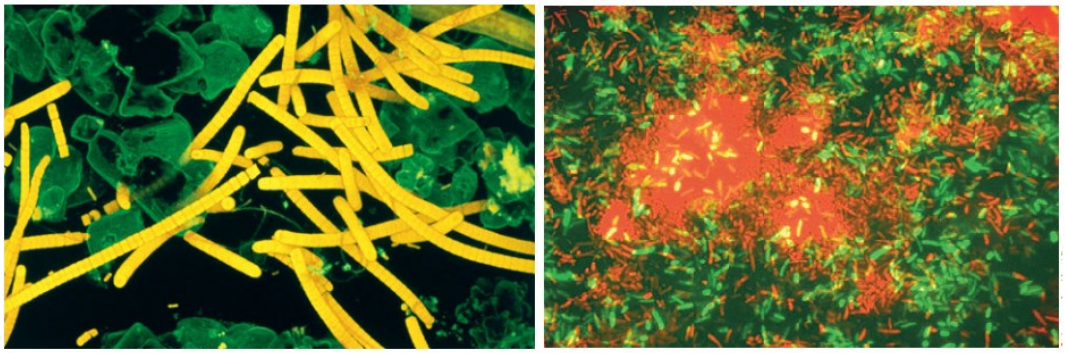

Figure 29: a) Confocal image of a filamentous cyanobacterium growing in a soda lake, b) Confocal image of a microbial biofilm community cultivated in the laboratory. The green, rod-shaped cells are Pseudomonas aeruginosa experimentally introduced into the biofilm. Other cells of different colours are present at different depths in the biofilm [170].

The components of a CSLM are the optical system, the laser light source, the detection system, and the scanning device (Figure 30) [177]. The CSLM principles are described in appendix A2.

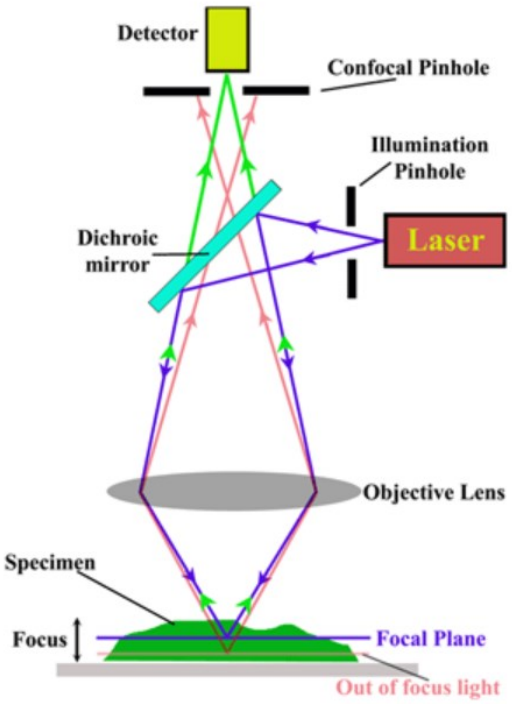

Figure 30: Schematic of an confocal laser scanning microscopy [178].

The use of CLSM is adopted when it is desirable to investigate the temporal dynamics of biofilm instead of only a final observation [176]. This technique is mainly used in MFCs to observe the colonization of the electrode over the time and the biofilm thickness [179], [180].

The main limitation of this technique is the selection of lasers with efficient fluorophore excitations, fluorophore can also reveal photobleaching in the x,y, and z planes [181]. Another important factor is the selection of the objective lenses and their working distances [181]. The costs of this technique depend on the system configuration but are expensive (starting at hundreds of thousands) and require experienced and highly trained users for an accurate measurement [169].

2.6.2.3 - Biomass dry weight

Biofilm dry weight gives a direct measurement of biofilm growth related with biofilm density (dry mass per wet volume) [182]. The biofilm density increases the reaction rate in the biofilm in early stages, although limits the substrate diffusion when achieved the critical biofilm density, after this point, the consumption rate is controlled mainly by diffusion, whereas the effective diffusion coefficient decreases on reaching inner regions of the microorganism layer [183]. This analysis implies the biofilm detachment from the electrode surface and its treatment to remove water and organic solids [169].

Biofilm dry mass is intimately tied to the overall electron-transfer processes occurring within the biofilm [184]. Choi et. al, [185] monitored the biofilm detachments based on the biofilm density when inducing shear stress.

This method is relatively cheap and easy to execute, however it is time consuming and do not give qualitative information of the microbial cells and the biofilm matrix [169], [186].

2.6.3 - Wastewater treatment evaluation

The objective of WWT is the protection of the quality of the receptor waters [187]. Therefore, different treatments are implemented to reduce the Chemical Oxygen Demand (COD), Biological Oxygen Demand (BOD), Total Organic Carbon (TOC), Total Suspended Solids (TSS), Nitrogen (N) and Phosphorus (P), and others parameters [187]. Total and fecal coliforms are employed as common indicator organisms [59].

COD indicates the microorganism activity in degrading the organic compounds following the reaction,

$$Organic\ Matter + O_2 + nutrients \xrightarrow{Microorganism} New\ Biomass + CO_2 + H_2O \quad (20)$$

COD removal rate is determined according to:

$$COD_{removal}(\%) = \frac{\Delta COD\ (mgL/O_2)}{COD_{wastewater}\ (mgL/O_2)} * 100 \quad (21)$$

In MFC the estimation of the COD removal rate is fundamental to evaluate its ability to perform a wastewater treatment and its CE [78]. In some cases it is possible to achieve a removal rate up to 90% and a CE of 80% [14]. For a cost-effective WWT using a MFC it should be achieved an organic removal rate of $5x10^3$–$1x10^4$ mgO_2/L [188].

BOD is the quantity of non-dissolved oxygen consumed in a water sample by microorganism for the degradation of organic matter, usually determined by the BOD_5, in respect to a period of 5 days at 20 ºC [187]. Easily measures the biodegradable organic carbon and is considered a method for evaluation the efficiency of the treatment processes [189].

The BOD_5 removal is determined according to

$$BOD, \frac{mg}{L} = \frac{DO_1 - DO_2}{P} \quad (22)$$

Where DO_1 is the dissolved oxygen (mg/L) of the diluted sample immediately after preparation (mg/L), D_2 the dissolved oxygen (mg/L) of diluted sample after 5-day of incubation at 20ºC (mg/L) and P the fraction of the wastewater sample volume to total combined volume.

TOC is an indirect measurement of the amount of carbon in a sample associated with organic compounds or carbon compounds derived from living things (e.g. proteins, lipids and urea) [169]. TOC measurements are often used as a qualitative nonspecific indicator of water quality and quantification of the biofilm accumulation [169]. It is less precise than BOD and COD but it is easier to perform [59].

WW contains a variety of solid materials with an ample variation in magnitude, from rags to colloidal material [189]. TSS removal is one of the most important physical parameters of WW and has been used in MFCs as well [190].

2.7 - Integrating Processes

Researchers have conducted significant efforts to improve the MFC performance as mentioned along the previous chapters. To make a MFC competitive with the convectional technologies used to perform WWTs its integration with other processes can lead to some benefits [16].

Integrating a MFC in a WWT system can increase their energy and resource utilization efficiencies, leading into a neutral or positive energy balance of plant and a better effluent quality [12]. MFCs can be a processing unit after the primary treatment and in the activated sludge or after the anaerobic digestion process, or even as standalone process to remove organic compounds [9]. MFCs can be combined with up-flow anaerobic sludge blanket reactor (MFC-UASB), integrated with an activated sludge process, such as anaerobic digestion, combined with anaerobic fluidized bed membrane reactor, or integrated with a rotating biological contactor (RBC) [191]. Coupling a MFC with a traditional WW biological treatment can yield higher denitrification and nitrogen and COD removal rates, almost complete removal of TSS, increase the energy output, being an opening potential to improve the feasibility of these systems [12], [16], [191].

The combination of MFCs with membrane-based technologies, such as ion exchange, forward osmosis, reverse osmosis, reverse electrodialysis and ultrafiltration membranes, have also been investigated [191]. Integration of membrane bioreactor with MFC (MBR-MFC) was tested for the ammoniacal nitrogen, organic matter and total phosphorus removal, Sun et. al [192] achieved 94%, 85% and 87% removal for total organic carbon, total nitrogen and total phosphorus respectively. Ultrafiltration membranes were integrated with tubular MFCs for a better effluent quality and treatment efficiency [12]. Liu et. al, [193] with a membrane bioreactor (MBR) considerable mitigated the membrane fouling [14].

MFC can be integrated with aerated lagoons and wetlands [16]. A constructed wetland-microbial fuel cells (CW-MFC) can achieve a performance at least as good as a conventional CW and simultaneously harvest energy, from the EAB metabolic activity and their interaction with the electrodes installed in the system [66]. Applications have evolved from conventional pollutants like organic matter and nutrients to more complex compounds such as pharmaceuticals [66], [194]. Rashid et. al, [195] showed that using algae biomass combined with activated sludge as a substrate in a MFC allows a much higher power density and mitigate waste [14].

Water crisis is for the first time in the human history a serious concern and desalination can be a win-win solution to restore the water cycle [196], [197]. The MDC adapt the MFCs configuration to perform desalination, integrating an electrodialysis cell to achieve wastewater treatment, seawater desalination and electricity generation [198].

To achieve the global energy transition and extensive decarbonisation of several platforms, such as grid, transport and industrial processes, hydrogen will be needed [199]. Microbial electrolysis cell (MEC) combines metabolism of microorganisms and electrochemistry, is a novel and emerging technology that transform degradable substrates into hydrogen due to an external potential input [200] [201], [202]. An MEC-MFC couple system has potential for biohydrogen production from wastes, plus the MFC also supply energy to the MEC reducing its energy demand and costs [203].

MFC hybrid systems are a different and attractive approach to improve the viability of MFCs. The examples here presented were selected from a vast list of possibilities reported in literature. Figure 31 illustrate some of these MFC hybrid systems [191].

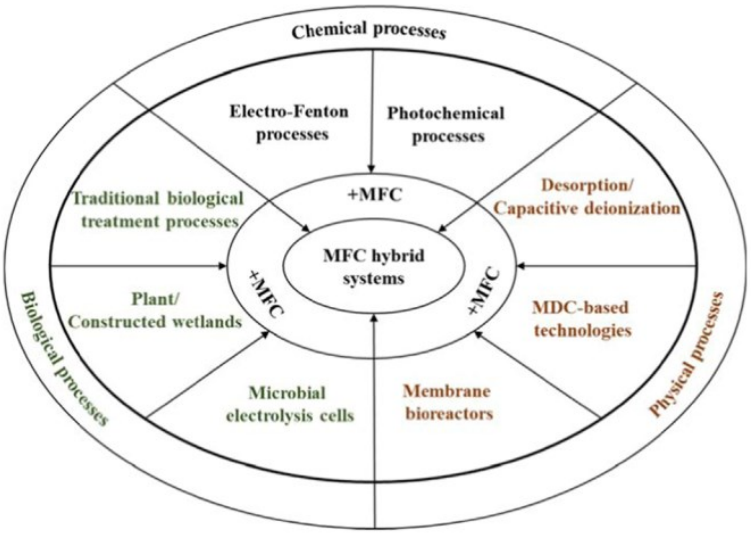

Figure 31: MFC hybrid systems [191].

2.8 - Challenges and Perspectives

Extensive studies on MFCs have been performed in the past two decades. Almost 7500 results are found on ScienceDirect when searching for “Microbial Fuel Cells”. Since 2010, research results where 6900 of the 7500, showing a considerable interest on the MFCs development.

Challenges and perspectives of the MFC technology contemplate research on metabolic mechanisms, electrochemically active microorganisms, biofilm activity, design and architecture of the reactor, MFC stacks and hybrid processes [16].

MFCs need to be scaled up by several orders of magnitude from the laboratory scale (10^{-6} to 10^{3} m^3) to a scale suitable for wastewater treatment (1 to 10^{3} m^3) [96]. Performance of MFCs is limited by their internal resistance derived from proton mass transfer, poor oxygen reduction kinetics at the cathode, and other factors as being sad in previous chapters [204]. Low power densities resulted by MFC operation can be increased by reducing the polarization losses. Further losses originated by unnecessary reactions, such as the direct oxidation of substrate by oxygen diffusion into the anaerobic compartment or microbial metabolic reactions, which do not benefit the process, should be also targeted [82].

MFCs have not been operated at the full capacity of the anodic microbial metabolism because of the internal resistance limitations, it is essential to understand the microbiology of the anodic microbial catalysts and the associated mechanism of electrons transfer to the electrode [204].

Microbial metabolism at the anode has still not given the full strength for a superior MFC operation due to internal resistance limitations, better comprehension in microbial catalysts and involved mechanisms of electrons transfer to the electrode must learned. [204].

Eletron transfer mechanisms of *G. sulfurreducens* and *S. oneidensis* have been widely study, although its necessary to understand and strength the EET mechanism of others EAB, it is also necessary to conduct efforts and investigation on the microbial electron uptake from cathodes. Concerning the three-phase (air, water and electrode) interface the selection of cathode materials is a challenge, research can be done on biocathodes or in advanced nanomaterials as cathodic catalysts however the costs can be expensive [16], [205].

Driving force for bacterial adsorption to polarized electrode or biofilm formation of electroactive microorganisms on electrodes are linked to the type of electrode material. A better understanding of these processes and modifications of the electrode surface is needed to improve the MFCs performance [205]. It is also required the increase of population density of the active bacteria in the electrode which seems to be limited not only from the availability of attachment points on the

electrode, but also from biofouling and catalyst inactivation, as shows Figure 13 [73]. Another issue relays in the non-functionality of the EAB at low temperatures and a consequently microbial biocatalyst inactivity, thus, the bioanodes or biocathodes activity can be inhibited [12]. Enhancing the insights into all the interactions between the microorganisms and the electrode is an effective strategy for the development of future MFCs with enhanced performances [205]

Efforts should be directed to address a suitable balance between ion transfer and oxygen permeation. Alternatives to the expensive Nafion membranes such as porous separator materials are a promising approach [60]. A critical issue in MFCs application for WWT is the biofouling of the membrane as it causes negative effects on ion and mass transfer. Therefore, the development of materials with antifouling properties should be a target of investigation [14], [60].

Electrode materials are vulnerable to corrosion and precipitation of by-products that result in its ineffectiveness with time. Studies need to discuss the stability of the electrode materials to provide a valuable guideline for their long-term viability in industrial applications [12], [14]. Support of heavy biofilm combined with water weight it is also a challenge, because some materials are not expected to be suitable to scale-up due to inherent lack of durability or structure strength as carbon paper or graphite rods. Conductive coatings for support material structures may be a solution [14].

MFCs may present conductivity problems with some WW effluents (as municipal), the dilution of high polluted effluents in sea or brackish waters improve the conductivity.

MFCs power output has been increasing through the years stating potential to these systems. MFCs must overcome the high internal energy losses and yield desire power outputs at large scale with cost-effectiveness [73]. The application of stacked MFCs in parallel or in series significantly increase the current and voltage. Nevertheless, voltage reversal and ionic short circuit remain a big concern for practical application. Voltage reversal occurs due to an unbalanced substrate distribution and a consequently unequal electrode potential between the different MFC units, ionic short circuit can be influenced by electrolyte ionic conductivity, distance between two MFCs and anode-cathode distance [206] [16].

As mentioned in chapter 2.6 hybrid processes can improve the potential use of MFCs, however this synergistic effect with other wastewater treatment technologies needs better understanding [16]. Integrating devices that can capture and store energy and boost the power output of MFC it's a field that needs to be explored, power converter-based energy storage devices can replace external resistors, harvesting and storing the energy generated [65].

The higher MFC costs, as a result of the anode and cathode materials (major portion) followed by membrane, current collector materials, and other essential parts, can be 30 times higher than

traditional activated sludge treatment systems for domestic wastewater, know how to reduce costs is a concern when address MFCs systems [9], [16]. In the market penetration sulfonated ion-exchange membranes are not of practical interest unless costs can be greatly reduced, some AEMs can be of interest [60]. The power ouputs can be increased increasing the electrode surface areas, but this will lead to higher costs, its necessary to come up with low-cost materials for both anode and cathode [60]. Inexpensive materials such as semicoke and activated carbon seems to meet interesting power densities [9]. In the meantime should exist some focus on passive microbial electrochemical systems, such as short-circuited MFCs, that can harvest conditions to treat low concentration pollution and relay on low upkeep and little investment systems [59].

Life cycle assessment (LCA) is a tool for reporting and evaluation of the outputs and potential environmental impacts of products and processes [207]. Few LCA studies have been done for MFCs, but at the moment the major negative environmental impacts result from the production of carbon fibre electrodes, membranes and stainless-steel components for current collectors, mesh and brushes [9]. By using this tool potential benefits and feasibility of the MFCs can be highlighted in relation to the other technologies [208].

MFC is a complex system involving biological, chemical and electrochemical processes, energy, mass and charge transfer, so the different phenomena that affect the MFC behaviour must be widely understood [50]. Modelling and mathematical tools are powerful for understanding the operation and the processes that occur in a working MFC, relieving the experimental costs and work, which is time consumption, while giving simulations of various configurations and operating conditions, that can highlight the MFCs optimization [50], [96]. Mathematical modelling and simulations must gain extra attention since provide several benefits and understandings [96].

3

Microbial fuel cell for winery wastewater treatment – case study

3.1 - Materials and Methods

3.1.1 - Synthetic Winery Wastewater Composition

The synthetic winery wastewater (SWWW) used in the experiments, as the name suggests, simulates a real winery wastewater effluent. The composition of this SWWW is shown in The substrate (source of carbon) of this SWWW is essentially glucose and fructose. The pH was adjusted to 7 with NaOH at 2M. The sterilization was assured by filtration using a pore diameter of 0.22 µm filter and then the SWWW was stored at 4ºC. and is based on the composition of combined outflows from different wineries, from pressing operations, washing of crusher and press, inflow and outflow from a holding tank and settling tank during the peak season in the Stellenbosch region, South Africa [209]. The substrate (source of carbon) of this SWWW is essentially glucose and fructose. The pH was adjusted to 7 with NaOH at 2M. The sterilization was assured by filtration using a pore diameter of 0.22 µm filter and then the SWWW was stored at 4ºC.

Table 11: SWWW composition.

Total volume (L)	1
Glucose (g)	1.8
Fructose (g)	1.8
YNB (g)*	1.7
Citric acid (mg)	1
Tartaric acid (mg)	2
Malic acid (mg)	2
Lactic acid (mg)	2
Propanol (mg)	1.24
Butanol (mg)	1
i-amyl alcohol (mg)	3.8
Acetic acid (mg)	250
Ethanol (mg)	10
Ethyl acetate (mg)	4
Propionic acid (mg)	8
Valeric acid (mg)	1
Hexanoic acid (mg)	0.5
Octanoic acid (mg)	0.7
$(NH_4)_2SO_4$ (g)	5

***YNB – Yeast Nitrogen Base**

3.1.2 - *Zygosaccharomyces bailii* Inoculum

As it was said in the chapter 1.1.3 the inoculum was a single yeast culture of Z. *bailii.* Prior the inoculation of the MFC, the *Z. bailii* pure culture was let to grow as the following description explains. *Z. bailii* was first incubated for 2 days in a rich medium, yeast extract-peptone-dextrose (YPD), at 30 ºC and under 120 rpm of agitation, providing the specific conditions for yeast growth. After that, the culture was centrifugated at 4000 rpm for 10 min, resulting in a differentiation of the biomass (cells) and the liquid media. The cells were than suspended in SWWW and let to grow at the same previously described conditions to acclimate cells in the SWWW. After that *Z. bailii* inoculum is ready to be placed in the MFCs. The MFCs ran in duplicate so the inoculum of the duplicates was the same, to ensure the same inoculum conditions. The volume was split to half and add to each MFC. The average of yeast concentration in the inoculums of all the experiments was 6.6 ± 0.1 logCFU/mL.

3.1.3 - Microbial Fuel Cell Construction and Operation

The MFC design was a SCMFC with a bottle-type configuration (Figure 32) made of glass and acquired to the Normax company. This type of MFC as the name suggests has a design of a bottle and consists of an anodic chamber and an air-cathode. From now on, in this work this MFC design will be named as B-MFC. This configuration was obtained from the modification of a Duran GLS80 bottle with a volume of 500 mL. It presents five sampling ports (two on the top of the

thread and three at the lateral) and a flange for the MEA (more details can be found in Appendix B).

The cathode electrode was a plain carbon cloth coated with 0.5 mg/cm^2 of Pt-black, acquired to FuelCellsEtc. The anode electrode was a carbon fibre graphite brush acquired to the Mill-Rose. The anode and the cathode were separated by a Nafion 117 membrane with an active area of 27 cm^2, acquired to the FuelCellsEtc. To prevent leakage, two rubber gaskets were placed on each side of the membrane. The cathode current collector was made of stainless-steel, has a thickness of 0.5 mm and 143 pores with a diameter of 3 mm and were acquired to Neves & Neves. The cell has also, two end plates to support and seal the MEA and to allow the cell assembly (Figure 33 and Figure 34). The B-MFC worked with a volume of 700 mL (Figure 34).

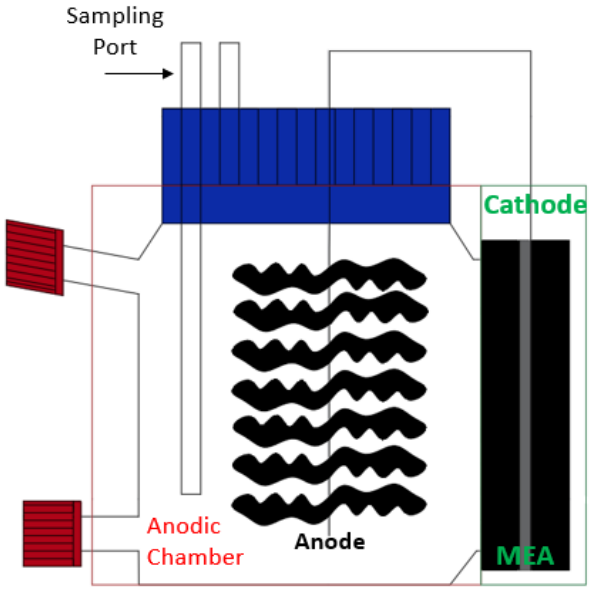

Figure 32: Schematic representation of the B-MFC used in the experiments; MEA – membrane electrode assembly (membrane and cathode electrode); Anode - carbon fibre graphite brush.

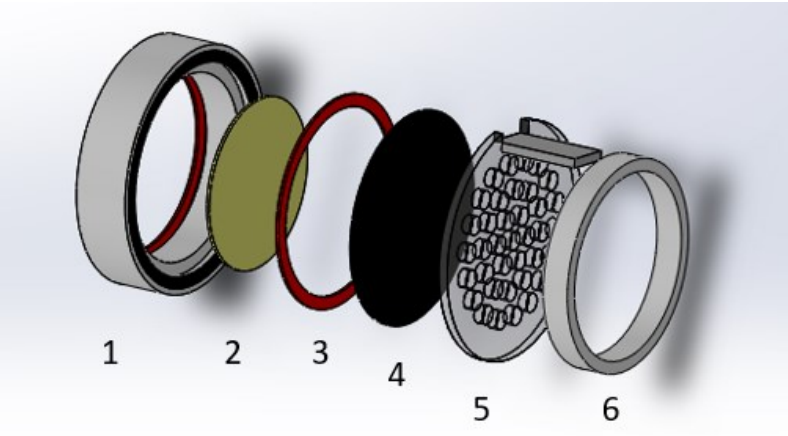

Figure 33: Schematic representation of cathode side; 1 and 6- end plates, 2-Nafion membrane, 3-isolating gasket, 4-cathode electrode and 5- cathode current collector.

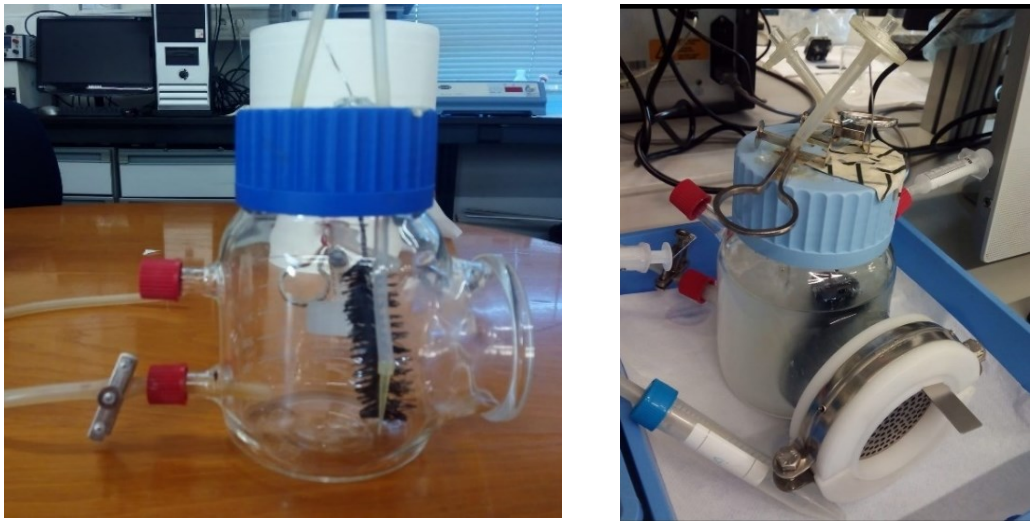

Figure 34: B-MFC used in the experiments; left – Anodic chamber with the anode electrode, carbon brush; right – B-MFC after assembly, with the MEA.

The MFC, anode, cathode and other MFC components such as gaskets were sterilized by autoclaving, at 121ºC during 15 min, followed by oven at 60 ºC until the utilization. The experiments were performed under deaerated conditions at the anode side and at room temperature, 20.1 ± 0.5 ºC that was periodically registered during the experiments. The B-MFC worked with 700 mL of volume at open circuit voltage (OCV), with no external electrical stimulus.

The Nafion 117 was pre-treated before its use following the procedure presented in Figure 35. Nafion 117 was emerged in a 3% H_2O_2 solution at 80 ºC and during 1h, followed by distilled water and by a 0.5 M H_2SO_4 solution at the same temperature and time (80 ºC, 1h). Finally, the membrane was washed and stored in sterilized distilled water at room temperature until needed [179].

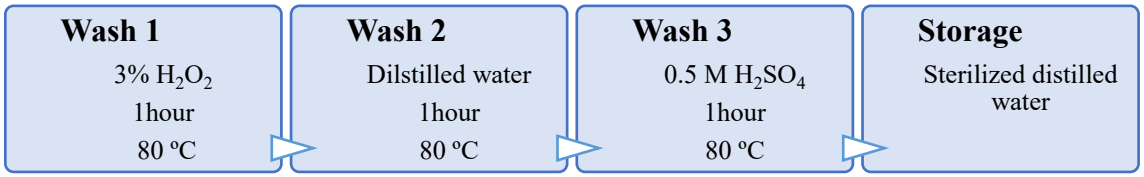

Figure 35: Nafion 117 pre-treatment.

Before the MFC start-up, the MEA components (membrane and cathode electrode) were placed in the B-MFC flange and were screwed by a clamp with 1.5 N.m of torque (Figure 34).

On the following steps, all the procedures were done aseptically by working near the Bunsen burner flame to avoid contamination. *Z. bailii* inoculum (200mL) was transferred to the anode of

the B-MFC, and the remaining volume, 500 mL, was filled with the SWWW slowly and without touching the anode to avoid the yeast cells detachment. Afterwards, a multimeter was connected to the system for measuring and monitoring the reactor voltage (OCV).

Each B-MFC experiment ran in sequential batch mode with batch cycles of 72 hours, running in a total of 360 hours (15 days, 5 batch cycles). The experiments for each condition tested were performed in duplicate. At the end of each cycle, the effluent was renewed. To accomplished that, it was ensured aseptic conditions and it was removed a volume of 500 mL from the reactor and was added an identical volume, 500 mL, of fresh SWWW. Not all the effluent is removed from the reactor to maintain Z. *bailii* viable cells. After the effluent renewal, the B-MFC was sealed and the samples were collected with sterilized syringe for further determination of colony forming units (CFU's). Samples from the removed effluent were also taken to conduct TOC, COD, conductivity and pH analyses. At the end of each experiment, it was performed the biofilm extraction, which allowed the quantification of the biofilm developed at the anode electrode. During the experiments polarization curves were also carried.

3.1.4 - Analytical Analyses

3.1.4.1 - Conductivity and pH

Conductivity and pH were measured for the samples described in the previous sub-chapter. In this way, it were obtained 5 values per experiment. Conductivity was performed by an electrolytic conductivity tester (DiST®4 HI98304, Hanna Instruments) which also measures the temperature and pH by a pH probe (BL931700 and H12114P, Hanna Instruments).

3.1.4.2 - *Zygosaccharomyces bailii* culturability

The *Z. bailii* culturability was obtained by the colony forming units (CFU) measurement. The planktonic cells culturability (referred later in this work as bulk cells) was evaluated at the beginning of each batch cycle so 5 values were obtained per experiment. The cells on the anode surface culturability (referred later as biofilm cells) were measured at the end of the experiment so 1 value was obtained per experiment. The CFU were obtained by the spread-drop plate count on YPD agar petri dishes. Decimal dilutions were performed in triplicate and petri dishes were incubated for 48 hours at 30 ºC before count the cells. The count was performed on dishes that presented CFUs in the range of 25-250 [210].

3.1.4.3 - Biofilm characterization

The biofilm attached to the anode electrode was resuspended in 20 mL of buffer (2 mM Na_3PO_4, 2 mM NaH_2PO_4, 9 mM NaCl and 1 mM KCL, at a pH of 7) and 1 mL was removed to quantify

the CFU. The remaining volume was used to perform the EPS extraction by adding cation exchange resin Dowex® Marathon® C sodium form (Na^+ form, strongly acidic, 20-50 mesh, Sigma-Aldrich, Portugal) and keeping the solution at 400 min^{-1} and 4 ºC for 4 h. Further, the extracellular components, matrix, were separated from the cell, (pellet, by centrifugation at 3777 g for 15 min [211].

The biofilm mass was quantified in terms of total volatile solids (TVS) according to the standard method number 2540 (A to D) from Standard Methods [212]. The homogenized biofilm suspension (5mL of matrix and 5mL of pellet) was used to quantify the biofilm and was performed in triplicate. The TVS is expressed in terms of mass per volume.

For a better insight of the biofilm formed it was estimated the parameter α (CFU/mg), which evaluates the biofilm viability [210]:

$$\alpha = \frac{C_{CFU}}{B_t} \quad (26)$$

C_{CFU} (CFUs/mL) = concentration of CFUs presented at the anode electrode.
B_t (mg/mL) = TVS of the biofilm attached to the anode electrode.

3.1.4.4 - Wastewater Treatment Efficiency

For the SWWW treatment evaluation it were conducted COD and TOC analyses. Each of these parameters were analysed at the end of each batch cycle.

The COD concentration (mgO_2/L) was determined based on the Standard Methods, method number 5220 D [213], which is a potassium dichromate closed reflux, colorimetric method. The COD removal efficiency was calculated with equation 27 which is similar to equation 24:

$$COD_{removal}(\%) = \frac{COD_{SWWW} - COD_{CycleX}}{COD_{SWWW}} \times 100 \quad (27)$$

COD_{SWWW} represents the COD concentration of the SWWW feed to the reactor at the beginning of the experiment (without inoculum), and the COD_{CycleX} represents the COD concentration at the end of the batch cycle (Appendix E). Each sample was analysed in triplicate. Before the COD quantification, the sample removed from the anode compartment was centrifugated at 3777g for 20 min.

The TOC concentration (mg/L) was determined based on the Standard Methods, method number 5310 A [214] and the TOC removal efficiency was calculated using equation 28:

$$TOC_{removal}(\%) = \frac{TOC_{SWWW} - TOC_{CycleX}}{TOC_{SWWW}} \times 100 \quad (28)$$

TOC_{SWWW} represents the TOC concentration of the SWWW feed to the reactor at the beginning of the experiment (without inoculum), and the TOC_{cycleX} represent the TOC concentration at the end of the batch cycle (Appendix F). Each sample was analysed in triplicate. Before the TOC quantification, the sample removed from the anode compartment was centrifugated at 3777g during 20 min.

3.1.5 - Polarization and Power Density Curves

The first polarization curve was done when the cells are presenting steady OCV, the voltage measured by the multimeter is constant indicating the system stabilization. The polarizations were done one day before the end of the batch cycle. By that, 2 polarization curves were realized at each experiment.

These analyses were performed using a ZENNIUM electrochemical workstation (ZAHNER - Eletrik) and in galvanostatic mode, imposing a current and measuring the voltage. The cell voltage was registered after 5 min of setting the current, to ensure that the system is near steady-state conditions. The current value imposed on the MFCs starts in $5x10^{-4}$ mA, subsequently increased to $1x10^{-3}$ mA, than to $3x10^{-3}$ mA, $6x10^{-3}$ A, $9x10^{-3}$ mA, $1x10^{-2}$ mA and $3x10^{-2}$ mA. This procedure was conducted until reaching 50 mV, to avoid affecting the yeast cells. These measurements allow obtaining the polarization curves that are a representation of the voltage (mV) as a function of the current (mA) or the current density (mA/m^2), the current normalizing per the membrane active area.

Power density (P) can be calculated by multiplying the current and the voltage and normalizing per PEM active area (equation 29),

$$P = \frac{I}{A} \times U \quad (29)$$

3.1.6 - Statistical Analysis

The experimental data were analysed and processed in the excel program. The analysis were performed at least in duplicate, in some cases triplicate, namely for the COD and TOC removal rate, culturability, total solids and total volatile solids. From a statistical analysis the mean and the standard errors were calculated using excel commands and the relative error was determined following the procedure described in Appendix I. Additionally, for the COD and TOC removal it was also determined the covariance and the correlation factor (CC) using the formulas presented in Appendix G. The covariance gives a sense of the direction, if (>0) the two variables move

together, if (<0) the two variables move in opposite directions, if (=0) the two variables are independent, covariance doesn't have a defined range. The CC informs on causality, how a variable is related with other, and its values are between -1 and 1, this is ($-1 \leq CC \leq 1$). If $-1 < CC < 0$ there is an imperfect negative correlation, if $CC = -1$ there is a perfect negative correlation, if $0 < CC < 1$ there is an imperfect positive correlation, if $CC = 1$ there is a perfect positive correlation, in this case the entire variability of one variable is explained by the other.

3.2 - Results and discussion

This chapter describes the results of the two experiments performed, A_0 and A_1, and its discussion. Table 12 depicts the features of A_0 and A_1 experiments.

Table 12: Description of the A_0 and A_1 experiments.

Experiment	Medium	Inoculum	Anode (diameter)	Cathode (catalyst)	Current collector (pore size)	Membrane
A_0	SWWW	*Z. bailii*	Graphite Brush (⌀ 2.5 cm)	Carbon cloth 0.5 mgPt/cm^2	Stainless Steel (3 mm)	Nafion 117
A_1	SWWW	*Z. bailii*	Graphite Brush (⌀ 5 cm)	Carbon cloth 0.5 mgPt/cm^2	Stainless Steel (3 mm)	Nafion117

As can be seen, the anode of A_1 experiment has 2x the diameter of the anode of the A_0 experiment. Therefore, the effect of the anode size on the B-MFC efficiency was the aim of this study.

3.2.1 - Conductivity and pH

As mentioned, the conductivity and the pH are important parameters that influence the MFC performance. Figure 36 presents the pH and conductivity (mS/cm) values for the 5 cycles of both experiments. Additional data is present in Appendix D.

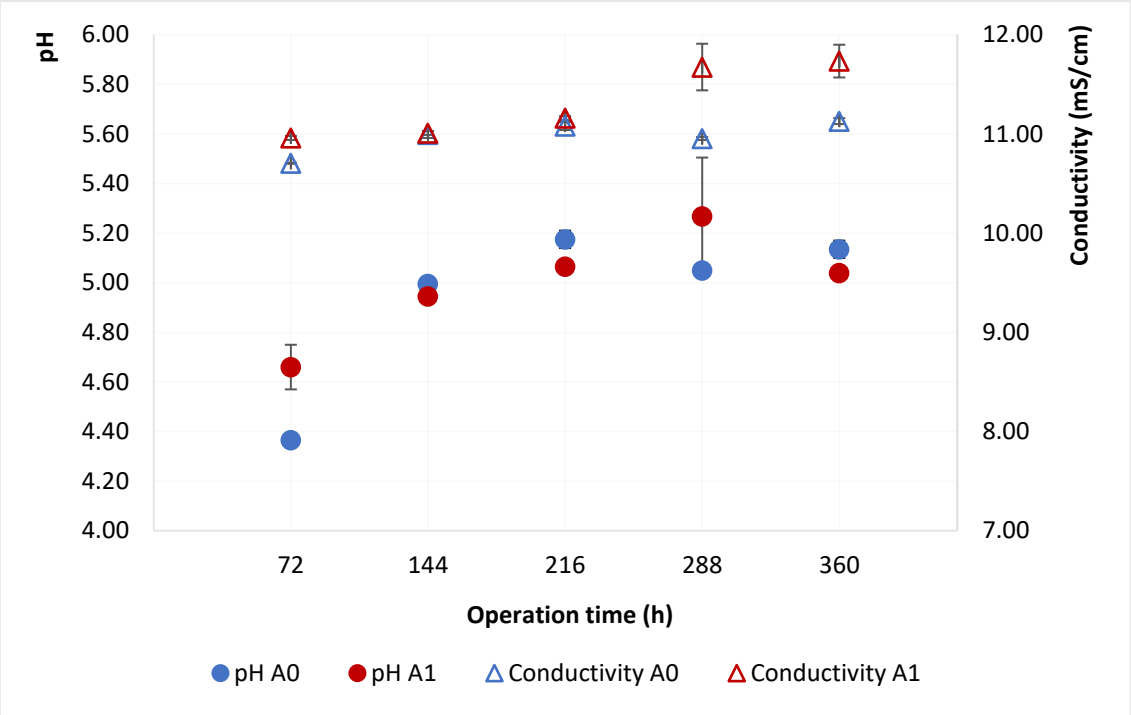

Figure 36: Representation of pH and conductivity of A_0 and A_1.

The pH values of A_0 ranged from 4.37 ± 0.015 to 5.18 ± 0.035 and of A_1 ranged from 4.66 ± 0.09 to 5.27 ± 0.238. Both experiments exhibited the lowest pH value at the 72h of operation. Deviations after the stabilization of the system, at 216h to 360h presented the smallest flotation values: 1% to A_0 and 4% to A_1 which could indicate a good signal of stability. The pH of SWWW was adjusted to 7, however after 72h the pH decreased at least 2 units on each batch cycle. The anode acidification is a well-known phenomenon and is commonly attributed to the production of protons by microbial activity and consequent accumulation by the inefficient proton diffusion through the PEM [62]. Also, can be due to the *Z. bailii* metabolic activity, the degradation of glucose to acetic acid and other by-products [215].

The conductivity values of A_0 ranged from 10.71 ± 0.01 mS/cm to 11.13 ± 0.03 mS/cm and A_1 from 10.96 ± 0.02 mS/cm to 11.74 ± 0.17 mS/cm. The amplitude of the maximum and minimum values between the same experience is short (4% and 6% for A_0 and A_1, respectively) which could indicate stability of the system. Analysing the conductivity behaviour, at 144h and 216h the values are almost equal for both experiments, representing a deviation less than ±0.05. For relative error besides 288 hours with (6%), both systems presented similar conductivity behaviour in the hours of study (<5%). However, A_1 achieved higher conductivity compared with A_0 and an increasing trend over the operating time, the stability of bulk cells in experiment A_1 (as shown next in Figure 37) was higher than A_0 what could justify the better value of conductivity seen.

The overall conductivity range presented by SWWW can be considered favourable to the MFC performance since it approximates the optimal conductive capacity of the solution which is 20

mS/cm [16], [85]. Furthermore, the conductivity is found to be higher than other WWs such as 5.6 mS/cm for a rice milling industry WW, 1.2 to 3.3 mS/cm for domestic WW and 3.23 mS/cm for brewery WW [85], [216], [217].

3.2.2 - *Zygosaccharomyces bailii* culturability and biofilm characterization

The CFU assay was carried out to quantify the number of culturable yeast cells in the bulk and at the anode and evaluate possible contaminations inside the anodic chamber. Figure 37 presents the yeast concentration, in logCFU/mL during the operation time.

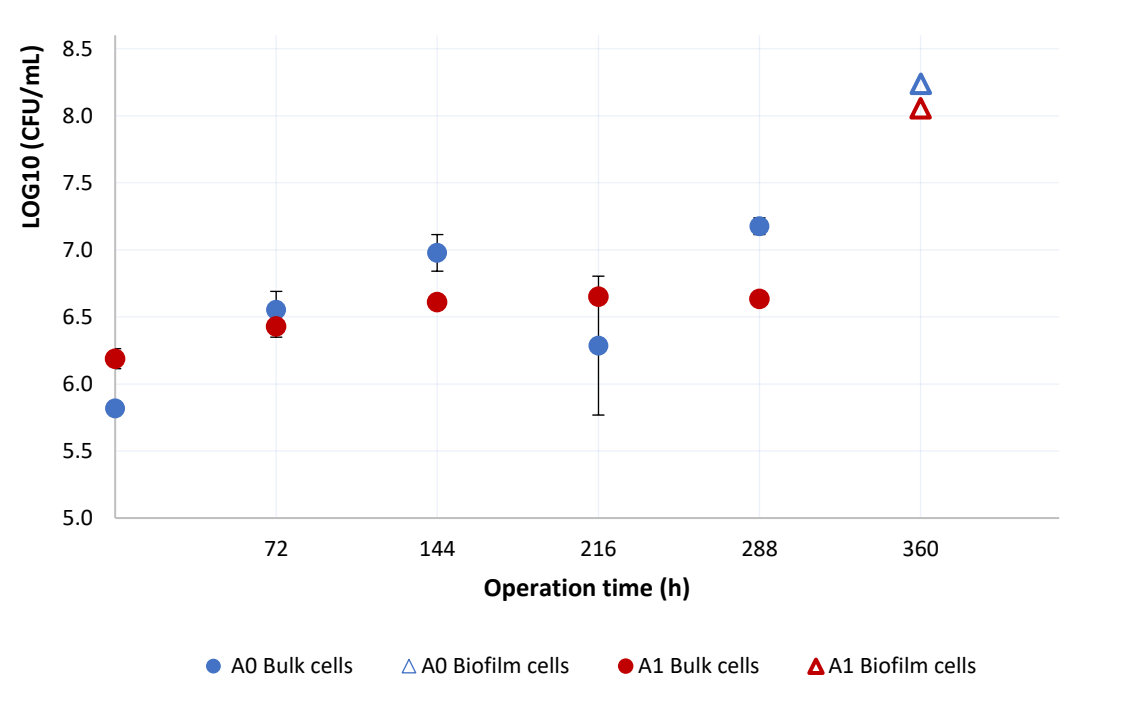

Figure 37: Z. bailii concentration in the bulk at the beginning of each batch cycle (0h, 72h, 144h, 216h and 288h) and on the anode (360h).

In the bulk, at 0h, 72h and 144h, it was observer a similar behaviour among both experiments, showing an increase of the cells concentration during the operation time. In experiment A_1 from 144h to the end, the yeast cells growth remains practically unaltered, exhibiting stability over the cycles. The experiment A_0 followed a different path, with a decrease of 12% from 144h to 216h of operation.

The maximum concentration achieved was 7.18 ± 0.06 logCFU/mL (288h) and 6.65 ± 0.04 logCFU/mL (216h) for A_0 and A_1, respectively. The highest similarity among experiments was seen at 72 h (± 0.06) and the higher deviation was seen at 288 hours (± 0.27).

As mentioned, Figure 37 also presents the culturability on the anode at the end of experiments, biofilm. Both experiments presented the highest culturability at the biofilm, indicating an

adhesion of the cells to the anode electrode. A_0 achieved the highest culturability, 8.24 logCFU/mL compared with 8.06 logCFU/mL in A_1, the relative error was 2% and the deviation was ± 0.09, by that the adhesion and grow in the anode electrodes was similar in both experiments.

Table 13 presents the TVS and α for both experiments.

Table 13: TVS and α values for A_0 and A_1.

	A_0	A_1	Relative error
TVS (mg/L)	2.83 ± 0.17	3.13 ± 0.02	9%
log (α)	7.79	7.56	-

TVS are higher in experiment A_1 indicating more organic content in the biofilm of experiment A_1 than experiment A_0. In addition, A_1 presented a small deviation between the duplicates (± 0.02) than A_0 (± 0.165). The α was higher in experiment A_0, meaning that the viability of cells in relation with the biofilm dry weight was greater in experiment A_0, what is related with the low TVS found in this experiment. These results go against what is expected, since usually higher electrode areas enable the adhesion of more cells to its surface and consequently more electron acceptance contributing for better electrochemistry processes [218]. A_1 presents an electrode with the double of filaments length, which increase substantially the area of the electrode, providing more area for cell adherence, as shown in Figure 38. However, results showed the opposite.

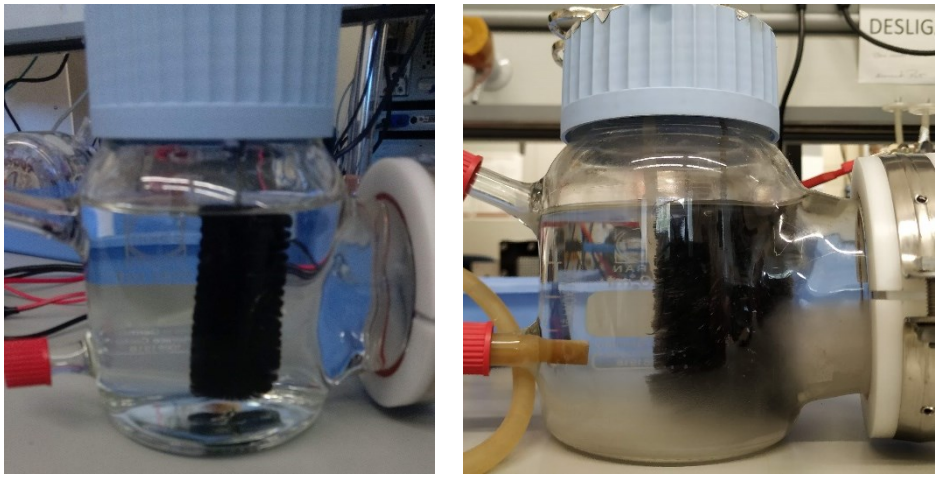

Figure 38: Experiments A_0 (on the left) and A_1 (on the right) evidencing the size differences on anodes.

A_1 presents a higher area, however, the filaments are more distant from each other, and A_0 presents a more dense configuration. Based on that, it could explain the lowest viability on the A_1 experiment. In fact, the anode structure of A_1 can facilitate cells detachment in the edge of the filaments at the time of SWWW renew since they not seem so "sheltered" as in A_0, also the extend length of the filaments can possible provide a weak cohesion and difficult cell adhesion.

3.2.3 - Wastewater treatment efficiency

Table 14 presents the average values of CODremoval and TOCremoval after the stabilization of the system, when electrochemistry stability of the MFC was shown, in the end of the last three cycles: at 216h, 288h and 360h. Additional data can be visualized in (appendix E,F).

Table 14: Average values of CODremoval and TOCremoval for A_0 and A_1 for 216h, 288h, and 360h working period, as well the relative error.

Average $COD_{removal}$ (%)			Average $TOC_{removal}$ (%)		
A_0	A_1	Relative error (%)	A_0	A_1	Relative Error (%)
25	34	25	50	61	17

Both the COD and the TOC removal rates were higher in A_1 than in A_0, the relative error of both parameters between the experiments reflects the superiority of A_1, with higher 25% COD removal and 17% TOC removal.

The COD removal rates are low when compared with other MFCs used for the WWW treatment. Cusick et. al, [219] achieved in a SCMFC a COD removal of 65%. Rengasamy and Berchmans [134] achieved 41% in a DCMFC. Penteado et. al, [219] presented a COD removal lower, 17%, and attributed that to an unbalanced nutrients/COD ratio [86], [219]. The lower COD removal rates found may be due to a bad homogenization when preparing the solutions for the COD determination.

Figure 39 presents the TOCremoval at the end of the last three cycles: at 216h, 288h and 360h.

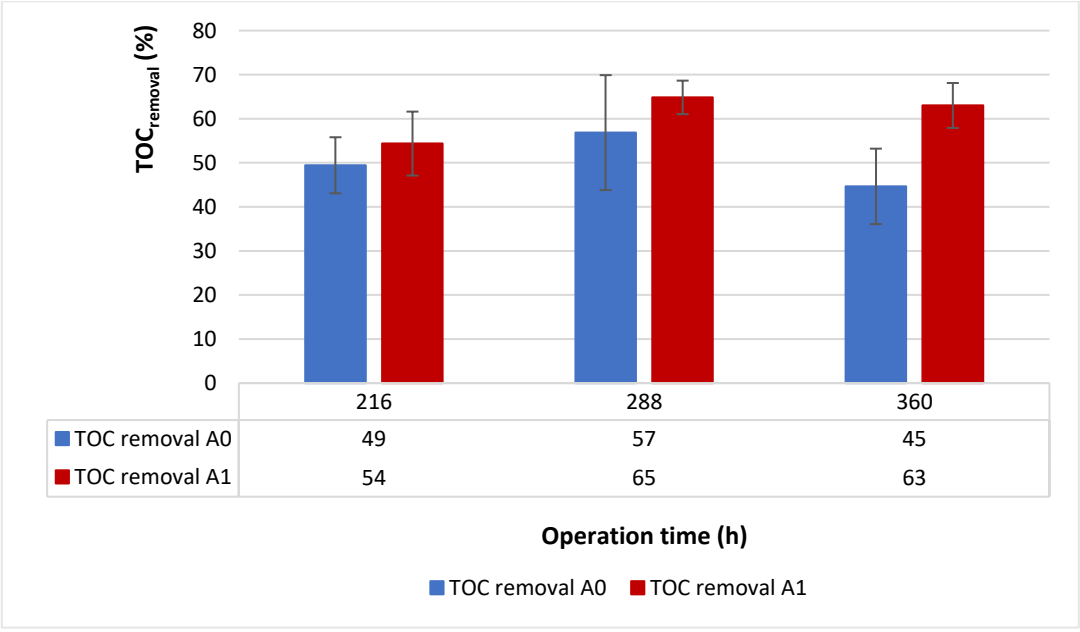

Figure 39: Total organic carbon removal for both experiments.

Both experiments present a similar TOC removal at 216h with a fluctuation over than 9%, although did not show similarity in the subsequent hours, at 288 h the fluctuation was over than 12% and was higher at 360 h, fluctuation over 29%. Overall, A_1 had a better performance regarding the TOC removal and almost an equal TOC removal at 288h and 360h. At the same time experiment from 288h to 360h, A_0 showed a big decrease (21%). Crossing the culturability of the bulk cells with the COD and TOC removal rate in A_0 it is possible to admit that important differences between duplicates exist. Another possibility is that the deaerated conditions were not provided properly on one of the duplicates and *Z. bailii* adopted fermentation path and ethanol (or other end products and biomass production) may had been produced [215]. This can support the accentuate decrease of the TOC removal since based on this possibility organic compounds concentration increased.

The highest TOC removal was achieved in both experiments at 288h, 57% and 65% for A_0 and A_1, respectively, in A_0 at this time was present the highest bulk cells (logCFU/mL) value, what can be the major reason to this TOC removal, in A_1 the bulk cells (logCFU/mL) value was almost unaltered in the last 3 cycles so the reason may be related with the overall stability of the system. Finally, once again the deviations presented in (Figure 39) indicate better approximation between the duplicates for A_1 than for A_0.

For better discussion was determined the COD/TOC relation that is present in Table 15.

Table 15: Ratio COD/TOC of A_0 and A_1.

	A_0	**A_1**
Time (h)	**COD/TOC**	**COD/TOC**
216	3.31 ± 0.16	3.79 ± 0.02
288	3.44 ± 0.01	3.50 ± 0.15
360	3.11 ± 0.04	3.66 ± 0.15

This ratio provides information about the degradation of organic matter by *Z. bailii* during the working period. Since TOC represents only the organic matter and COD account for organic and inorganic material, an equilibrium on this ratio during the working period indicates that the yeast activity present an equilibrated organic matter degradation without the formation of products from the fermentative activity.

As shown in Table 15, the A_0 presents a COD/TOC rate range from 3.44 to 3.11 (10%), what indicates a similar organic matter content degradation, the great fluctuation occurs from 288h to 360h (10%), 216h and 288h had a similar organic matter degradation content (4%). The range in A_1 is between 3.79 and 3.50 (8%), a lower value, what can infer a correct and equilibrated degradation of organic matter.

From the covariance determination is state that both variables move together in both experiences (>0, appendix G). In A_0 variables are very related since coefficient correlation is 0.9 (appendix G). In A_1 they are extremely related since coefficient value is 1 (appendix G). Despite the differences of COD and TOC removal between both experiments the behaviour is the same, COD removal is related with the TOC removal and vice-versa, from the SWWW composition there are no inorganic compounds, also if fermentative path occur the end products are also organics compounds, results that the COD removal and TOC removal are side by side, if one increases the other too increases, if one decreases the other too decreases.

3.2.4 - Polarization and Power Density Curves

Figure 40 presents the polarization and power density curves for A_0 and A_1. The polarization curve is resultant of the average of 4 polarization curves per experiment, representing the overall experiment performance (polarizations performed at the last two batch cycles, which present better replicability, and in duplicate for each reactor). The results of the individual polarization and power density measurements can be found in Appendix H.

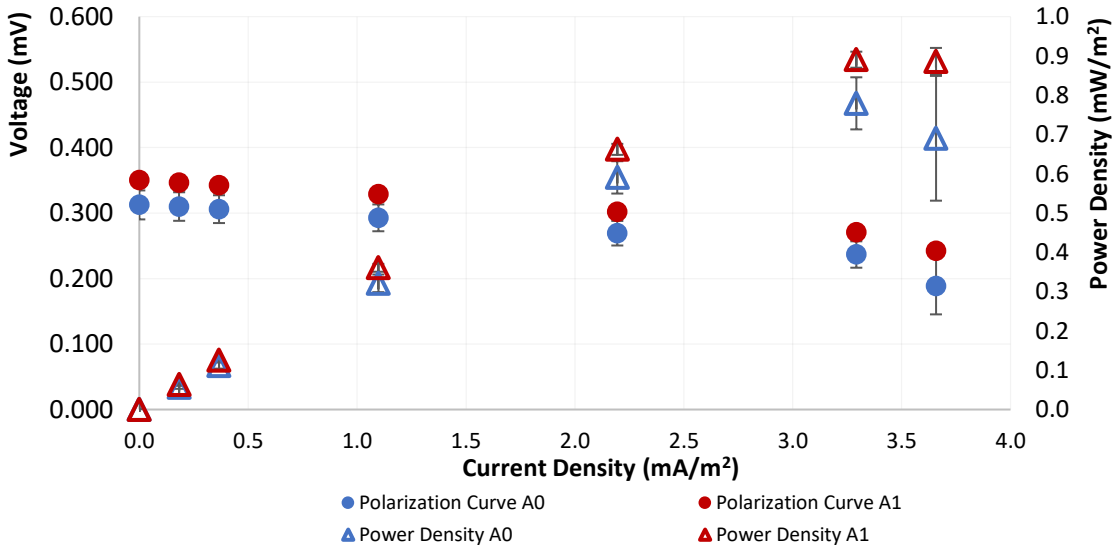

Figure 40: Polarization and power density curves for A0 and A1.

A_0 achieved a maximum power density of 0.78 ± 0.07 (mW/m^2) and A_1 achieved a maximum power density of 0.89 ± 0.03 (mW/m^2) at a current density of 3.66 (mA/m^2). This states that A_1 presented better performance than A_0, with a relative error of 12%. From Table 14 it was seen that A_1 presented a higher COD removal rate, which could indicate a better degradation of the organic matter increasing the power generation.

The highest OCV value was for A_1, 0.350 ± 0.01 mV, compared with 0.313 ± 0.02 mV from A_0. A_1 was able to toughly sustain the current imposed during the tests with more stability, generating a better power output. As already mentioned, a higher anode area provides a higher cells adhesion

and a decrease of the cell internal resistance that may increase de power density [220]. Despite that, the results of the cell culturability show exactly the opposite. The higher anode electrode area could not provide high cell adhesion but may be responsible for changing an important parameter that influences the MFC performance: the distance between the anode and cathode electrodes. A look on Figure 38 allows to see the difference on the distance of the anode filaments and MEA for both MFCs. This decrease on the distance could overpass some protons diffusion limitations towards the cathode. Moreover, besides a lower viability, the distribution of cells in the anode surface may be improved and could provide high direct electron transfer.

The error in power density start to be noticeable at a current of 2.0 (mA/m^2), although for experiment A_1 they are attenuated but are very significant for experiment A_0, especially for the 360h, what once again suggests the differences in duplicates of A_0. The error its related with the difficult in stablish a pseudo-steady-state condition on the MFC that seems to be harder after 2.0 (mA/m^2), the reason can be related with mass transfer losses that are more evident at high currents, thus, while recording in a galvanostatic method the steady state can be affected by changes in the biofilm, in the concentration of substrate, or concentration of electroactive metabolites, changing with potential and time [139]. As mentioned A_0 was more vulnerable to error what must be related once again with a worse overall stability of the system (bulk cells fluctuation over time).

Table 16 summarizes the relative errors between the experiments for the maximum voltage and power density achieved.

Table 16: Relative error for the voltage and power density at 288h and 360h.

Time (h)	A_0	A_1	Relative error	A_0	A_1	Relative error
	U (mV)		%	P (mW/m^2)		%
288	0.33	0.35	6	0.84	0.90	7
360	0.30	0.35	14	0.71	0.87	18

At 288h experiments show a relative error lower than 10% for both measurements which means Z. *bailii* activity was similar as well as the response of the system. The distance of relative error when evaluating the parameters at 360h is greater than 288h, and results for experiment A_1 are better.

Figure 41 relates the maximum power density achieved with the COD removal at 288h and 360h for both experiments. To be precise, the polarization curves were performed one day before the sampling harvest for the COD measurements. However, to facilitate the comparison between these parameters, the time is assumed to be the same, corresponding at the end of the batch cycle.

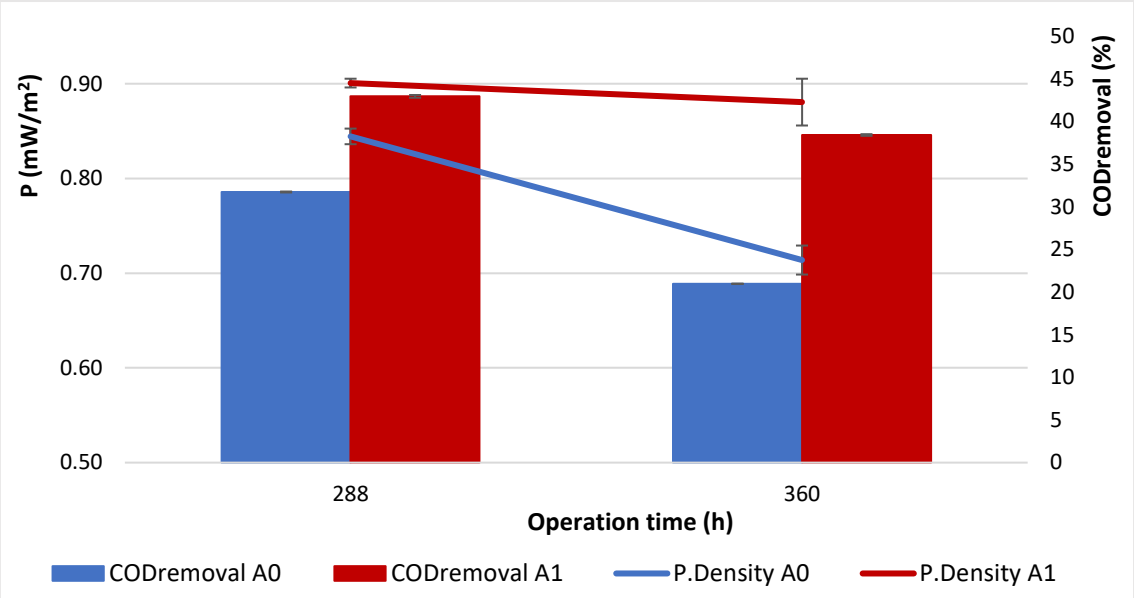

Figure 41: Relation between CODremoval and power density at 288h and 360h for A_0 and A_1.

As can be seen, A_0 presented a lower COD removal and power density than A_1. Although, both experiments decreased performance over the time. A_0 presented a reduction of 34% and 15% for, respectively, the COD removal and power density, while A_1 presented only a reduction of 11% and 2% for, respectively, COD removal and power density.

Figure 41 also shows that with higher values of power density higher COD removal rates are found. However, both parameters are influenced by microbial activity meaning that this cannot be assumed as a direct relation. This analyse presents the electrochemistry component related with activity in the electrode and wastewater treatment component related with activity in the solution.

3.3 - Conclusions

To infer the capability of a MFC using yeast *Z. bailii* to perfom the treatment of a SWWW and simultaneously produce energy, typical performance parameters, such as COD removal and power density were assigned. Experience A_1 with a large anode electrode surface granted a higher power density (0.89 mW/m^2) and COD removal efficiency (34%) than experience A_0. For both studies, the best appraisal was reflected at 288h of the working period although the results are low that the desirable.

Z. bailii presented similar results concerning the UFCs/ml in the biofilm, 8.24 logUFC/mL and 8.06 logUFC/mL for experiment A_0 and experiment A_1 respectively. The quantification of the total volatile solids reveals more organic content in A_1. Results indicate that *Z. bailii* adhered on the anodes, indicating biofilm formation. Besides, it was possible to see a "white deposit" on the electrodes, strongly suggesting the same. However, further confirmation is mandatory.

The measurement of pH, conductivity, and ratio COD/TOC also highlighted the behaviour of *Z. bailii* for the submitted operations and environmental conditions, where both B-MFC had approximated results, conductivity values were in the range of 10.70 to 11.90 uS/cm^2 what is a good conductivity in solution for MFC, pH values without great deviation from pH=5, and a equilibrated ratio COD/TOC in the last three batch cycles. On this analysis (pH and conductivity) it is possible to infer that replicability between the duplicates was very good however others analyses didn´t present the same results, like the concentration of bulk cells in experiment A_0, or the power density at high currents. For experiment A_0 should had been done another experiment (triplicate).

From the literature is visible the capacity of *Z. bailii* to grow in winery wastewater due to is characteristics, as being the most preservative-resistant organism known, an aggressive food spoilage microorganism, highly fermentative, etc. In this study, as shown by the bulk cells concentration *Z. bailii* grow on the SWWW at the anodic chamber of the B-MFC, however the COD removal was lower than the desirable.

Concluding, the structure and surface area of the anode electrode was a crucial system design that provided better performance of experiment A_1. In relation to the surface area of the electrode, experiment A_1 should have shown higher yeast adhesion due to higher surface area although the adhesion was higher in experiment A_0, what is related with the structure of the anode electrode, the dense and short filaments of experiment A_0 seem to give more protection to biofilm cohesion and better adhesion than the long filaments of experiment A_1. Experiment A_1 on other way presented a higher biofilm organic content (evaluated by TVS) and the long filaments might have improve the distribution of cells in the anode surface with a consequent enhance of direct electrons transfer, alongside implied a short electrode spacing that could overpass protons diffusion limitation towards the cathode, this factors combined turn up to be responsible for the better power density. Techniques to characterize the matrix of the biofilm in terms of sugars and polysaccharides and biofilm thickness should have been conducted.

Infer that all the reactor design and the membrane-electrode-assembly turn up to be a coherent unit since no water leakage or unwanted contaminations were seen in the 360 hours working period through experiments.

4

Final Remarks

MFCs are a promising and renewable technology to incorporate in the electricity grid and substitute conventional wastewater treatment plants if energy production can be strengthened and the wastewater treatment efficiencies meet the legislation values. An increase of the MFC performance depend on extensive, complex and detailed factors since are involved three branches of studies, chemistry, energy and microbiology.

The scope of research is vast and difficult, concerning the lack of knowledge of different influencing aspects, such as biofilm formation, oxygen reduction rate, electron transfer, electrode material, among others. EAB and biofilm activity are related with the intracellular and extracellular electrons transfer and transport mechanisms affecting the power generation, result of internal resistance that negatively affects the power production. Therefore, better knowledge and forms to reduce it need to appear. Electron transfer in microorganisms respiratory chain affects the energy use and energy generated (Figure 9), understand the respiratory chain and manage to move the electrons to an early potential stage of the respiratory chain will increase the energy generation. The surface chemistry and configuration of electrode materials affect the power output, its necessary to find the best relations. Concerning the biofilm formation and quantification, the use of characterization techniques should be realized to spread and compare reliable and interesting results with better insight.

It was mentioned the potential energy hold in wastewaters (3-10 times the energy required to treat it), what is an incredible motivation for developing MFC technology, since the inherent energy in the organic content of the WW can be sufficient to treat hit, stepping in the sustainability. WW can be multiform, complex, recalcitrant and high strength, becoming hard or impossible to singular microorganism to break and transform complex organic compounds in simple ones, to fight this hassle consortium of microbes have better characteristics and applicability in diverse WWT since they have superior ability to break the complex organics compounds and may provide higher power density. By that finding the best microbe communities suitable to the type of WW to treat is a step to take. In this picture and to grant better magnitude it is also important to achieve

the best conductivity in solution and adjust the pH to a proper value towards the development of the microorganisms.

As in all projects, capital can be the barrier or the approval, reducing costs is a priority, based on this assumption MFC have different defined possibilities. Membranes need to be effective, with high proton transfer, antifouling properties, low oxygen cross over, and long-term use, Nafion is a great choice but very expensive, Selemion can be an alternative, also recent studies in hybrid membranes and membrane materials derived from nanotechnology infer good properties and low cost. Referring electrodes, they present more options, and some are very interesting in capital cost, as carbon cloth and carbon paper, ensure the long-term use can be a problem, especially when treating wastewater. Cathodes configuration as air cathodes are cost acceptable but need the use of catalyst (as Pt) for achieve considerable power output what enhance the costs, at the time catalyst alternatives are few, almost restricted to metal catalysts (expensive), nonprecious metals or biocatalyst that seems promising. Current collectors are considered less costly in relation to cathodes, membranes, catalyst, and anodes, so it is more important to make an approach to its long-term and efficiency rather than costs. The reactor chamber is reported in the initial investment but since degradation it is not a problem the costly-effective approach is not of concern. It is important to have in mind that design and choice of materials is in continuously development and improvement.

Investments and reliability are of concern in a research project, before starting a MFC study, deep evaluation in design configuration, materials and experimental conditions must be prioritized. The experimental research should relay in reproducibility and replicability, aspects to consider are the electrodes areas and materials, space between electrodes, type of current collector, microorganisms, membrane thickness, material, and active area, working volume, among others. A single chamber MFC with a membrane electrode assembly air exposed seems to be a good choice for studies, it has several known advantages, to mention, the short electrode spacing that could provide better power output, less costs due to no need of aeration and the sustainability and availability of the air cathode.

In the last decade research on MFCs was boosted, focusing different types of substrates, configurations, microorganisms, types of materials, but is still need a prominence on bigger scales. Right investments for the implementation of MFCs in remote regions with low electrical facilities as well insufficient wastewater treatments plants is a reality that should be planned. Also, integrating MFCs in wastewater treatments plants to decrease the costs of activated sludge systems seems to be a possibility in a near future

5

References

[1] A. Vainio, V. Varho, P. Tapio, A. Pulkka and R. Paloniemi, "Citizens' images of a sustainable energy transition," *Energy,* vol. 183, pp. 606-616, 2019.

[2] H. Vijay, R. Bocca, P. Gomez, S. Dahlke and M. Bazilian, "The energy transitions index: An analytic framework for understanding the evolving global energy system," *Energy Strategy Reviews,* vol. 26, no. 100382, 2019.

[3] M. Tvaronaviciene, J. Baublys, J. Raudeliuniene and D. Jatautaitė, "Global energy consumption peculiarities and energy sources: Role of renewables," in *Energy Transformation Towards Sustainability*, Elsevier, 2019, pp. 1-49.

[4] M. &. Eddy, G. Tchobanoglous, F. L. Burton and H. D. Stensel, Wastewater Engineering Treatment Disposal Reuse (5th edition), Mcgraw-Hill, 2013.

[5] A. Roshana and M. Kumar, "Water end-use estimation can support the urban water crisis management: A critical review," *Journal of Environmental Management,* vol. 268, no. 110663, 2020.

[6] W.-W. Li and H.-Q. Yu, "Advances in Energy-Producing Anaerobic Biotechnologies for Municipal Wastewater Treatment," *Engineering,* vol. 2, pp. 438-446, 2016.

[7] M. S. Miah, R. Kazi, N. U. U. Uddin and Bhuiyan, "Effluent Treatment Plant: A Tool for Protecting Environment from Pollution," *University Journal of Business,* vol. 33, 2012.

[8] P. Aelterman, K. Rabaey, P. Clauwaert and W. Verstraete, "Microbial fuel cells for wastewater treatment," *Water Science & Technology ,* vol. 54, pp. 9-15, 2006.

[9] V. G. Gude, "Wastewater treatment in microbial fuel cells - an overview," *Journal of Cleaner Production,* vol. 122, pp. 287-307, 2016.

[10] P. K. Gaur, Principles of Water and Wastewater Treatment, SBS Publishers & Distributors Ltd, 2012.

[11] E. D.Penteado, C. M. Fernandez-Marchante, M. Zaiat, P. Cañizares, E. R. Gonzalez and M. A. Rodrigo, "Influence of sludge age on the performance of MFC treating winery wastewater," *Chemosphere,* vol. 151, pp. 163-170, 2016.

[12] S. S. Kumara, V. Kumara, S. K. Malyan, J. Sharma, T. Mathimani, M. S. Maskarenj, P. C. Ghosh and A. Pugazhendhie, "Microbial fuel cells (MFCs) for bioelectrochemical treatment of different wastewater streams," *Fuel,* vol. 254, no. 115526, 2019.

[13] K. Rabaey, G. Lissenns and W. William Verstraete, "Microbial fuel cells: Performances and perspectives," in *Biofuels for Fuel Cells: Renewable Energy from Biomass Fermentation*, IWA Publishing, 2005, pp. 377-399.

[14] M. Do, H. Ngo, W. Guo, Y.Liu, S. Chang, D. Nguyen, L. Nghieem and B. Ni, "Challenges in the application of microbial fuel cells to wastewater treatment and energy production: A mini review," *Science of The Total Environment,* vol. 639, pp. 910-920, 2018.

[15] P. L. McCarty, J. Bae and J. Kim, "Domestic Wastewater Treatment as a Net Energy Producer-Can This be Achieved?," *Environmental Science & Technology,* vol. 45, pp. 7100-7106, 2011.

[16] L. He, Y. Chen, H. Lu, X. Cheng, B. Chang and Z. Wang, "Advances in microbial fuel cells for wastewater treatment," *Renewable and Sustainable Energy Reviews,* vol. 71, pp. 388-403, 2017.

[17] H. R. Schultz, "Global Climate Change, Sustainability, and Some Challenges for Grape and Wine Production," *Journal of Wine Economics,* vol. 11, pp. 181-200, 2016.

[18] H. Fraga, I. G. d. C. Atauri, A. C. Malheiro, J. Moutinho-Pereira and J. A. Santos, "Viticulture in Portugal: A review of recent trends and climate change projections," *Journal International des Sciences de la Vigne et du Vin,* vol. 51, pp. 61-69, 2017.

[19] K. Mosse, A. Patti, E. Christen and T. Cavagnaro, "Review: Winery wastewater quality and treatment optionsin Australia," *Australian Journal of Grape and Wine Research,* vol. 17, pp. 111 - 122, 2011.

[20] http://www.oiv.int/, "International Organisation of Vine and Wine," 2020.

[21] L. Ioannou, G. Puma and D. Fatta-Kassinos, "Treatment of winery wastewater by physicochemical, biological and advanced processes: A review," *Journal of Hazardous Materials,* vol. 286, pp. 343-368, 2014.

[22] S. Berchmans, A. Palaniappan and R. Karthikeyan, "Electrical Energy from Wineries—A New Approach Using Microbial Fuel Cells," in *Food Industry Wastes: Assessment and Recuperation of Commodities (1st Edition)*, Elsevier, 2013, pp. 237-247.

[23] A. Saraiva, G. Rodrigues, H. Mamede, J. Silvestre, I. Dias, M. Feliciano, P. O. e. Silva and M. Oliveira, "The impact of the winery's wastewater treatment system on the winery water footprint," *Water Science and Technology,* vol. 80, p. 1823–1831, 2019.

[24] M. Oliveira, C. Cunha-Queda and E. C. N. F. D. Duarte, "Aerobic treatment of winery wastewater with the aim of water reuse," *Water Science & Technology,* vol. 60, pp. 1217-1223, 2009.

[25] H. L. Shepherd, M. E. Grismer and G. Tchobanoglous, "Treatment of High-Strength Winery Wastewater Using a Subsurface-Flow Constructed Wetland," *Water and Environment Journal ,* vol. 73, pp. 394-403, 2001.

[26] K. Garcia, "Winery Process Wastewater Management Handbook: Best Practices and Technologies," Sustainable Winegrowing British Columbia, 2018.

[27] W. C. Quayle, A. Fattore, R. Zandona, E. W. Christen and M. Arienzo, "Evaluation of Organic Matter Concentration in Winery Wastewater: A case study from Australia," *Water Science & Technology,* vol. 60, pp. 2521-2528, 2009.

[28] P. Day, J. Cribb, A.-M. Boland, M. Shanahan, D. D. Oemcke, D. A. Kuma, G. Cowey, K. Forsyth and A. Burgi, "Winery Wastewater Management & Recycling: Operational Guidelines," Grape and Wine Research and Development Corporation, 2011.

[29] F. Jourjon, S. Khaldi, M. Reveillere, C. Thibault, A. Poulard, P. Chretien and J. Bednar, "Microbiological characterization of winery effluents: An inventory of the sites for different treatment systems," *Water Science Technology,* vol. 51, pp. 19-26., Water Sci Technol 2005.

[30] N. Kuanyshev, G. M. Adamo, D. Porro and P. Branduardi, "The spoilage yeast Zygosaccharomyces bailii: Foe or friend?," *Yeast,* vol. 34, pp. 359-370, 2017.

[31] D. S. Thomas and R. R. Davenport, "Zygosaccharomyces bailii- a profile of characteristics and spoilage activities," *Food Microbiology,* vol. 2, pp. 157-169, 1985.

[32] M. Stratford and C. J. Capell, "SOFT DRINKS | Microbiology," in *Encyclopedia of Food Sciences and Nutrition (2nd Edition)*, Elsevier Science, 2003, pp. 5358-5366.

[33] P. Kalathenos, J. Sutherland and T. Roberts, "Resistance of some wine spoilage yeasts to combinations of ethanol and acids present in wine," *Journal of Applied Bacteriology,* vol. 78, pp. 245-250.

[34] P. Branduardi, M. Valli, L. Brambilla, M. Sauer, L. Alberghina and D. Porro, "The yeast Zygosaccharomyces bailii: a new host for heterologous protein production, secretion and for metabolic engineering applications," *FEMS Yeast Research,* vol. 4, pp. 493-504, 2004.

[35] S. A. James and M. Stratford, "Yeast Spoilage of Foods and Beverages," in *The Yeasts (5th Edition)*, Elsevier, 2011, pp. 53-63.

[36] B. Bryson, A Short History of Nearly Everything, Black Swan, 2003.

[37] A. L. Dicks and D. A. J. Rand, "Introducing Fuel Cells," in *Fuel Cell Systems Explained (3rd Edition)*, John Wiley & Sons Ltd., 2018.

[38] M. Faraday, Experimental Researches in Electricity, Dover Publications, 2004.

[39] D. Anthony, J. Rand, R. M. Dell and R. Dell, Hydrogen Energy: Challenges and Prospects (1st Edition), Royal Society of Chemistry, 2007.

[40] R. Kumar, M. Farooque and B. Ernst, Fuel Cell Handbook (6th Edition), National Energy Technology Laboratory, 2002.

[41] C. C. Lee, Environmental Engineering Dictionary (3rd Edition), Rockville, MD : Government Institutes, 1989.

[42] S. T. Revankar and P. Majumdar, Fuel Cells: Principles, Design, and Analysis (1st Edition), CRC Press, 2013.

[43] K. Scott and E. Yu, Microbial Electrochemical and Fuel Cells: Fundamentals and Applications (1st Edition), Woodhead Publishing, 2015.

[44] K. Scoot, Sustainable and Green Electrochemical Science and Technology, John Wiley & Sons Ltd, 2017.

[45] R. O'Hayre, S.-W. Cha, W. Colella and F. B. Prinz, "Fuel Cell Characterization," in *Fuel Cell Fundamentals (3rd Edition)*, Wiley, 2016.

[46] S. Basu, Recent Trends in Fuel Cell Science and Technology, Springer;, 2007.

[47] C. Spiegel, Designing and Building Fuel Cells (1st Edition), McGraw-Hill Education, 2007.

[48] N. Karami, "Control of a Hybrid System Based PEMFC and Photovoltaic Panels," *Thesis for PhD ,* 2014.

[49] B. E. Logan and J. M. Regan, "Microbial Fuel Cells: Challenges and Aplications," *Environmental Science & Technolgy,* vol. 40, p. 5172–5180, 2006.

[50] V. B. Oliveira, M. Simões, L. F. Melo and A. M. F. R. Pinto, "Overview on the developments of microbial fuel cells," *Biochemical Engineering Journal,* vol. 73, pp. 53-64, 2013.

[51] L. Galvani, "Commentary on the effect of electricity on muscular motion," *Am. J. Phys.,* 1954.

[52] M. C. Potter, "Electrical effects accompanying the decomposition of organic compounds," *Royal Society ,* vol. 84, p. 260–276, 1911.

[53] S. V. Mohan, J. S. Sravan, S. K. Butti, K. V. Krishna, J. A. Modestra, G. Velvizhi, A. N. Kumar, S. Varjani and A. Pandey, "Microbial Electrochemical Technology: Emerging and Sustainable Platform," in *Microbial Electrochemical Technology: Sustainable Platform for Fuels, Chemicals and Remediation*, Elsevier, 2018, pp. 3-18.

[54] F. Kracke, I. Vassilev and J. O. Krömer, "Microbial electron transport and energy conservation – the foundation for optimizing bioelectrochemical systems," *Frontiers in Microbiology,* vol. 6, p. 575, 2015.

[55] A. Federico, P. Sebastià and H. Falk, "Microbial electrochemical technologies: maturing but not mature," *Microbial Biotechnology,* vol. 11, pp. 18-19, 2018.

[56] S. Roy and S. Pandit, "Microbial Electrochemical System: Principles and Application," in *Microbial Electrochemical Technology: Sustainable Platform for Fuels, Chemicals and Remediation*, Elsevier, 2019, pp. 19-48.

[57] C. Santoro, C. Arbizzani, B. Erable and I. Ieropoulos, "Microbial fuel cells: From fundamentals to applications. A review," *Jornal of Power Sources,* vol. 356, pp. 225-244, 2017.

[58] O. Obata, J. Greenman, H. Kurt, K. Chandran and I. Ieropoulos, "Microbial Fuel Cell anodic bacterial community and antibacterial agents: resilience and vulnerability test," *Bioelectrochemistry,* vol. 134, no. 107500, 2020.

[59] H. Smida, T. Flinois, E. Lebe`gue, C. Lagrost and F. Barrie`re, "Microbial Fuel Cells - Wastewater Utilization," *Surface Science and Electrochemistry,* vol. 218, pp. 328-336, 2018.

[60] K. Scott, "Membranes and separators for microbial fuel cell," in *Microbial Electrochemical and Fuel Cells: Fundamentals and Applications*, WoodHead Publishing , 2015, pp. 153-178.

[61] D. Sangeetha, K. Vaidhegi and S. Moogambigai, "Membranes for Microbial Fuel Cells," in *Microbial Electrochemical Technology: Sustainable Platform for Fuels, Chemicals and Remediation*, Elsevier, 2018.

[62] H.-S. Lee, B. R. Dhar and A. Hussain, "Electron Transfer Kinetics in Biofilm Anodes: Conductive Extracellular Electron Transfer," in *Microbial Electrochemical Technology: Sustainable Platform for Fuels, Chemicals and Remediation*, Elsevier, 2019.

[63] M. A. Lal and S. C. Bhatla, Plant Physiology, Development and Metabolism, Springer Nature, 2018.

[64] V. G. Debabov, "Electricity from Microorganisms," *Microbiology,* vol. 77, pp. 149-157, 2007.

[65] M. Sun, L.-F. Zhai, W.-W. Li and H.-Q. Yu, "Harvest and Utilization of Chemical Energy in Wastes by Microbial Fuel Cells," *Chemical Society Reviews,* vol. 45, pp. 2847-2870, 2016.

[66] C. A. R. Vargas, A. Prado and C. A. Arias, "Microbial Electrochemical Technologies for Wastewater Treatment: Principles and Evolution from Microbial Fuel Cells to Bioelectrochemical-Based Constructed Wetlands," *Water,* vol. 10, p. 1128, 2018.

[67] R. Veerubhotla, J. L. Varanasi and D. Das, "Biofilm Formation Within Microbial Fuel Cells," in *Progress and Recent Trends in Microbial Fuel Cells*, Elsevier, 2018, pp. 231-242.

[68] T. Storck, B. Virdis and D. J. Batstone, "Modelling extracellular limitations for mediated versus direct interspecies electron transfer," *The ISME Journal,* vol. 10, p. 621–631, 2016.

[69] S. A. Patil, C. Hägerhäll and L. Gorton, "Electron transfer mechanisms between microorganisms and electrodes in bioelectrochemical systems," *Bioanalytical Reviews,* vol. 1, pp. 71-129, 2012.

[70] R. L. Heydorn, C. Engel and K. D. Rainer Krull, "Strategies for the Targeted Improvement of Anodic Electron Transfer in Microbial Fuel Cells," *ChemBioEng Reviews,* vol. 7, pp. 4-17, 2019.

[71] S. K. Butti, G. Velvizhi and M. L. K. Sulonen, "Microbial electrochemical technologies with the perspective of harnessing bioenergy: Maneuvering towards upscaling," *Renewable and Sustainable Energy Reviews,* vol. 53, pp. 462-476, 2016.

[72] R. M. Snider, S. M. Strycharz-Glaven, S. D. Tsoi, J. S. Erickson and L. M. Tender, "Long-range electron transport in Geobacter sulfurreducens biofilms is redox gradient-driven.," *Proceedings of the National Academy of Sciences,* vol. 109, pp. 15467-15472, 2012.

[73] G. C. Premier, I. Michie, H. C. Boghani, K. R. Fradler and J. R. Kim, "Reactor design and scale-up," in *Microbial Electrochemical and Fuel Cells*, Woodhead Publishing, 2016, pp. 215-244.

[74] S. P. Jung and S. Pandit, "Important Factors Influencing Microbial Fuel Cell Performance," in *Microbial Electrochemical Technology: Sustainable Platform for Fuels, Chemicals and Remediation*, Elsevier, 2018, pp. 377-406.

[75] P. Aelterman, S. Freguia, J. Keller, K. Rabaey and W. Verstraete, "The anode potential regulates bacterial activity in microbialfuel cells," *Communications in agricultural and applied biological sciences,* vol. 73, pp. 85-90, 2008.

[76] B. E. Logan, B. Hamlers, R. Rozendal, U. Chroder, J. Keller, S. Freguia, P. Aelterman, W. Verstraete and K. Rabaey, "Microbial Fuel Cells: Methodology and Technology†," *Environmental Science & Technology,* vol. 40, p. 5181–5192, 2006.

[77] J. Khera and A. Chandra, "Microbial Fuel Cells: Recent Trends," *Proceedings of the National Academy of Sciences,* vol. 82, p. 31–41, 2012.

[78] F. A. Unal, M. H. Calimli, H. Burhan, F. Sismanoglu, B. Yalcin and F. Sen, "Microbial Fuel Cells Characterization," in *Microbial Fuel Cells: Materials and Applications*, Materials Research Foundations, 2019, pp. 75-100.

[79] A. J. Slatea, K. A. Whitehead, D. A. Brownson and C. E. Banksa, "Microbial fuel cells: An overview of current technology," *Renewable and Sustainable Energy Reviews,* vol. 101, pp. 60-81, 2019.

[80] Y. Fan, E. Sharbrough and H. Liu, "Quantification of the Internal Resistance Distribution of Microbial Fuel Cells," *Environmental Science & Technology,* vol. 42, pp. 8101-8107, 2008.

[81] X. Dominguez-Benetton, S. Sevda, K. Vanbroekhoven and D. Pant, "The accurate use of impedance analysis for the study of microbial electrochemical systems," *Chemical Society Reviews,* vol. 41, pp. 7228-7246, 2012.

[82] C. Kuppam, A. Kadier, G. Kumar, R. A. Nastro and V. Jeevitha, "Challenges in Microbial Fuel Cell and Future Scope," in *Microbial Fuel Cell: A Bioelectrochemical System that Converts Waste to Watts (1st Edition)*, Springer, 2018, pp. 483-499.

[83] V. Gude, "Microbial fuel cells for wastewater treatment and energy generation," in *Microbial Electrochemical and Fuel Cells: Fundamentals and Applications*, Woodhead Publishing, 2016, pp. 247-285.

[84] B. E. Logan and J. M. Regan, "Electricity-producing bacterial communities in microbial fuel cells," *Trends in Microbiology,* vol. 14, pp. 512-518, 2006.

[85] D. Pant, G. V. Bogaert, L. Diels and K. Vanbroekhoven, "A review of the substrates used in microbial fuel cells (MFCs) for sustainable energy production," *Bioresource Technology,* vol. 101, pp. 1533-1543, 2010.

[86] P. Pandey, V. N. Shinde, R. L. Deopurkar, S. P. Kale, S. A. Patil and D. Pant, "Recent advances in the use of different substrates in microbial fuel cells toward wastewater treatment and simultaneous energy," *Applied Energy,* vol. 168, pp. 706-723, 2016.

[87] G. Sun, A. Thygesen and A. S. Meyer, "Acetate is a superior substrate for microbial fuel cell initiation preceding bioethanol effluent utilization," *Applied Microbiology and Biotechnology,* vol. 99, pp. 4905 - 4915, 2015.

[88] B. E. Logan, "Exoelectrogenic bacteria that power," *Nature Reviews Microbiology,* vol. 7, p. 375–381, 2009.

[89] K. V. Krishna, K. Swathi, M. Hemalatha and S. V. Mohan, "Bioelectrocatalyst in Microbial Electrochemical Systems and Extracellular Electron Transport," in *Microbial Electrochemical Technology: Sustainable Platform for Fuels, Chemicals and Remediation*, Elsevier, 2018, pp. 117-141.

[90] K. C. Wrighton, P. Agbo, F. Warnecke, K. A. Weber, E. L. Brodie, T. Z. D. Santis, P. Hugenholtz, G. L. Andersen and J. D. Coates, "A novel ecological role of the Firmicutes identified in thermophilic microbial fuel cells," *The ISME Journal (,* vol. 2, p. 1146–1156, 2008.

[91] Y. Hubenova and M. Mitov, "Extracellular Electron Transfer in Yeast-Based Biofuel Cells: A Review," *Bioelectrochemistry,* vol. 106, pp. 177-185, 2015.

[92] E. T. Sayed and M. A. Abdelkareem, "Yeast as a Biocatalyst in Microbial Fuel Cell," in *Old Yeasts - New Questions*, Rijeka, 2016.

[93] S. B. Ummalyma, D. Sahoo, A. Pandey and K. V. Prajeesh, "Microalgae–Microbial Fuel Cell," in *Microbial Fuel Cells Materials and Applications*, Materials Research Forum, 2019, pp. 1-20.

[94] N. Patel, D. Rai, M. Z. A. Khan, S. Soni, U. Mishra and B. Bhunia, "Microbial Fuel Cell Operating Conditions," in *Microbial Fuel Cells: Materials and Applications*, Material Research Forum, 2019, pp. 53-74.

[95] E. Tamboli and J. S. Eswari, "Microbial Electrochemical Technology," in *Microbial electrochemical technology sustainable platform for fuels chemicals and remediation*, Elsevier, 2018, pp. 407-435.

[96] F. Hernández-Fernández, A. P. Ríos, M. Salar-García, V. O.-M. L. Lozano-Blanco, C. Godínez, F. Tomás-Alonso and J. Quesada-Medina, "Recent progress and perspectives in microbial fuel cells for bioenergy generation and wastewater treatment," *Fuel Processing Technology,* vol. 138, pp. 284-297, 2015.

[97] R. Kumar, L. Singh and Z. A. Wahid, "Microbial Fuel Cells: Types and Applications," in *Waste Biomass Management – A Holistic Approach*, Springer, 2017.

[98] P. Aelterman, K. Rabaey, H. T. Pham, N. Boon and W. Verstraete, "Continuous Electricity Generation at High Voltages and Currents Using Stacked Microbial Fuel Cells," *Environmental Science & Technology,* vol. 40, p. 3388–3394, 2006.

[99] A. Dumitru and K. Scott, "Anode materials for microbial fuel cells," in *Microbial Electrochemical and Fuel Cells: Fundamentals and Applications*, Woodhead Publishing, 2016, pp. 117-152.

[100] J. Luo, M. Chi, H. Wang, H. He and M. Zhou, "Electrochemical surface modification of carbon mesh anode to improve the performance of air-cathode microbial fuel cells," *Bioprocess and Biosystems Engineering,* vol. 36, p. 1889–1896, 2013.

[101] J. Wei, P. Liang and X. Huang, "Recent progress in electrodes for microbial fuel cells," *Bioresource Technology,* vol. 102, pp. 9335-9344, 2011.

[102] H. Rismani-Yazdi, S. M. Carver, A. D. Christy and O. H. Tuovinen, "Cathodic limitations in microbial fuel cells: An overview," *Journal of Power Sources,* vol. 180, pp. 683-694, 2008.

[103] X. Wang and N. Li, "Air-Cathodes," in *Microbial Electrochemical Technology: Sustainable Platform for Fuels, Chemicals and Remediation*, Elsevier, 2018, pp. 99-115.

[104] M. J. Lawati, T. Jafary, M. Said and B. A. Al-Mamun, "A mini review on biofouling on air cathode of single chamber microbial fuel cell; prevention and mitigation strategies," *Biocatalysis and Agricultural Biotechnology ,* vol. 22, 2019.

[105] P. Chatterjee, M. Ghangrekar and D. Leech, "A brief review on recent advances in air-cathode microbial fuel cells," *Environmental Engineering and Management Journal,* vol. 17, pp. 1531-1544, 2018.

[106] S. Bajracharya, A. ElMekawy, S. Srikanth and D. Pant, "Cathodes for microbial fuel cells," in *Microbial Electrochemical and Fuel Cells: Fundamentals and Applications*, Elsevier, 2016, pp. 179-213.

[107] K. Chandrasekhar, "Effective and Nonprecious Cathode Catalysts for Oxygen Reduction Reaction in Microbial Fuel Cells," in *Microbial Electrochemical Technology: Sustainable Platform for Fuels, Chemicals and Remediation*, Elsevier, 2018, pp. 485-501.

[108] M. Ghasemi, M. Ismail, S. K. Kamarudina, K. Saeedfar, W. R. W. Daud, S. H. A. Hassan, L. Y. Heng, J. Alam and S.-E. Oh, "Carbon nanotube as an alternative cathode support and catalyst for microbial fuel cells," *Applied Energy,* vol. 102, pp. 1050-1056, 2013.

[109] M. Zhou, M. Chi, J. Luo, H. He and T. Jin, "An overview of electrode materials in microbial fuel cells," *Journal of Power Sources,* vol. 196, no. 4427-4435, 2011.

[110] R. K. Gautam and A. Verma, "Electrocatalyst Materials for Oxygen Reduction Reaction in Microbial Fuel Cell," in *Microbial Electrochemical Technology: Sustainable Platform for Fuels, Chemicals and Remediation*, Elsevier, 2018, pp. 451-483.

[111] K. Scott, "Electrochemical principles and characterization of bioelectrochemical systems," in *Microbial Electrochemical and Fuel Cells: Fundamentals and Applications*, Woodhead Publishing, 2016, pp. 29-66.

[112] P. Clauwaert, D. v. d. Ha, N. Boon, K. Verbeken, M. Verhaege, K. Rabaey and W. Verstraete, "Open Air Biocathode Enables Effective Electricity Generation with Microbial Fuel Cells," *Environmental Science & Technology,* vol. 21, p. 7564–7569, 2007.

[113] M. Miskan, M. Ismaila, M. Ghasemi, J. M. Jahima, D. Nordin and M. H. A. Bakar, "Characterization of membrane biofouling and its effect on the performance of microbial fuel cell," *International Journal of Hydrogen Energy,* vol. 41, pp. 543-552, 2016.

[114] E. Yang, K.-J. Chae, M.-J. Choi, Z. Hee and I. S. Kim, "Critical review of bioelectrochemical systems integrated with membrane-based technologies for desalination, energy self-sufficiency, and high-efficiency water and wastewater treatment," *Desalination,* vol. 452, pp. 40-67, 2019.

[115] M. Shabani, H. Younesi, M. Pontié, A. Rahimpour, M. Rahimneja and A. A. Zinatizadeh, "A critical review on recent proton exchange membranes applied in microbial fuel cells for renewable energy recovery," *Journal of Cleaner Production,* vol. 264, no. 121446, 2020.

[116] S. Gottesfeld, D. R. Dekel, M. Page, C. Bae, Y. Yan, P. Zelenay and Y. S. Kim, "Anion exchange membrane fuel cells: Current status and remaining," *Journal of Power Sources,* vol. 375, pp. 170-184, 2017.

[117] J. X. Leong, W. R. W. Daud, M. Ghasemi, K. B. Liew and M. Ismail, "Ion exchange membranes as separators in microbial fuel cells for bioenergy conversion: A

comprehensive review," *Renewable and Sustainable Energy Reviews,* vol. 28, pp. 575-587, 2013.

[118] K.-J. Chae, M. Choi, F. Ajayi, W. Park, I. S. Chang and I. S. Kim, "Mass Transport through a Proton Exchange Membrane (Nafion) in Microbial Fuel Cells," *Energy & Fuels,* vol. 22, p. 169–176, 2008.

[119] I. Rivera, U. Schröder and S. A. Patil, "Microbial Electrolysis for Biohydrogen Production: Technical Aspects and Scale-Up Experiences," in *Microbial Electrochemical Technology: Sustainable Platform for Fuels, Chemicals and Remediation Biomass, Biofuels and Biochemicals*, pp. 871-898.

[120] G. Palanisamy, H.-Y. Jung, T. Sadhasivam, M. D. Kurkuri, S. C. Kim and S.-H. Roh, "A comprehensive review on microbial fuel cell technologies: Processes, utilization, and advanced developments in electrodes and membranes," *Journal of Cleaner Production,* vol. 221, pp. 598-621, 2019.

[121] A. Nandy, V. Kumar, S. Mondal, K. Dutta, M. Salah and P. P. Kundu, "Performance evaluation of microbial fuel cells: effect of varying electrode configuration and presence of a membrane electrode assembly," *New Biotechnology,* vol. 32, pp. 272-281, 2014.

[122] J. R. Kim, G. C. Premier, F. R.Hawkes, R. M.Dinsdale and A. J.Guwy, "Development of a tubular microbial fuel cell (MFC) employing a membrane electrode assembly cathode," *Journal of Power Sources,* vol. 187, pp. 393-399, 2009.

[123] O. Lefebvre, Y. Shen, Z. Tan, A. Uzabiaga, I. S. Chang and H. Y.Ng, "A comparison of membranes and enrichment strategies for microbial fuel cells," *Bioresource Technology,* vol. 102, pp. 6291-6294, 2011.

[124] F. Hernández-Fernández, A. P. d. l. Ríos, M. Salar-García, V. O.-M. L. Lozano-Blanco, C. Godínez, F. Tomás-Alonso and J. Quesada-Medina, "Recent progress and perspectives in microbial fuel cells for bioenergy generation and wastewater treatment," 2015.

[125] G. Mohanakrishna, S. Mohan and S. Mohan, "Carbon based nanotubes and nanopowder as impregnated electrode structures," *Applied Energy,* vol. 95, pp. Pages 31-37, 2012.

[126] H. Liu and B. E. Logan, "Electricity Generation Using an Air-Cathode Single Chamber Microbial Fuel Cell in the Presence and Absence of a Proton Exchange Membrane," *Environmental Science & Technology,* vol. 38, p. 4040–4046, 2004.

[127] A. L. Vázquez-Larios, O. Solorza-Feria, H. M. Poggi-Varaldo, R. G. González-Huerta, M. Teresa Ponce-Noyola, E. Ríos-Leal and N. Rinderknecht-Seijasc, "Bioelectricity production from municipal leachate in a microbial fuel cell: Effect of two cathodic catalysts," *International Journal of Hydrogen Energy,* vol. 39, pp. 16667-16675, 2014.

[128] S. Velasquez-Orta, I. Head, T.P.Curtis and K.Scott, "Factors affecting current production in microbial fuel cells using different industrial wastewaters," *Bioresource Technology,* vol. 102, pp. 5105-5112, 2011.

[129] B. Jong, P. Liew, M. L. Juri, B. Kim, A. M. Dzomir, K. Leo and M.R. Awang, "Performance and microbial diversity of palm oil mill effluent microbial fuel cell," *Applied Micorbiology,* vol. 53, pp. 660-667, 2011.

[130] G.Velvizhi and S. Mohan, "Biocatalyst behavior under self-induced electrogenic microenvironment in comparison with anaerobic treatment: Evaluation with pharmaceutical wastewater for multi-pollutant removal," *Bioresource Technology,* vol. 102, pp. 10784-10793, 2011.

[131] Y. Zhang, J. S. Noori and I. Angelidaki, "Simultaneous organic carbon, nutrients removal and energy production in a photomicrobial fuel cell (PFC)," *Energy & Environmental Science,* vol. 4, p. 4340–4346, 2011.

[132] Y. Yuan, Q. Chen, S. Zhou, L. Zhuang and P. Hu, "Improved electricity production from sewage sludge under alkaline conditions in an insert-type air-cathode microbial fuel cell," *Journal of Chemical Technology and Biotechnology,* vol. 87, pp. 80-86, 2011.

[133] T. P. Sciarria, G. Merlino, B. Scaglia, A. D'Epifanio, B. Mecheri, S. Borin, S. Licoccia and F. Adani, "Electricity generation using white and red wine lees in air cathode microbial fuel cells," *Journal of Power Sources,* vol. 274, pp. 393-399, 2015.

[134] K. Rengasamy and S. Berchmans, "Simultaneous degradation of bad wine and electricity generation with the aid of the coexisting biocatalysts Acetobacter aceti and Gluconobacter roseus," *Bioresource Technology,* vol. 104, pp. 388-393, 2012.

[135] R. M. Ziara, B. I. Dvorak and J. Subbiah, "Sustainable Waste-to-Energy Technologies: Bioelectrochemical Systems," in *Sustainable Food Waste-To-energy Systems*, Academic Press, 2018, pp. 111-140.

[136] E. D. Penteado, C. M. Fernandez-Marchante, M. Zaiat, E. R. Gonzalez and M. A. Rodrigo, "Influence of carbon electrode material on energy recovery from winery wastewater using

a dual-chamber microbial fuel cell," *Journal Environmental Technology,* vol. 38, pp. 1333-1341, 2016.

[137] S. Cheng, B. A. Dempsey and B. E. Logan, "Electricity Generation from Synthetic Acid-Mine Drainage (AMD) Water using Fuel Cell Technologies," *Environmental Science & Technology,* vol. 23, p. 8149–8153, 2007.

[138] L. Huang and B. E. Logan, "Electricity generation and treatment of paper recycling wastewater using a microbial fuel cell," *Applied Microbiology and Biotechnology 349–355,* vol. 80, p. 349–355, 2008.

[139] F. Zhao, R. C. T. Slade and J. R. Varcoe, "Techniques for the study and development of microbial fuel cells: an electrochemical perspective," *Chemical Society Reviews,* vol. 38, pp. 1926-1239, 2009.

[140] A. K. Manohar, O. Bretschger, K. H. Nealson and F. Mansfeld, "The use of electrochemical impedance spectroscopy (EIS) in the evaluation of the electrochemical properties of a microbial fuel cell," *Bioelectrochemistry,* vol. 72, pp. 149-154, 2008.

[141] M. T. F. Abedul, "Dynamic electroanalysis: an overview," in *Laboratory Methods in Dynamic Electroanalysis*, Elsevier, 2019, pp. 1-10.

[142] P. M. D. Serra, A. Espírito-Santo and M. Magrinho, "A steady-state electrical model of a microbial fuel cell through multiple-cycle polarization curves," *Renewable and Sustainable Energy Reviews,* vol. 117, 2020.

[143] G. Nikhil and S. V. Mohan, "Bioelectrochemical Energy Transitions Persuade Systemic Performance," in *Microbial Electrochemical Technology Sustainable Platform for Fuels, Chemicals and Remediation*, Elsevier, 2018, pp. 437-449.

[144] F. A. Unal, M. H. Calimli, H. Burhan, F. Sismanoglu, B. Yalcin and F. Sen, "Microbial Fuel Cells Characterization," in *Microbial Fuel Cells: Materials and Applications*, 2019.

[145] L. E. Doyle and E. Marsili, "Methods for enrichment of novel electrochemically-active microorganisms," *Bioresource Technology,* no. 195, pp. 273-282, 2015.

[146] X. Zhang, D. J. Philips, D. H. Roume, D. K. Guo, P. K. Rabaey and D. A. Prévoteau, "Rapid and Quantitative Assessment of Redox Conduction Across Electroactive Biofilms by using Double Potential Step Chronoamperometry," *ChemElectroChem,* vol. 4, pp. 1026-1036, 2017.

[147] S. S. Kumar, V. Kumar and S. Basu, "Electroanalytical Techniques for Investigating Biofilms in Microbial Fuel Cells," in *Bioelectrochemical Interface Engineering (1st Edition)*, Wiley & Sons, Inc, 2019.

[148] D. Czerwińska-Główka and K. Krukiewicz, "A journey in the complex interactions between electrochemistry and bacteriology: from electroactivity to electromodulation of bacterial biofilms," *Bioelectrochemistry,* vol. 131, no. 107401, 2020.

[149] E. Marsili, J. B. Rollefson, D. B. Baron, R. M. Hozalski and D. R. Bond, "Microbial Biofilm Voltammetry: Direct Electrochemical Characterization of Catalytic Electrode-Attached Biofilms," *Applied and Environmental Microbiology,* vol. 74, p. 7329–7337, 2008.

[150] C. Grobbler, B. Virdis, A. Nouwens, F. Harnischd, K. Rabaeye and P. L.Bond, "Effect of the anode potential on the physiology and proteome of Shewanella oneidensis MR-1," *Bioelectrochemistry,* vol. 119, pp. 172-179, 2018.

[151] M. Jarosz, J. Grudzień, K. Kamiński, K. Gawlak, K. Wolski, M. Nowakowska and G. D. Sulka, "Novel bioelectrodes based on polysaccharide modified gold surfaces and electrochemically active Lactobacillus rhamnosus GG biofilms," *Electrochimica Acta,* vol. 296, pp. 999-1008, 2019.

[152] N. Sekar and R. Ramasamy, "Electrochemical Impedance Spectroscopy for Microbial Fuel Cell Characterization," *Journal of Microbial & Biochemical Technology,* 2013.

[153] R. P. Ramasamy, V. Gadhamshetty, L. J. Nadeau and G. R. Johnson, "Impedance spectroscopy as a tool for non-intrusive detection of extracellular mediators in microbial fuel cells," *Biotechnology and Bioengineering,* vol. 104, pp. 882-891, 2009.

[154] A. K. Manohar, O. Bretschger, K. H. Nealson and F. Mansfeld, "The polarization behavior of the anode in a microbial fuel cell," *Electrochimica Acta,* vol. 53, pp. 3508-3513, 2008.

[155] Z. He, Y. Huang, A. K. Manohar and F. Mansfeld, "Effect of electrolyte pH on the rate of the anodic and cathodic reactions in an air-cathode microbial fuel cell," *Bioelectrochemistry,* vol. 74, pp. 78-82, 2008.

[156] M. Sindhuja, N. S. Kumar, V. Sudha and S. Harinipriya, "Equivalent circuit modeling of microbial fuel cells using impedance spectroscopy," *Journal of Energy Storage,* vol. 7, pp. 136-146, 2016.

[157] S. Roy and S. Pandit, " Microbial Electrochemical System: Principles and Application," in *Microbial Electrochemical Technology: Sustainable Platform for Fuels, Chemicals and Remediation*, 2018.

[158] K. Scott, "Electrochemical principles and characterization of bioelectrochemical systems," in *Microbial Electrochemical and Fuel Cells: Fundamentals and Applications*, 2016.

[159] S. Becerro, J. Paredes, M. Mujika, E. P. Lorenzo and S. Arana, "Electrochemical Real-Time Analysis of Bacterial Biofilm Adhesion and Development by Means of Thin-Film Biosensors," *IEEE Sensors Journal,* vol. 16, 2016.

[160] S. Srikanth, E. Marsili, M. C. Flickinger and D. R. Bond, "Electrochemical characterization of Geobacter sulfurreducens cells immobilized on graphite paper electrodes," *Biotechnology and Bioengineering,* vol. 99, pp. 1065-1073, 2007.

[161] Ya-Juan, Q. Yan, Q. Long, Zou, X.-S. Wu and J.-H. Liu, "Biofilm promoted current generation of Pseudomonas aeruginosa microbial fuel cell via improving the interfacial redox reaction of phenazines," *Bioelectrochemistry Volume 117, October 2017, Pages 34-39,* vol. 117, pp. 34-39, 2017.

[162] M. Méndez-Tovar, J. V. García-Meza and I. González, "Electrochemical Monitoring of Acidithiobacillus Thiooxidans Biofilm Formation on Graphite Surface With Elemental Sulfur," *Bioelectrochemistry,* vol. 128, pp. 30-38, 2019.

[163] M. T. Madigan, J. M. Martinko, K. S. Bender, D. H. Buckley and D. A. Stahl, "Major Microbial Habitats and Diversity," in *Brock Biology of Microorganisms (13th Edition)*, Pearson Education Inc, 2004.

[164] T. Tolker-Nielsen, "Biofilm Development," in *Microbial Biofilm*, ASM Press, 2015.

[165] Y. López and S. M. Soto, "The Usefulness of Microalgae Compounds for Preventing Biofilm Infections," *Antibiotics,* vol. 9, 2019.

[166] H.-C. Flemming and J. Wingender, "The biofilm matrix," *Nature Reviews Microbiology,* vol. 8, pp. 623-633, 2010.

[167] J. Kramer, S. Soukiazian, S. Mahoney and J. Hicks-Garner, "Microbial fuel cell biofilm characterization with thermogravimetric analysis on bare and polyethyleneimine surface modified carbon foam anodes," 2012.

[168] G. D. Saratale, R. Ganesh Saratale, M. K. Shahid, G. Zhend, G. k. Kumar, H.-S. Shin, Y.-G. Choi and S.-H. Kim, "A comprehensive overview on electro-active biofilms, role of exo-electrogens and their microbial niches in microbial fuel cells (MFCs)," *Chemosphere,* vol. 178, pp. 534-547, 2017.

[169] C. Wilson, R. Lukowicz, S. Merchant, H. Valquier-Flynn, J. Caballero, J. Sandoval, M. O. Okuom, C. Huber, T. D. Brooks, E. Wilson, B. Clement, C. D. Wentworth and H. Andrea E, "Quantitative and Qualitative Assessment Methods for Biofilm Growth: A Mini-review," *Research & Reviews | Journal of Engineering and Technology,* vol. 6, 2017.

[170] M. T. Madigan, J. M. Martinko, K. S. Bender, D. H. Buckley and D. A. Stahl, "A Brief Journey to the Microbial World," in *Brock Biology of Microorganisms*, Pearson Education Inc, 2012.

[171] A. K. Singh, "Experimental Methodologies for the Characterization of Nanoparticles," in *Engineered Nanoparticles: Structure, Properties and Mechanisms of Toxicity*, Elsevier Inc, 2016, pp. 125-170.

[172] M. Walock, "Thesis Nanocomposite coatings based on quaternary metalnitrogen," *PhD Thesis A& ParisTech,,* 2012.

[173] J. Webb and J. H. Holgate, "MICROSCOPY | Scanning Electron Microscopy," in *Encyclopedia of Food Sciences and Nutrition (2nd Edition)*, Academic Press, 2003, pp. 3922-3928.

[174] S. K L and F. M C, "The Use of Confocal Scanning Laser Microscopy and Other Tools to Characterize Escherichia coli in a HighCell-Density Synthetic Biofilm," *Biotechnology and Bioengineering,* vol. 20, pp. 340-356., 1996.

[175] J. R. Lawrence and T. R. Neu, "Confocal laser scanning microscopy for analysis of microbial biofilms.," in *Methods in Enzymology*, vol. 310, Elsevier, 1999, pp. 143-144.

[176] N. Kamjunke, U. Spohn, M. Füting, G. Wagner, E.-M. Scharf, S. Sandrock and B. Zippel, "Use of confocal laser scanning microscopy for biofilm investigation on paints under field conditions," *International Biodeterioration & Biodegradation,* vol. 69, pp. 17-22, 2012.

[177] X. Zhou and Y. Li, "Techniques for Oral Microbiology," in *Atlas of Oral Microbiology: From Healthy Microflora to Disease*, Academic Press, 2015, pp. 15-40.

[178] S. Shah, J. Yang, J. P. Crawshaw, O. Gharbi and E. Boek, "Predicting Porosity and Permeability of Carbonate Rocks From Core-Scale to Pore-Scale Using Medical CT Confocal Laser Scanning Microscopy and Micro CT," in *SPE Annual Technical Conference and Exhibition*, 2013.

[179] A. Baudler, I. Schmidt, M. Langner, A. Greiner and U. Schröder, "Does it have to be carbon? Metal anodes in microbial fuel cells and related bioelectrochemical systems," *Energy Environ. Sci.,* vol. 8, pp. 2048-2055, 2015.

[180] A. Bridier, E. D.-L. Quemener, C. Bureau, P. Champigneux, L. Renvoise, J.-M. Audic, E. Blanchet, A. Bergel and T. Bouchez, "Successive Bioanode Regenerations to Maintain Efficient Current Production From Biowaste," *Bioelectrochemistry,* vol. 106, pp. 133-140, 2015.

[181] N. Sharif, S. Khoshnoudi-Nia and S. M. Jafari, "Confocal laser scanning microscopy (CLSM) of nanoencapsulated food ingredients," in *Characterization of Nanoencapsulated Food Ingredients*, Academic Press, 2020.

[182] W. G. Characklis, M. G. Trulear, J. D. Bryers and N. Zelver, "Dynamics of biofilm processes: methods," *Water Research,* vol. 16, pp. 1207-1216, 1982.

[183] Ş. Şeker, H. Beyenal and A. Tanyolaç, "The effects of biofilm thickness on biofilm density and substrate consumption rate in a differential fluidizied bed biofilm reactor (DFBBR)," *Journal of Biotechnology,* vol. 41, pp. 39-47, 1995.

[184] J. T. Babauta and H. Beyenal, "Biofilm Electrochemistry," in *Biofilms In Bioeletrchemical Sytems*, Wiley, 2015.

[185] Y. Choi and E. Morgenroth, "Monitoring biofilm detachment under dynamic changes in shear stress using laser-based particle size analysis and mass fractionation," *Water Science and Technology,* vol. 47, p. 69–76, 2003.

[186] J. Azeredo, N. F. Azevedo, R. Briandet, N. Cerca, T. Coenye, A. R. Costa, M. Desvaux, G. D. Bonaventura, M. Hébraud, Z. Jaglic, M. Kačániová, S. Knøchel, A. Lourenço, F. Mergulhão and R. L. Meyer, "Critical review on biofilm methods," *Critical Reviews in Microbiology,* vol. 43, pp. 313-351, 2016.

[187] G. Kiely and J. M. Veza, "Ingeniería ambiental: fundamentos, entornos, tecnologías y sistemas de gestión," McGraw-Hill Interamericana de España, 2003.

[188] P. Clauwaert, P. Aelterman, T. H. Pham, L. D. Schamphelaire, M. Carballa, K. Rabaey and W. Verstraete, "Minimizing losses in bio-electrochemical systems - the road to applications," *Applied Microbiology and Biotechnology,* vol. 79, p. 901–913, 2008.

[189] M. &. Eddy and G. Tchobanoglous, Wastewater Engineering Treatment Disposal Reuse (5th Edition), McGraw-Hill, 2005.

[190] Z. Z. Ismail and A. Y. Radeef, "The Effect of Total Suspended Solids on the Electricity Generation in Microbial Fuel Cell Treating Actual Potato Chips Processing Wastewater," *University of Baghdad Engineering Journal ,* vol. 26, no. 55-62, 2020.

[191] Y. Zhang, M. Liu, M. Zhou, H. Yang, L. Liang and T. Gu, "Microbial fuel cell hybrid systems for wastewater treatment and bioenergy production - Synergistic effects, mechanisms and challenges," *Renewable and Sustainable Energy Reviews,* vol. 103, pp. 13-29, 2019.

[192] F.-y. Sun, X.-m. Wang and X.-y. Li, "An innovative membrane bioreactor (MBR) system for simultaneous nitrogen and phosphorus removal," *Process Biochemistry,* vol. 48, pp. 1749-1756, 2013.

[193] J. Liu, L. Liu, B. Gao and F. Yang, "Integration of bio-electrochemical cell in membrane bioreactor for membrane cathode fouling reduction through electricity generation," *Journal of Membrane Science,* vol. 430, pp. 196-202, 2013.

[194] Y.-L. Oon, S.-A. Ong, Li-NgeeHo, Y.-S. Wong, F. A. Dahalan, Y.-S. Oon, H. K. Lehl and W.-E. Thunga, "Synergistic effect of up-flow constructed wetland and microbial fuel cell for simultaneous wastewater treatment and energy recovery," *Bioresource Technology,* vol. 23, pp. 90-197, 2016.

[195] N. Rashid, Y.-F. Cui, M. S. U. Rehmana and J.-I. Han, "Enhanced electricity generation by using algae biomass and activated sludge in microbial fuel cell," *Science of The Total Environment,* vol. 456, pp. 91-94, 2013.

[196] W. A. Jury, H. Jr and J. Vaux, "The Emerging Global Water Crisis: Managing Scarcity and Conflict Between Water Users," *Advances in Agronomy,* vol. 95, pp. 1-76, 2007.

[197] A. Pistocchi, T. Bleninger, C.Breyer, U. Caldera, C. Dorati, D.Ganora, M.M.Millan, C. Paton, D.Poullis, F. S. Herrero, M. Sapiano, R.Semiat, C. Sommariva, S. Yuece and G. Zaragoza, "Can seawater desalination be a win-win fix to our water cycle?," *Water Research Volume,* vol. 182, no. 115906, 2020.

[198] T. H. Kwan, F. Katsushi, Y. Shen, S. Yin, Y. Zhang, K. Kase and Q. Yao, "Comprehensive review of integrating fuel cells to other energy systems for enhanced performance and enabling polygeneration," *Renewable and Sustainable Energy Reviews ,* vol. 128, no. 109897, 2020.

[199] H. Europe, "Hydrogen Roadmap Europe: A sustainable pathway for the European Energy Transition (1st Edition)," Bietlot, 2019.

[200] S. V. Mohan and A. Pandey, "Sustainable Hydrogen Production: An Introduction," in *Biohydrogen (Second Edition): Biomass, Biofuels, Biochemicals*, Elsevier, 2019, pp. 1-23.

[201] A. Kadier, Y. Simayi, P. Abdeshahian, N. F. Azman, K. Chandrasekhar and M. S. Kalil, "A comprehensive review of microbial electrolysis cells (MEC) reactor designs and configurations for sustainable hydrogen gas production," *Alexandria Engineering Journal,* vol. 55, pp. 427-443, 2016.

[202] K. Y. Show, Y. G. Yan and D.-J. Lee, "Biohydrogen Production: Status and Perspectives," in *Biohydrogen (Second Edition): Biomass, Biofuels, Biochemicals*, 2019, pp. 391-411.

[203] M. Sun, G.-P. Sheng, L. Zhang, C.-R. Xia, Z.-X. Mu, X.-W. Liu, H.-L. Wang, H.-Q. Yu, R. Qi, T. Yu and M. Yang, "An MEC-MFC-Coupled System for Biohydrogen Production from Acetate," *Environmental Science & Technology,* vol. 42, p. 8095–8100, 2008.

[204] B. H. Kim, I. S. Chang and G. M. Gadd, "Challenges in Microbial Fuel Cell Development and Operation," *Applied Microbiology and Biotechnology,* vol. 76, p. 485–494, 2007.

[205] J. Philips, K. Verbeeck, K. Rabaey and J. Arends, "Electron transfer mechanisms in biofilms," in *Microbial Electrochemical and Fuel Cells Fundamentals and Applications*, Elsevier, 2016, pp. 67-113.

[206] S. Bajracharya, "Microbial fuel cell coupled with anaerobic treatment processes for wastewater treatment," in *Integrated Microbial Fuel Cells for Wastewater Treatment*, Elsevier Inc. All, 2020, pp. 295-311.

[207] G. S. Murthy, "Systems Analysis Frameworks for Biorefineries," in *Biofuels: Alternative Feedstocks and Conversion Processes for the Production of Liquid and Gaseous Biofuels (2th Edition)*, Academic Press, 2019, pp. 77-92.

[208] T. Zhang and P.-L. Tremblay, "Possible Industrial Applications for Microbial Electrosynthesis From Carbon Dioxide," in *Microbial Electrochemical Technology Sustainable: Platform for Fuels, Chemicals and Remediation*, Elsevier, 2019, pp. 825-842.

[209] L. Malandra, G. Wolfaardt, A. Zietsman and M. Viljoen-Bloom, "Microbiology of biological contactor for winery wastewater treatment," *Water Research,* vol. 37, pp. 4125-4134, 2003.

[210] C. H. Collins, P. M. Lyne and J. M. Grange, Microbiological methods (7th Editon), Butterworth-Heinemann, Oxford, 1999.

[211] J. V. Boas, V. B. Oliveira, L. R. C. Marcon, D. P. Pinto, M. Simões and A. M. F. R. Pinto, "Effect of operating and design parameters on the performance of a microbial fuel cell with Lactobacillus pentosus," *Biochemical Engineering Journal,* vol. 104, pp. 34-40, 2015.

[212] A. W. APHA, Standard Methods for the Examination of Water and Wastewater (20th Edition), American Public Health Association, American Water Works Association, Water Environment Federation, 1998.

[213] A. W. APHA, Standard Methods for the Examination of Water and Wastewater (20th edition), American Public Health Association, American Water Works Association, Water Environment Federation, 1998.

[214] SHIMADZU, TOC Application Handbook, SHIMADZU Corporation .

[215] M. Stratford, H. Steels, G. Nebe-von-Caron, M. Novodvorska, K. Hayer and D. B. Archer, "Extreme resistance to weak-acid preservatives in the spoilage yeast Zygosaccharomyces bailii," *International journal of food microbiology ,* vol. 166, pp. 126-134, 2013.

[216] R. Rathour, V. Kalola, J. Johnson, K. Jain, D. Madamwar and C. Desai, "Treatment of Various Types of Wastewaters Using Microbial Fuel Cell Systems," in *Microbial Electrochemical Technology: Sustainable Platform for Fuels, Chemicals and Remediation*, Elsevier, 2018, pp. 665-692.

[217] Y. Ahn and B. E. Logan, "Effectiveness of domestic wastewater treatment using microbial fuel cells at ambient and mesophilic temperatures," *Bioresource Technology,* vol. 101, pp. 469-475, 2010.

[218] G. D. Saratale, R. G. Saratale, M. KashifShahid, GuangyinZhen, GopalakrishnanKumar, H.-S. Shin, Y.-G. Choi and S.-H. Kim, "A comprehensive overview on electro-active biofilms, role of exoelectrogens and their microbial niches in microbial fuel cells (MFCs)," *A comprehensive overview on electro-active biofilms, role of exo-electrogens and their microbial niches in microbial fuel cells (MFCs),* 2017.

[219] R. D. Cusick, P. D. Kiely and B. E.Logan, "A monetary comparison of energy recovered from microbial fuel cells and microbial electrolysis cells fed winery or domestic wastewaters," *International Journal of Hydrogen Energy,* vol. 35, pp. 8855-8861, 2010.

[220] B. Saba, A. D. Christy, Z. Yu, A. C. Co, R. Islam and O. H. Tuovinen, "Characterization and performance of anodic mixed culture biofilms in submersed microbial fuel cells," *Bioelectrochemistry,* vol. 113, pp. 79-84, 2016.

[221] B. Gadella, T. v. Haeften, K. v. Bavel and J. A. Valentijn, "Multi-photon excitation microscopy for advanced biomedical imaging," *BioMedical Engineering OnLine,* 2003.

[222] P. Hutzler, R. Fischbach, W. Heller, T. P. Jungblut, S. Reuber, R. Schmitz, M. Veit, G. Weissenbo and J.-P. Schnitzler, "Tissue localization of phenolic compounds in plants by confocal laser scanning microscopy," *Journal of Experimental Botany ,* vol. 49, pp. 953-965, 1998.

Appendix

Appendix A - Supporting information (Principles of function of the techniques for biofilm quantification)

A.1 Scanning electron microscopy

High-energy electrons produced at the top of the column, are accelerated downward where they passed the anode and are focused by a series of magnetic lens to hit the surface of the sample mounted on a movable stage under vacuum, the surface is scanned by moving the electron-beam coils [171]. The acceleration voltage is proportional to the penetration depth of the electrons into the sample where they are scattered due to elastic and inelastic collisions, additional determines the shape as well as the size of the electron beam interaction volume. Collision with atoms that have low atomic number (Z) result in a higher penetration depth and are mainly inelastic, thus, electrons form a pear-shaped interaction volume in the size region of micrometres. Atoms with higher Z increase the elasticity of collisions resulting in larger scattering angles, thus, more spherical interaction volumes. Energy and scattering angle of reflected electrons turns out to be related to the elemental and phase composition of the sample, therefore compositional analysis become more reliable and more significant for the differences in Z [78], [171], [172],.

Reflected electrons can be separated in secondary electrons and back-scattered electrons. Secondary electrons ejected from the sample via inelastic scattering (low Z) have typically low energy, result of kinetic energy loss due to inelastic collision, this electrons are from the first nanometers of the sample surface, are detected at lower deflection angles and primarily used for imaging the sample surface morphology [78], [172]. The energy loss can be emitted in the form of a photon (x-rays) or transmitted to another electrons which are ejected from its orbital (Auger process) [172]. Backscattered electrons are a result of elastic scattering (higher Z) with kinetic energy higher than 5eV, deflection angles larger than 90º and are used to image atomic contrast and reveal crystallographic information, providing better compositional analysis [78] [172].

A.2 Confocal scanning laser microscopy

In CSLM the laser light focuses a determined spot of the specimen, illuminating it. At this point exist 2 lights pathways, the excitation (purple line), and the emission (red line) [181]. Excitation light passes through a pinhole and becomes a parallel beam that is reflected when encounters the dichroic mirror onto the objective lens [177], [181]. After passing through the objective lens the light beam focuses a small spot on the biological sample, emitting a fluorescent light (emission

pathway) from the sample [177], [181], [221]. Fluorescence is collected by the objective lens and scanning system, and reflects off the dichroic mirror, the fluorescent light passes through a pinhole at the focal point while out of focus lights is eliminated, allowing only the illuminated spot to enter in the detector, elimination of unfocused light depends on the numerical aperture of the microscope lens and the size of the pinhole [177], [181], [221].

Moving the focused spot across the sample by a x-y light deflector a sequentially point by point and line by line is detected and a 2-D image is created using the scan system [222]. Taking consecutive series of x-y scans at different depths and using computer image processing and 3-D image reconstruction software, high resolution 3-D image can be obtained from the sample [221].

Scanned areas resolution may differ in 512x512, 512x768, or 1024x1024, when the scan rate is increased resolution is lost and when the scan rate is low photobleaching is increased [175].

Appendix B - Microbial Fuel Cell Design

Figure B1 presents a scheme of the MFC used in experiments and shows the positioning of the lateral sampling ports.

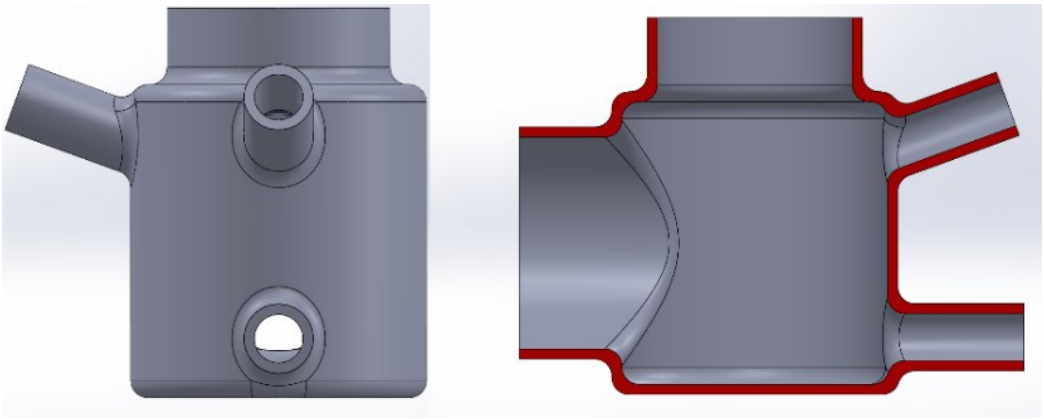

Figure B1: Schematic representation of the MFC with the lateral sampling ports shown in detail.

Appendix C - Synthetic Winery Wastewater Characterization

The characterization of SWWW in terms of COD and TOC is depicted on table C1.

Table C1: Concentration of COD and TOC in the SWWW.

COD (mgO_2/L)	3923
TOC (mg/L)	1802

Appendix D - Conductivity, pH and temperature

The experiments ran in duplicate. Duplicates of A_0 and A_1 are named as I and II. The conductivity, the pH and the temperature of the effluent is in tables D1 for A_0 and in C1 for A_1.

Table D1: Experimental data of conductivity, pH and temperature of A_0 at the end of each batch cycle, at 72h, 144h, 216h, 288h and 360h.

A_0

	I			II		
Time (h)	**Conductivity (mS/cm)**	**T (ºC)**	**pH**	**Conductivity (mS/cm)**	**T (ºC)**	**pH**
72	10.70	21.40	4.38	10.71	21.50	4.35
144	11.03	21.30	4.97	10.96	21.30	5.01
216	11.12	21.40	5.21	11.04	21.90	5.14
288	10.97	20.90	5.06	10.94	21.00	5.04
360	11.16	21.90	5.17	11.10	22.10	5.10
Average	**11.00**	**21.38**	**4.96**	**10.95**	**21.56**	**4.93**

Table D2: Experimental data of conductivity, pH and temperature of A_1 at the end of each batch cycle, at 72h, 144h, 216h, 288h and 360h.

A_1

	I			II		
Time (h)	**Conductivity (mS/cm)**	**T (ºC)**	**pH**	**Conductivity (mS/cm)**	**T (ºC)**	**pH**
72	10.98	21.10	4.75	10.94	21.20	4.57
144	10.99	20.60	4.95	11.03	21.04	4.94
216	11.14	21.70	5.07	11.18	21.80	5.06
288	11.91	20.00	5.03	11.44	20.00	5.05
360	11.57	20.70	5.02	11.90	21.00	5.06
Average	**11.32**	**20.82**	**4.96**	**11.57**	**21.01**	**5.03**

Appendix E - Chemical Oxygen Demand

The concentration of COD and CODremoval for duplicates of A_0 and A_1 are in table D1.

Table E1: Concentration of COD and CODremoval of the duplicates of A_0 and A_1. The COD concentration was obtained at the last of the three cycles at 216h, 288h and 360h.

	A_0		**A_1**	
	I		I	
Time (h)	**COD (mgO_2/L)**	**$COD_{removal}$ (%)**	**COD (mgO_2/L)**	**$COD_{removal}$ (%)**
216	3352	15	3439	12
288	2893	26	2866	27
360	3208	18	2038	48
	II		**II**	
216	2629	33	2791	29
288	2463	37	1609	59
360	2992	24	2793	29

Appendix F - Total Organic Carbon

The concentration of TOC and TOCremoval for duplicates of A_0 and A_1 are in table F1.

Table F1: Concentration of TOC and TOCremoval of the duplicates of A_0 and A_1. The COD concentration was obtained at the last of the three cycles at 216h, 288h and 360h.

	A_0		**A_1**	
	I		I	
time (h)	**TOC (mg/L)**	**$TOC_{removal}$ (%)**	**TOC (mg/L)**	**$TOC_{removal}$ (%)**
216	1065	41	914	49
288	837	54	786	56
360	1019	43	534	70
	II		II	
216	757	58	730	59
288	718	60	481	73
360	975	46	799	56

Appendix G - Covariance & Coefficient Correlation

Covariance can be determined by equation G1,

$$Covariance = \frac{\sum_{i=1}^{n}(x_i - x_{average}) * (y_i - y_{average})}{n-1} \quad \text{(G1)}$$

Coefficient correlation (CC) can be given by equation G2,

$$CC = \frac{Covariance\ (x,y)}{StandarDeviation\ (x) * StandarDeviation(y)} \quad \text{(G2)}$$

Table G1 presents the covariance value and CC of 216h, 288h and 360h.

Table G1: Determination of covariance and CC of the CODremoval and TOCremoval in A_0 and A_1.

A_0

Time (h)		$COD_{removal}$	$TOC_{removal}$		(x-χ) * (y-χ)
216		23.8	49.4		1.5
288		31.7	56.9		40.8
360		21.0	44.7		25.6
	Mean	25.5	50.3	Sum	67.9
	Standard.Dev	5.6	6.1	Sample Size	3
				Covariance	**34**
				Corr.Coeff	**0.99**

A_1

Time (h)		$COD_{removal}$	$TOC_{removal}$		(x-χ) * (y-χ)
216		20.6	54.4		85.5
288		43.0	64.8		36.8
360		38.4	63.0		10.1
	Mean	34.0	60.7	Sum	132.4
	Standard.Dev	11.8	5.6	Sample Size	3
				Covariance	**66**
				Corr.Coeff	**1.00**

Appendix H - Polarization Curves

Polarization and power density curves for duplicates of A_0 and A_1 are in tables H1 and H2.

Table H1: Experimental data of polarization and power density curves at 288h and 360h.

A_0							
288h							
I				II			
I (A)	U (mV)	I (mA/m^2)	P (mW/m^2)	I (A)	U (mV)	I (mA/m^2)	P (mW/m^2)
0	0.344	0.000	0.00	0	0.316	0.000	0.00
$5x10^{-7}$	0.341	0.183	0.06	$5x10^{-7}$	0.314	0.183	0.06
$1x10^{-6}$	0.336	0.366	0.12	$1x10^{-6}$	0.311	0.366	0.11
$3x10^{-6}$	0.321	1.097	0.35	$3x10^{-6}$	0.301	1.097	0.33
$6x10^{-6}$	0.292	2.195	0.64	$6x10^{-6}$	0.283	2.195	0.62
$9x10^{-6}$	0.254	3.292	0.84	$9x10^{-6}$	0.259	3.292	0.85
$1x10^{-5}$	0.218	3.658	0.80	$1x10^{-5}$	0.237	3.658	0.87
$3x10^{-5}$	0.074	10.973	0.81				
360h							
I (A)	U (mV)	I (mA/m^2)	P (mW/m^2)	I (A)	U (mV)	I (mA/m^2)	P (mW/m^2)
0	0.308	0.000	0.00	0	0.282	0.000	0.00
$5x10^{-7}$	0.305	0.183	0.06	$5x10^{-7}$	0.280	0.183	0.05
$1x10^{-6}$	0.300	0.366	0.11	$1x10^{-6}$	0.277	0.366	0.10
$3x10^{-6}$	0.283	1.097	0.31	$3x10^{-6}$	0.266	1.097	0.29
$6x10^{-6}$	0.255	2.195	0.56	$6x10^{-6}$	0.247	2.195	0.54
$9x10^{-6}$	0.212	3.292	0.70	$9x10^{-6}$	0.222	3.292	0.73
$1x10^{-5}$	0.176	3.658	0.64	$1x10^{-5}$	0.124	3.658	0.45
$3x10^{-5}$	0.049	10.973	0.54				

Table H2: Experimental data of polarization and power density curves at 288h and 360h.

A_1							
288h							
I				II			
I (A)	U (mV)	I (mA/m^2)	P (mW/m^2)	I (A)	U (mV)	I (mA/m^2)	P (mW/m^2)
0	0.351	0.000	0.00	0	0.350	0.000	0.00
$5x10^{-7}$	0.348	0.183	0.06	$5x10^{-7}$	0.347	0.183	0.06
$1x10^{-6}$	0.344	0.366	0.13	$1x10^{-6}$	0.343	0.366	0.13
$3x10^{-6}$	0.332	1.097	0.36	$3x10^{-6}$	0.330	1.097	0.36
$6x10^{-6}$	0.307	2.195	0.67	$6x10^{-6}$	0.303	2.195	0.67
$9x10^{-6}$	0.275	3.292	0.91	$9x10^{-6}$	0.272	3.292	0.90
$1x10^{-5}$	0.247	3.658	0.90	$1x10^{-5}$	0.248	3.658	0.91
$3x10^{-5}$	0.126	10.973	1.38	$3x10^{-5}$	0.122	10.973	1.34
360h							
I (A)	U (mV)	I (mA/m^2)	P (mW/m^2)	I (A)	U (mV)	I (mA/m^2)	P (mW/m^2)
0	0.364	0.000	0.00	0	0.336	0.000	0.000
$5x10^{-7}$	0.362	0.183	0.07	$5x10^{-7}$	0.329	0.183	0.06
$1x10^{-6}$	0.357	0.366	0.13	$1x10^{-6}$	0.327	0.366	0.12
$3x10^{-6}$	0.339	1.097	0.37	$3x10^{-6}$	0.314	1.097	0.35
$6x10^{-6}$	0.306	2.195	0.67	$6x10^{-6}$	0.291	2.195	0.64
$9x10^{-6}$	0.275	3.292	0.91	$9x10^{-6}$	0.260	3.292	0.84
$1x10^{-5}$	0.248	3.658	0.91	$1x10^{-5}$	0.226	3.658	0.83
$3x10^{-5}$	0.131	10.973	1.44	$3x10^{-5}$	0.112	10.973	1.23

Appendix I - Relative Error

$$Relative\ Error\ (\%) = ABS\frac{Value_i - Value_{ii}}{Value_i} * 100$$

Where i=parameter in analyse and ABS = Absolute value of the number (excel command).